ผลกระทบของสภาวะการเดินระบบและการปนเปื้อนของไอออน ในกระบวนการรวมตะกอนและออกซิเดชันทางไฟฟ้า สำหรับการปรับปรุงคุณภาพน้ำ

นางสาวววดลาย เทง

วิทยานิพนธ์นี้เป็นส่วนหนึ่งของการศึกษาตามหลักสูตรปริญญาวิศวกรรมศาสตรมหาบัณฑิต
สาขาวิชาวิศวกรรมสิ่งแวดล้อม ภาควิชาวิศวกรรมสิ่งแวดล้อม
คณะวิศวกรรมศาสตร์ จุฬาลงกรณ์มหาวิทยาลัย
ปีการศึกษา 2560

Effect of Operating Conditions and Ion Contaminations on Electro Coagulation and Oxidation Processes for Water Quality Improvement

Miss Vouchlay Theng

A Thesis Submitted in Partial Fulfillment of the Requirements
for the Degree of Master of Engineering Program in Environmental Engineering
Department of Environmental Engineering
Faculty of Engineering
Chulalongkorn University
Academic Year 2017

Thesis Title	Effect of Operating Conditions and Ion Contaminations on Electro Coagulation and Oxidation Processes for Water Quality Improvement
By	Miss Vouchlay Theng
Field of Study	Environmental Engineering
Thesis Advisor	Associate Professor Pisut Painmanakul, Ph.D.
Thesis Co-Advisor	Nattawin Chawaloesphonsiya, Ph.D.

Accepted by the Faculty of Engineering, Chulalongkorn University in Partial Fulfillment of the Requirements for the Master's Degree

....Dean of the Faculty of Engineering
(Associate Professor Supot Teachavorasinskun, D.Eng.)

THESIS COMMITTEE

....Chairman
(Assistant Professor Pichaya Rachdawong, Ph.D.)

....Thesis Advisor
(Associate Professor Pisut Painmanakul, Ph.D.)

....Thesis Co-Advisor
(Nattawin Chawaloesphonsiya, Ph.D.)

....Examiner
(Assistant Professor Chaiyaporn Puprasert, Ph.D.)

....Examiner
(Associate Professor Sutha Khaodhiar, Ph.D.)

....External Examiner
(Marupatch Jamnongwong, Ph.D.)

วาวดลาย เทง : ผลกระทบของสภาวะการเดินระบบและการปนเปื้อนของไอออน ในกระบวนการรวมตะกอนและออกซิเดชันทางไฟฟ้า สำหรับการปรับปรุงคุณภาพน้ำ (Effect of Operating Conditions and Ion Contaminations on Electro Coagulation and Oxidation Processes for Water Quality Improvement) อ.ที่ปรึกษาวิทยานิพนธ์หลัก: รศ. ดร. พิสุทธิ์ เพียรมนกุล, อ.ที่ปรึกษาวิทยานิพนธ์ร่วม: ดร. ณัฐวิญญ์ ชวเลิศพรศิยา, 185 **หน้า.**

งานวิจัยนี้มีวัตถุประสงค์เพื่อศึกษาการกำจัดความขุ่นและสารประกอบอินทรีย์ในน้ำ (Natural Organic Matter, NOM) ด้วยกระบวนการรวมตะกอนทางไฟฟ้า (Electro Coagulation, EC) และกระบวนการออกซิเดชันทางไฟฟ้า (Electro Oxidation, EO) โดยมีปัจจัยที่ทำการศึกษา ได้แก่ ผลกระทบจากการปนเปื้อนของไอออน (เฟอรัสและแคลเซียม) และสภาวะการเดินระบบ (ค่า pH เริ่มต้นและความหนาแน่นของกระแสไฟฟ้า) ทำการทดลองกับน้ำสังเคราะห์ที่มีส่วนผสมของเบนโทไนท์ให้มีความขุ่น 100 NTU และกรดฮิวมิค (Humic Acid, HA) 70 มิลลิกรัมต่อลิตร จากการทดลองพบว่า สภาวะที่เหมาะสมในการกำจัดความขุ่น HA และความขุ่นร่วมกับ HA ด้วยกระบวนการ EC คือ การต่อขั้วไฟฟ้าแบบอนุกรม (Bipolar) ที่ระยะห่างระหว่างขั้ว 2 เซนติเมตร ความหนาแน่นของกระแสไฟฟ้า 3 มิลลิแอมแปร์ต่อตารางเซนติเมตร และระยะเวลาเดินระบบ 20 นาที จากการศึกษาผลกระทบจากการปนเปื้อนของไอออนต่อกระบวนการ EC พบว่า เฟอรัส แคลเซียม และค่า pH เริ่มต้นเป็นปัจจัยที่มีผลกระทบอย่างมีนัยสำคัญต่อการกำจัดความขุ่น ขณะที่ความหนาแน่นของกระแสไฟฟ้า เฟอรัส และค่า pH เริ่มต้นเป็นปัจจัยที่มีผลกระทบอย่างมีนัยสำคัญต่อการกำจัด HA โดยมีสภาวะที่เหมาะสมคือ เฟอรัสและแคลเซียมที่ความเข้มข้น 1 และ 18 มิลลิกรัมต่อลิตร ค่า pH เริ่มต้นเท่ากับ 8 และความหนาแน่นของกระแสไฟฟ้า 3.4 มิลลิแอมแปร์ต่อตารางเซนติเมตร อย่างไรก็ตาม น้ำทิ้งจากกระบวนการ EC ที่ทดลองในสภาวะการเดินระบบที่ไม่เหมาะสมถูกนำมาบำบัดต่อด้วยกระบวนการ EO โดยใช้อลูมิเนียมเป็นขั้วแคโทดที่ต่อขนาน (Monopolar) กับแกรไฟต์เคลือบด้วยคาร์บอนนำไฟฟ้าเป็นขั้วแอโนด พบว่า ที่ความหนาแน่นของกระแสไฟฟ้า 5.5 มิลลิแอมแปร์ต่อตารางเซนติเมตร และระยะเวลาเดินระบบ 20 นาที เป็นสภาวะการทดลองที่เหมาะสมซึ่งมีประสิทธิภาพการกำจัด HA 37 กรัมต่อลิตร จากการทดลองในงานวิจัยนี้สามารถกล่าวได้ว่า การปรับปรุงคุณภาพน้ำด้วยกระบวนการ EC ตามด้วยการทิ้งให้ตกตะกอน เป็นรูปแบบที่เหมาะสมสำหรับบำบัดตัวอย่างน้ำสังเคราะห์ในงานวิจัยนี้ให้ผ่านตามมาตรฐานน้ำทิ้งของ WHO

ภาควิชา วิศวกรรมสิ่งแวดล้อม ลายมือชื่อนิสิต ....

สาขาวิชา วิศวกรรมสิ่งแวดล้อม ลายมือชื่อ อ.ที่ปรึกษาหลัก ....

ปีการศึกษา 2560 ลายมือชื่อ อ.ที่ปรึกษาร่วม ....

5970418421 : MAJOR ENVIRONMENTAL ENGINEERING
KEYWORDS: ELECTROCOAGULATION (EC), ELECTROOXIDATION (EO), ION CONTAMINATIONS AND OPERATING CONDITIONS

VOUCHLAY THENG: Effect of Operating Conditions and Ion Contaminations on Electro Coagulation and Oxidation Processes for Water Quality Improvement. ADVISOR: ASSOC. PROF. PISUT PAINMANAKUL, Ph.D., CO-ADVISOR: NATTAWIN CHAWALOESPHONSIYA, Ph.D., 185 pp.

The objective of this study is to investigate the effect of ion contaminations and operating conditions on Electro Coagulation (EC) and Oxidation (EO) in turbidity and natural organic matter (NOM) removal. The experiments were conducted in 4 liters column. Ferrous and calcium were chosen as contaminated ions. The operating condition was varied in terms of initial pH and current density. 100 NTU turbidity and 70 mg/L NOM were synthesized from bentonite and humic acid (HA), respectively. The results showed that bipolar arrangement of electrodes with 2 cm gap was the optimal condition in terms of gas flow rate and electrode corrosive ratio (Q_g/Loss) as well as the treatment performance. From kinetic study, turbidity was removed through destabilization mechanism while HA was removed faster by physical attractive force and sweep floc mechanism. The optimal operation time was found at 20 minutes. It was then selected for analyzing the effect of co-ions and operating conditions. Based on the result, calcium, ferrous, and initial pH were significant effect on turbidity removal while current density, initial pH, and ferrous were significant effect on HA removal. The optimal condition on turbidity removal was found at ferrous 1 mg/L, calcium 18 mg/L, initial pH 8, and current density 3.4 mA/cm^2. HA was obtained at ferrous 25 mg/L, calcium 8 mg/L, initial pH 5, and current density 4 mA/cm^2. The effluent of the worst condition of HA was then taken place for EO process. Aluminum cathode and conductive carbon coated onto graphite anode were the best condition for EO electrode material. The optimal condition was found at current density 5.5 mA/cm^2 and operating time 20 minutes in monopolar arrangement for EO process to remove 37 mg/L HA.

Department:	Environmental Engineering	Student's Signature	....
Field of Study:	Environmental Engineering	Advisor's Signature	....
Academic Year:	2017	Co-Advisor's Signature	....

ACKNOWLEDGEMENTS

I would like to express my sincere gratitude to my advisor, Assoc. prof. Pisut Painmanakul, Ph.D. for his enthusiastic encouragement, useful critiques, and keeping my progress on schedule in this research study. I also greatly thank to my co-advisor, Dr. Nattawin Chawaloesphonsiya for his motivation, lighting up idea, and patient guidance. My grateful thanks are also extended to all thesis committees: Asst. Prof. Pichaya Rachdawong, Ph.D, Assoc. Prof. Sutha Khaodhiar, Ph.D., Asst. Prof. Chaiyaporn Puprasert, Ph.D., and Dr. Marupatch Jamnongwong for the useful suggestions and feedbacks.

This research wishes to thank Collaborative Research Program (CR) under ASEAN University Network Southeast Asia Engineering Education Development Network Program (AUN/SEED-Net) of Japan International Cooperation Agency (JICA) JFY 2016-2017 for financial support.

The appreciation was also given to various people in teamwork under supervision of Dr. Pisut Painmanakul, namely Mr. Saret Bun, Mr. Nawadol Thongtaluang, and all my laboratory colleagues for their guidance in thesis writing, Thai translation, chemical substance purchase, and providing insight and expertise that greatly assisted the research.

Additionally, I would like to thank all lecturers, staffs, and technicians of the laboratory in Department of Environmental Engineering for providing invaluable knowledge as well as offering the resources and experimental guidance.

Last but not least, I would like to thank my parents for their support, motivation, and encouragement throughout my study.

CONTENTS

Page

Page

Page

Page

LISTS OF FIGURE

LISTS OF TABLE

ABBREVIATIONS

-	AOPs	Advanced Oxidation Process
-	BDD	Boron-Doped Diamond
-	BR	Batch Reactor
-	CC	Chemical Coagulation
-	CCD	Central Composite Design
-	CDWQS	Cambodian Drinking Water Quality Standard
-	CE	Current Efficiency
-	COD	Chemical Oxygen Demand
-	CSTR	Continuous Stirred Tank Reactor
-	DBPs	Disinfection By-Products
-	DO	Dissolved Oxygen
-	DOC	Dissolved Organic Compound
-	DOE	Design Of Experiment
-	DSA	Dimensionally Stable Anode
-	EC	Electrocoagulation
-	EDL	Electrical Double Layer
-	EF	Electroflotation
-	EO	Electrooxidation
-	HA	Humic Acid
-	HSs	Humic Substances
-	ISE	Ion Selective Electrode
-	MC-LR	Microcystin-LR
-	MIEX®	Magnetic Ion Exchange Resin
-	MTE	Metal Trace Elements
-	NHE	Normal Hydrogen Electrode
-	NOM	Natural Organic Matter
-	OM	Organic Matter
-	PAC	Powdered Activated Carbon
-	PFR	Plug Flow Reactor

-	RBF	River Bank/ Bed Filtration
-	RSM	Response Surface Methodology
-	SN	Signal-To-Noise
-	TDS	Total Dissolved Solid
-	TOC	Total Organic Carbon
-	UNICEF	The United Nations Children's Emergency Fund
-	USAID	United States Agency For International Development
-	UV	Ultraviolet
-	WHO	World Health Organization

CHAPTER 1
INTRODUCTION

1.1 Background

Surface water, groundwater and rainwater are the main sources of drinking water in Cambodia. In raining season, the large amount of raining water causes flooding and impacts to the quality of water. Meanwhile in dry season, water shortage usually occurs everywhere in rural area. Therefore, most of people decide to used groundwater for daily activities since it could provide adequate amount of water according to National Institute of Statistics (2008). However, several contaminants are found such as ferrous, hardness, chloride, and organic matter in groundwater. On the other hand, the source of water supplied in city is from surface water such as river and lake. Many undesirable agents such as suspended matter, bacteria, viruses, organic matter, etc., also have been found. Therefore, both groundwater and surface water are required to treat due to their unfit quality for human consumption.

Two common contaminants are turbidity and natural organic matter. Turbidity is caused by very small particulates in the water which synonymous with cloudiness and color. Suspended solid is not able to settle down by gravity since their stability results from a balance between electrostatic forces on interparticle repulsion and attraction of Van-der-Waals (Bejjany et al., 2017a). Conventional coagulation and flocculation have been widely used for removing turbidity. Coagulant can destabilize pollutants, it will be therefore removed in followed separation process. Organic substances also bring many disadvantage to human health. It causes physically color and odor. The bacterial oxidation of organic carbon from natural sources and human activities deplete dissolve oxygen in water. Moreover, it is a carrier of heavy metal and brings toxicity to environment. Remained natural organic matter (NOM) in disinfection process of water treatment can produce disinfection by-product which impact to the human health. NOM also help microbial re-growth in water distribution system (Joseph et al., 2012).

Generally, NOM and turbidity are removed by chemical coagulation and flocculation followed by filtration in conventional treatment. However, this process generates another pollution due to the usage of chemical reagents such as aluminum and iron metal salt. Therefore, some treatment techniques have been proposed to examine NOM and turbidity such as adsorption, membrane, biological process, and advanced oxidation process (AOP). However, many negative impacts are also found such as regeneration (adsorbents and ion-exchange), high cost of operation (advanced oxidation process), membrane fouling (membrane process), and long time of treatment (biological process) (Kac et al., 2017). Recently, electrocoagulation (EC) technology has been proposed in 1909 using aluminum and iron electrode in the USA (Holt et al., 1999). Since there is not required any chemical reagents and less sludge produced, Electro Coagulation and Oxidation were wildly used in large scale for reducing contaminants in water (Kuokkanen et al., 2013).

Therefore, the combination of Electro Coagulation (EC) and Oxidation (EO) was commonly considered for removing the turbidity and NOM from water.

1.2 Statement of problem

Even though, EC and EO are the effective processes to remove turbidity and NOM, respectively, but water does not contain only these two pollutants. Many ion species and pollutants have been found in raw water as shown in Table 1.1. In Cambodia, two contaminations commonly found in groundwater are high iron contents (76.51% exceed Cambodia drinking water standard), and water hardness (202.92 mg/L of calcium carbonate) that are also the obstacle of groundwater quality. The iron in groundwater occurs in form of dissolved Fe(II) in the absence of oxygen. Ferrous could be removed by oxidation in Electrochemical. The ferric hydroxide form is a coagulant and also adsorbent which bring positive effect in Electrochemical process (D Ghosh et al., 2008). For calcium, it was removed by forming calcium carbonate at the cathode side of the electrode (Zhao et al., 2014). However, the assessment of the effect of these co-ions (iron and hardness) and operating conditions on turbidity and NOM removal was limited in research studies.

Therefore, the objective of the study aimed to investigate the effect of iron, hardness, pH and current density on turbidity and NOM removal in Electro Coagulation and Oxidation process.

Table 1.1. Some contaminants found in groundwater source (Waller, 2016)

Contaminants	Potential health and other effects
Inorganic contaminants	
Aluminum	Increase turbidity or discolored water after treatment
Arsenic	Cause health problem: liver and kidney damage, blood hemoglobin decreases, carcinogen due to acute and chronic toxicity
Cadmium	Cause high blood pressure, replace zinc biochemically in the body, damage liver and kidney, and anemia Destroy testicular tissue and red blood cells and toxic to aquatic biota
Chloride	Deteriorate plumbing system, taste becomes noticeable Above secondary maximum contaminant level
Hardness	Decrease the lather formation of soap, increase scale formation in hot-water heaters.
Iron	Impart a bitter astringent taste to water and brown color
Mercury	Cause acute and chronic toxicity Target the kidneys and can cause nervous system disorders
Organic contaminants	
Volatile organic compounds	Cause cancer and liver damage, anemia, gastrointestinal disorder, skin irritation, blurred vision, exhaustion, weight loss, damage to the nervous system, and respiratory tract irritation
Pesticides	Cause poisoning, headaches, dizziness, gastrointestinal disturbance, numbness, weakness, and cancer Destroy nervous system, thyroid, reproductive system, liver, and kidneys
Plasticizers	Cause cancer, damage nervous and reproductive systems, kidney, stomach, and liver
Physical characteristics	
Turbidity	Objectionable for aesthetic reasons May not adversely affect health but may cause need for additional treatment
Color	Suggests that treatment is needed, aesthetically unpleasing

1.3 Hypotheses

The hypotheses of this study were:

- The optimal conditions of electrode configuration and arrangement in Electrocoagulation process may enhance the treatment performance of turbidity and natural organic matter (NOM)
- Ion contaminations and operating conditions (initial pH and current density)

may effect on turbidity and natural organic matter removal in Electrocoagulation process

- Electrode material and operating conditions of Electrooxidation process could improve natural organic matter removal

1.4 Objectives

The objectives of this research were divided into three main categories:

1) To optimize the treatment conditions of Electrocoagulation process in terms of turbidity and natural organic matter removal
2) To evaluate the effect of ions (ferrous and calcium) and operating conditions (initial pH and current density) on Electrocoagulation performance in terms of turbidity and natural organic matter removal, and predict mathematical model by using statistical design of experiment (DOE) methodology
3) To analyze electrode material and operating condition on natural organic matter removal in Electrooxidation process

1.5 Scopes of study

This research was conducted in laboratory of Department of Environmental Engineering, Chulalongkorn University. The synthetic water which contained turbidity, ions (calcium and ferrous), and natural organic matter was represented for fresh water. Bentonite and Humic acid (HA) were used for creating turbidity and natural organic matters in water, respectively. The scopes of this study were summarized following:

- Analyze the synthetic water characteristics and conventional treatment process
- Optimize electrode configuration and arrangement in terms of gas flow rate and electrode loss ratio, and treatment performance.
- Analyze the treatment efficiency and kinetic of EC in terms of turbidity and NOM removal at different current densities.
- Investigate the effect of individual iron, hardness, pH, and current density on turbidity and NOM removal in EC process.
- Examine the effect and optimization of co-existing ions and operating conditions on turbidity and NOM removal. Predicted models were constructed by using second polynomial equation.

- Assess the electrode material, kinetic, and effect of chloride on NOM removal in EO process. Design criteria for turbidity and NOM removal in continuous reactor were proposed.

CHAPTER 2

THEORY AND LITERATURE REVIEW

2.1 Theoretical background

2.1.1 Source of drinking water in Cambodia

In Cambodia, water supply system was operated after civil war. The major activity was to provide safety water to the emergency area in the period between 1979 and 1994. This work was significantly achieved. The percentages of water source for drinking in Cambodia are shown in Table 2.1. and the source for dry season is shown in Figure 2.1. It shows that the sources of drinking water come tube well, dug well, surface water, pipe, bought water, and other. The highest fraction is ground water (53%). Then, surface water is also play an important role too. The total estimation volume of surface water such as Tonle Sap and Mekong river and groundwater are about 17.6 x 10^9 m^3.

Table 2.1. Source of drinking water supply in Cambodia (Ministry of Rural Development, 2002)

Source %	Cambodia	Phnom Penh	Other urban	Rural
Piped in dwelling	5.1	45.4	7.2	0.7
Public Tap	1.3	2.9	1.6	1.1
Tube/piped well of borehole	19.0	8.0	24.8	19.4
Protected dug well	22.1	6.4	18.1	24.2
Rainwater	0.7	-	2.0	0.6
Tanker, truck or otherwise bought	6.1	31.5	12.8	2.6
Subtotal for protected sources	54.3	94.2	66.5	48.6
Unprotected dug well	15.5	0.4	9.7	17.8
Pond, river or stream	28.3	5.0	22.3	31.5
Other	1.9	0.4	1.5	2.0
Subtotal for unprotected sources	45.7	5.8	33.5	51.4
Total	100	100	100	100
Number of households ($x10^3$)	2093	174	214	1705

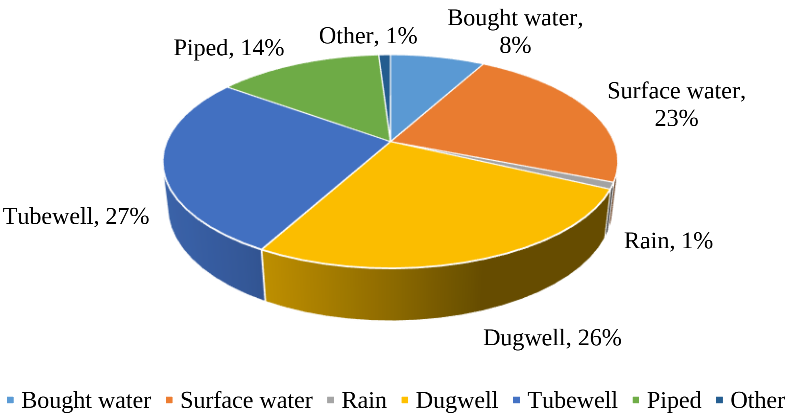

Figure 2.1. Cambodian drinking water source in dry season

Groundwater has been used for both rural area and some city for agriculture and daily consumption. According to USAID development program between 1960 to 1963, the depth of well in Cambodia was around 2 meters to 209 meters. Table 2.2 illustrated the contaminants in groundwater which was survey more than 5000 wells with 1.7 meters to 5.5 meters water depths.

Table 2.2. Groundwater data summarized from National Institute of Statistics (2008)

Parameter	Units	Sample	Mean	Max	Min	CDWQS[1]	Exceeding (%)
Health-impacting							
Arsenic	µg/L	8488	28.28	1000	0	50	12.49
Fluoride	mg/L	8484	0.68	110	0	1.5	4.21
Nitrate	mg/L as NO_3	8486	7.96	1361	0	50	3.09
Manganese	mg/L	8486	0.37	28	0	0.4[2]	19.48
Aesthetic impacting							
Iron	mg/L	8485	3.43	100	0	0.3	76.51
Manganese	mg/L	8486	0.37	28	0	0.1	40.45
Turbidity	NTU	8488	26.18	2960	0	5	46.55
Chloride	mg/L	8487	107.63	2303	0	250	20.42
pH		8482	6.72	9.95	0	6.5-8.5	29.5
Hardness	mg/L as $CaCO_3$	8488	202.92	3186	0	300	21.05
Salinity	ppt	8473	0.32	19	0	N/A	N/A

Note: [1] Cambodian drinking water quality standard (CDWQS)

[2] Manganese health standard of 0.4 mg/L from WHO

2.1.2 Natural organic matter

Organic substances contain compounds of carbon and hydrogen. The hydrocarbons could be formed only by a living organism called "organic". Nowadays, thousands types of organic compound has been artificial created by different purpose (Greeson, 1981).

The fractions of natural organic matter (NOM) contained in surface water or groundwater are hydrophobic, hydrophilic, carbohydrate, carboxylic acid, and amino acid. Around 49% comes from hydrophobic NOM which are the humic substance (Matilainen and Sillanpää, 2010). They are humic acid (HA) and fulvic acid. They have high functionalized carbon-rich polydisperse polyelectrolytes (Kac et al., 2017). NOM characteristic depends on the origins of water. It comes from the degradation of plant and animal, bacterial, algae (Särkkä, Vepsäläinen, et al., 2015). Natural organic matter

In Cambodia, organic matter (MO) could transport from surface water to groundwater around 44 meter (Lawson et al., 2016).

2.1.3 Turbidity

Turbidity is measured by the cloudiness of water. Generally, turbidity is measured by using light scatter. If there are many particle in water, the light scatter will be high. Therefore, the water has high turbidity.

The turbidity of the Tonle Sap Lake (Pursat site) is in the range of 30 to 50 NTU at 1.4 meter depth when the lake has flood. However, the turbidity increase in the range 150 to 300 NTU in range 1 meter depth to the surface of water. This high turbid water causes from natural organic matter which floats on the surface of water (Irvine et al., 2011).

2.1.4 Turbidity treatment

Many methods have been used to remove turbidity from water such as coagulation and filtration. Below is briefly summarized the technique to treat it.

a. Conventional coagulation

Jar test is a conventional method for turbidity removal. It is a valuable method in water treatment to evaluate the treatment efficiency of turbid water. Jar test was operated

Figure 2.2. Jar test flocculator

in batch mode with 6 impellers to determine the optimal coagulant dose necessary for treatment.

The mechanisms to remove turbidity are (Crittenden et al., 2012):

- Destabilization: the colloidal particle had negative charge and it was not able to settle down by gravity due to repulsion force. The positive coagulant could attach with colloidal particle to reduce repulsion force, so the pollutant started destabilizing in water.
- Flocculation: after destablization occurred, the flocs could be aggregated and able to settle down.
- Sedimentation: All flocs were settle down in sedimentation tank

The mechanisms of destabilization are:

- Electrical double layer (EDL) compression (Figure 2.3)
- Adsorption and Charge Neutralization: the characteristics of adsorption/neutralization are destabilization at lower concentration than indifferent electrolytes and adsorption occurs with the overdosing. Optimal dosage of coagulant is proportional to colloid concentration.—“stoichiometry of coagulation”.
- Inter-particle bridging: the polymer bridge could adsorb on the surface of particle. Therefore, it results in columbic (charge-charge) interactions, dipole interaction, hydrogen bonding, and Van de Waal force of attraction. The

Table 2.3. Chemical coagulants use in water treatment

Coagulants	Precipitates
$Al_2(SO_4)_3$	$Al(OH)_3$
$FeCl_3$	$Fe(OH)_3$
$MgCO_3$	$Mg(OH)_2$
CaO	$CaCO_3$

reaction mechanisms for polymers are shown in Figure 2.4.

- Precipitate and enmeshment: the metal salt such as $Al_2(SO_4)_3$ and $FeCl_3$ could forming the sweep floc and be able to remove by sedimentation. The chemical coagulant are shown in Table 2.3.

b. <u>Slow sand filtration</u>

Slow sand filtration (Figure 2.5) is a simple method for separating particle from water. The application of slow sand filters has been used in household across the globe. Slow send filtration remove turbidity through collision and attachment mechanism. The bacteria in sand filter could produce polymers which could help in turbidity removal. It does not employ chemical coagulants and commercially produced polymers. Traditionally, it was installed in 1 meter height and 1 meter of supernatant water. The diameter of filter varies from 0.15 to 0.35 millimeter (Logsdon et al., 2002).

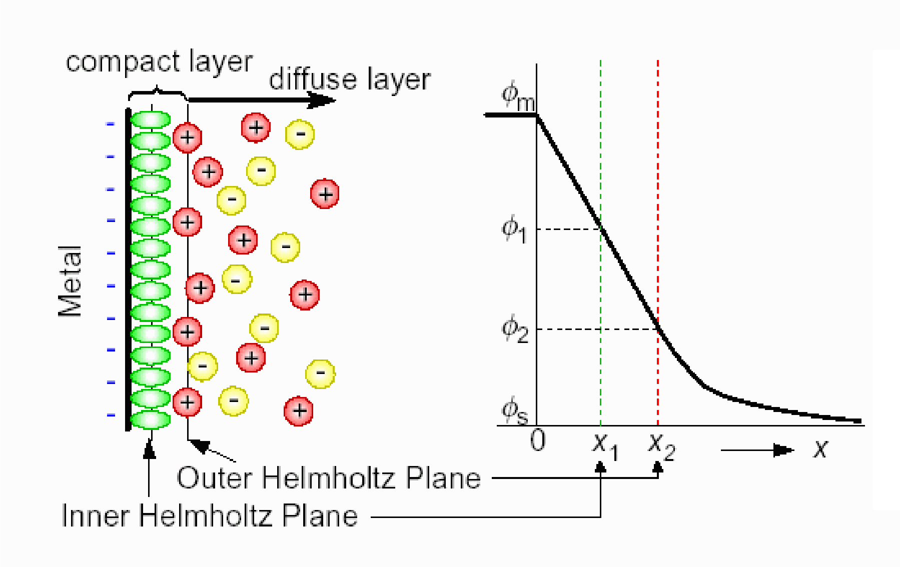

Figure 2.3. Electrical double layer, source:
<u>https://web.nmsu.edu/~snsm/classes/chem435/Lab14/double_layer.html</u>

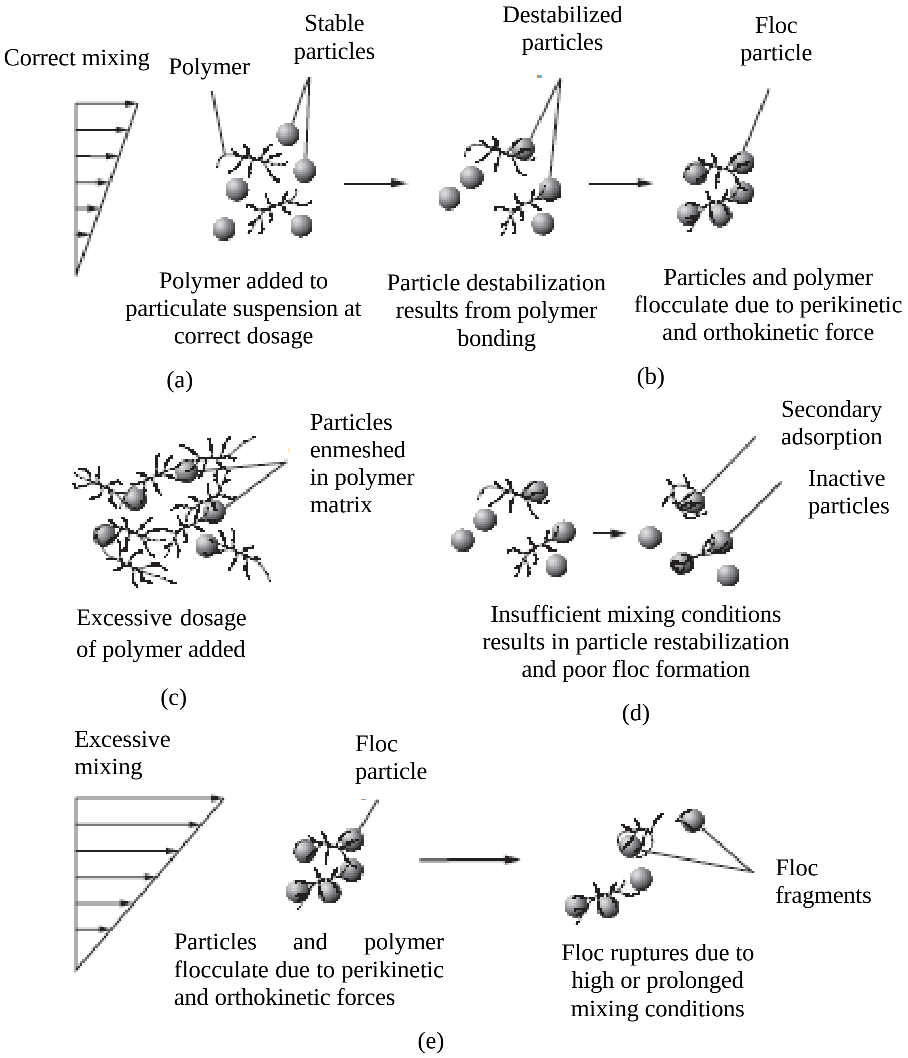

Figure 2.4. Schematic representation of the bridging model for the destabilization of particles by polymers (Crittenden et al., 2012)

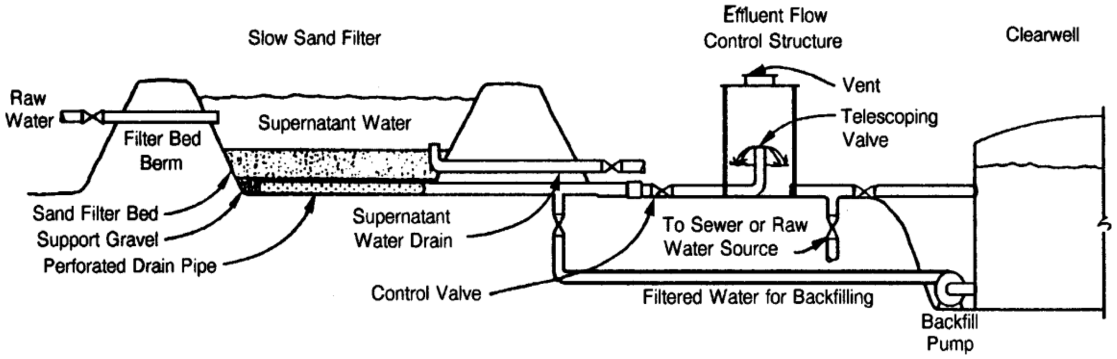

Figure 2.5. Open slow sand filter with effluent rate control (Water and Smith, 1990)

c. Pressure-driven membrane process

Membrane process is a modern technology for potable water treatment. It offers many benefits such as no chemical added, spend less time and easy operate, and small space operating. Membrane is used in order to remove particles, microorganism, and organic matter from water. There are many types of membrane being used (Zularisam et al., 2006):

- Reverse osmosis
- Nanofiltration
- Ultrafiltration
- Microfiltration

The important component of membrane is pressure-driven force. The pressure pulses the water go out through membrane filter as shown in Figure 2.6.

d. Electrocoagulation

Electrocoagulation (EC) is a complex process to remove pollutants from wastewater by using electricity to generate the coagulant. The mechanism of pollutant removal in EC process are in three steps (Mollah et al., 2004):

- Coagulant generation from electrode
- Destabilization
- Floc formation

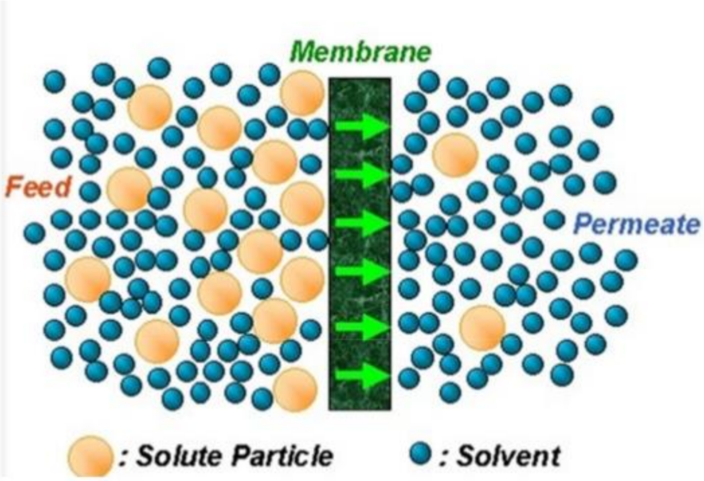

Figure 2.6. Membrane separation, source:
https://www.slideshare.net/Khawwam/lecture12-membrane-filtration

e. Summary of turbidity removal method

The summary of method for turbidity removal was shown in Table 2.4 Among these methods, Electrocoagulation is a good technique to remove turbidity from water since it can remove turbidity effectively, less sludge and environmental friendly. Therefore, Electrocoagulation was studied in this research.

2.1.5 Natural organic compound treatment

Since NOM has many disadvantages to the health, there are several methods have been proposed to treat it such as enhanced coagulation, electrooxidation, adsorption, membrane filtration, and advanced oxidation process. The briefly detail of each method was shown below:

a. Enhanced coagulation

In water treatment, coagulation was employed to treat the turbidity from the water. However, the reduction of turbidity did not reduce the amount of NOM in water. Thus, a suitable condition is needed to remove NOM through coagulation process called Enhanced coagulation. Enhanced coagulation uses effective coagulant dosage and optimized pH to remove TOC or minimized DOC residual after coagulation (Singer and Bilyk, 2002; Volk et al., 2002; Xie et al., 2012). Optimizing coagulant dosage is essential to avoid coagulant overdosing which affect the increasing of sludge and pH reduction. Meanwhile residual metal remained in treated water under-dosing. Total organic carbon is the important parameter to determine the coagulation dosage required.

Table 2.4. Summary methods for removing turbidity from raw water

Methods	Advantages	Disadvantages
Conventional treatment	High efficiency Simply treatment	Secondary pollutants (sludge)
Slow sand filtration	Convenient in setting up and use in rural area Low cost	Low efficiency Long time treatment Clogging
Membrane filtration	High efficiency	High cost of treatment Membrane fouling
Electrocoagulation	High efficiency Environmental friendly	Energy cost consumption Electrode corrosive

The efficiency of coagulation process is not dependent only pH, coagulant dosage and. types, but also others factor such as NOM characteristics and presence of divalent cations. However, the negative aspects of enhanced coagulation are the production of high levels of dissolved aluminum (coagulant) in settle water, production of very corrosive water for metals and concrete, more sludge than conventional treatment

b. Advanced oxidation process (AOPs)

Advanced oxidation process is the aqueous phase oxidation method to remove the target pollutants through intermediacy of highly reactive species such as hydroxyl (-OH) radical (Comninellis et al., 2008). OH radical is used to oxidize NOM as DBPs precursor by eliminating hydrogen atoms or adding electrophiles to their double bonds in NOM and DBPs cases. At the beginning of the mechanism, OH radicals received an electron from organic materials. Then, the process proceeded as carbon-centered radicals react with oxygen rapidly to form peroxyl radicals. This radical produced ketones, aldehydes and/ or CO_2 while it reacts among themselves (Lamsal et al., 2011).

c. River Bank/ Bed Filtration (RBF) system

Riverbank filtration is a water treatment technology to remove NOM from the water by extracting water from the river using pumping well in the adjacent alluvial aquifers (Jaramillo, 2012). The components of RBF consist of deposits of sand, gravel, large cobbles, and boulders. However, the ideal condition usually includes coarse-grained, permeable water-bearing deposits that hydraulically connects with riverbed materials

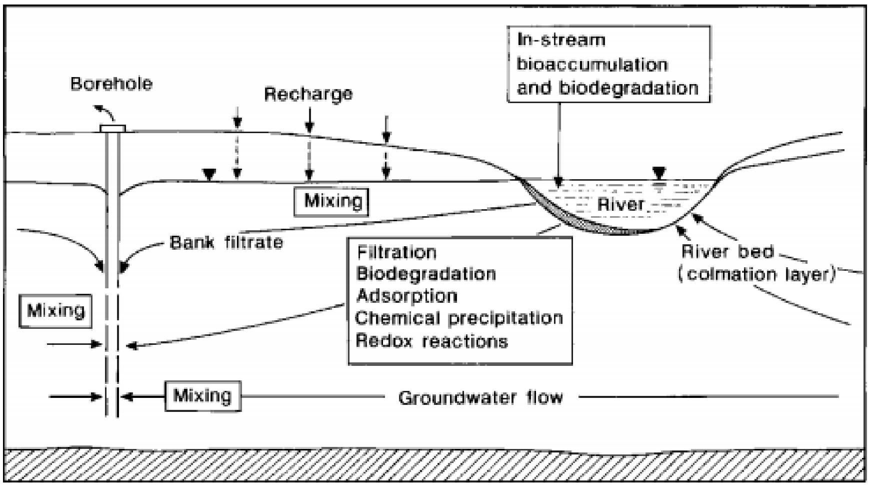

Figure 2.7. Riverbank filtration system

(Ray et al., 2003). The pollutant was treated by physical, chemical, and biological processes that take place, between the surface water and groundwater, and the substrate. The main processes in RBF in pollutant reduction are dispersion, physical filtration, biodegradation, ion exchange, dilution, and adsorption (Worch et al., 2002). The factors that make the treatment successfully are river water and groundwater quality, water residence time, porosity of the medium, temperature and pH conditions, oxygen concentration in the aquifer (Kuehn and Mueller, 2000).

d. Electrooxidation

Electrooxidation (EO) has been used in disinfection of various drinking water and wastewater. It can disinfect Escherichia coli in drinking water (Jeong et al., 2007). The main mechanism of EO is inactivation of bacteria by hydroxyl radicals produced by water discharge, and also involving direct oxidation at the electrode surface. EO can oxidize pollutants through direct oxidation and indirect oxidation.

EO has shown promising results in wastewater remediation for organic pollutants and disinfection of drinking water, it has its drawbacks. Disinfection by-products such as perchlorates and bromates can be produced during treatment. Thus, the concentration of chloride is important in EO process.

e. Summary of methods for NOM removal

NOM has been treated by different methods. Most researchers have been improved the technology to remove it from drinking water due to disadvantages. However, each method has its own advantages and disadvantage as shown in Table 2.5. Different country, area, and season need different methods for treating NOM. Based on table Table 2.5, it can figure out that EO is the best technic to remove NOM from wastewater.

2.1.6 Electrocoagulation (EC)

Electrocoagulation (EC) technology has been proposed in 1909 using aluminum and iron electrode in the USA. Since there is not required any chemical reagents and less sludge produced, electrocoagulation was wildly used in large scale for reducing contaminants in water for drinking purposes in 1946 (Sahu et al., 2014b). With this technology, three mechanisms are occurred—coagulation, flotation, and oxidation. The

Table 2.5. Summary advantages and disadvantages of methods for NOM removal

Treatment Method	Advantages	Disadvantages
Enhanced Coagulation	Hydrophobic NOM removal	Residual hydrophilic NOM and high coagulant consumption
Advanced Oxidation Process (AOPs)	Materialize/ Oxidize high molecular mass components of NOM to low molecular mass	Increase low molecular mass components, Not suitable for high alkalinity water, Incomplete oxidation may increase disinfection by-products formation, and High cost
River Bank Filtration (RBF)	Remove most of biodegradable materials	Residual hydrophilic NOM
Electro-oxidation	No additional chemical consumption and environmental friendly	Energy consumption, electrode corrosive, and high cost of electrode

metal cations are produced on the anion electrodes via electrolysis and these ions form various hydroxides in the water. In addition to this main reaction, several side reactions, such as hydrogen bubble formation and the reduction of metals on cathodes, also take place in the cell. Electrocoagulation is used for the treatment of aqueous wastewater containing heavy metals and metal trace elements (MTE) such as fluorine, arsenic, nickel as well as chromium (VI) as well as surface waters (Bejjany et al., 2017b).

a. Definition of electrocoagulation

The electrocoagulation (EC) process is an alternative technique by applying current density to treat contaminants or pollutants from water and wastewater (Erick Butler et al., 2011). EC is an interaction of EC, EO, and EF which have been shown in Figure 2.8. Generally, electrocoagulation is a technology based on the concepts of electrochemical cells, specifically called ‘‘electrolytic cells’’. In an electrolytic process, electrolyte is a liquid that serves a pair of immersed electrodes connecting to a source of direct current. The general electrolytic reactions describe about the system of electrochemical behavior. The basis of electrocoagulation is treat various pollutants from the water and wastewater by the formation of a coagulant species. The three main mechanism of main mechanisms (M. M Emamjomeh and M Sivakumar, 2009) are:

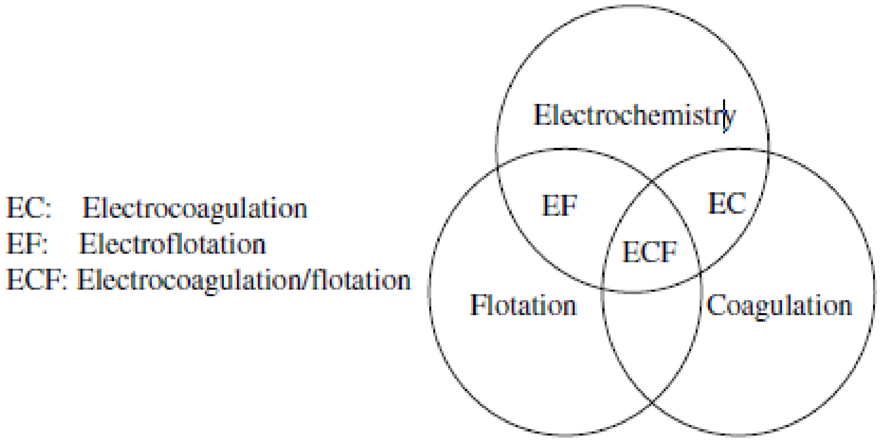

Figure 2.8. Interaction occurring within EC process (M. M. Emamjomeh and M. Sivakumar, 2009)

- Electrode oxidation
- Gas bubble generation
- Flotation and sedimentation of flocculation formed

b. <u>Electrocoagulation mechanism</u>

Electrochemical or electrocoagulation/flotation process has gained a great attention for removal of various pollutants and organic matters due to its simplicity. The mechanisms of treatment in EC process consist of oxidation, reduction, coagulation, decomposition, deposition, adsorption, absorption, flotation, and precipitation as shown in Figure 2.9. In EC, the main pairs of metal sheets in reactor tank called sacrificial electrodes (anodes and cathodes). The anode electrode (usually aluminum or iron) dissolve to produce metallic ions into solution and hydrogen gas is released at the cathode when a direct current. Then, the metal hydroxides were produced from the reaction of metallic ions and hydroxides. This metal hydroxides can adsorb and settle pollutants (Derayat et al., 2015; Motlagh, 2015). If in this process M is considered as metal anode, the following reactions will occur:

In anode:

$M_{(s)} \rightarrow M_{(aq)}^{n+} + n\ e^-$ eq. 2.1

$2H_2O + 2\ e^- \rightarrow 4H_2O + O_{2(g)} + 4\ e^-$ eq. 2.2

In cathode:

$M_{(aq)}^{n+} + n\ e^- \rightarrow M_{(s)}$ eq. 2.3

$2H_2O + 2\ e^- \rightarrow H_{2(g)} + 2OH^-$ eq. 2.4

If iron and aluminum electrodes are used, Fe^{3+} and Al^{3+} are produced. These metal ions after reaction with hydroxyl ions will produce metal hydroxides or poly-hydroxides. For example, aluminum produces in water are $Al(H_2O)_6^{3+}$, $Al(H_2O)_5OH^{2+}$, $Al(H_2O)_4OH^{1+}$ or monomer or polymer strains of Al $(OH)^{2+}$, $Al_2(OH)^{24+}$, $Al_6(OH)^{153+}$, $Al_{13}(OH)_3^{45+}$. These compounds increase the elimination efficiency. The final compound of the eliminated matter by this process depends on parameters such as electrode type and electrode shape.

EC is a technique involving the electrolytic addition of coagulating metal ions directly from sacrificial electrodes. These ions destabilize suspended, emulsified, or dissolved contaminants in an aqueous medium, similar to the addition of coagulating chemicals such as alum or ferric chloride, which allow the pollutants removal easily by sedimentation and flotation. This process includes a cell metal anode and uses direct electrical current. The electrocoagulation (EC) process has three stages (Malakootian and Yousefi, 2009b):

- Forming coagulants from the electrical oxidation of sacrificial anode
- Destabilizing pollutants, suspended solids, and emulsion breaking
- Combining unstable particles to form flocculation. Destabilization mechanisms in this process include electrical double-layer compression, adsorption and charge neutralization, enmeshment in a precipitate and inter-particle bridging.

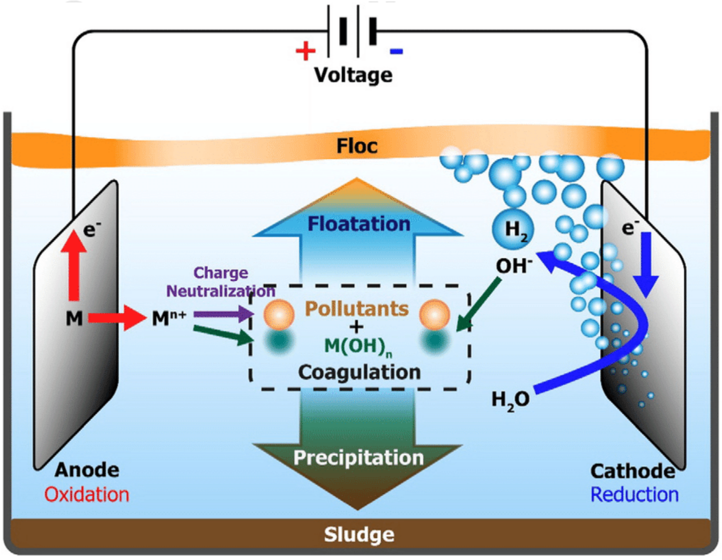

Figure 2.9. The mechanism of electrocoagulation (An et al., 2017)

c. Bubble production rate

In EC, the bubble of hydrogen and oxygen are produced when the current pass. The production rate of hydrogen gas bubble generation is (Sarkar et al., 2011):

$$Q_G = f \times \frac{IRT}{zFP} \qquad \text{eq. 2.5}$$

Where, Q_G: gas flowrate
F: Faraday's constant
T: temperature
P: pressure of the system
I: absolute current
z: number of electrons required to produce 1 mol of gas (for hydrogen z=2)
R: gas constant
f: the fraction of the total produced hydrogen that enters the bubbles, while the remaining portion (1-f) remains dissolved in the bulk solution. The value of f varies between zero (for no bubbles) and one (all of the gas is used to form bubbles).

For a given bubble diameter, d_b, the rate of bubbles generated per second, N_b, is given by:

$$N_b = \frac{Q_G}{V_b} = Q_G \Big/ \left(\pi d_b^3 \big/ 6 \right) \qquad \text{eq. 2.6}$$

d. Parameters of EC

Electrocoagulation process has many parameters affecting to its process (Sahu et al., 2014a). The important parameters of Electrocoagulation process are current density, time, electrode material, electrode spacing and arrangement, pH, and conductivity.

- *Current density and time*

In all the electrocoagulation process, current density is the most important parameter in controlling the reaction rate. Current density is the ratio of current to the active area of electrode. Rising current density can increase the removal efficiency of chemical oxygen demand, biochemical oxygen demand, suspended solid (Nasrullah et al., 2014). Current density directly determines the bubble generation rates, coagulant, and also influences to mass transfer and solution mixing at the electrodes. Electrolysis time also affects the treatment efficiency of the electrochemical process. A relationship between electrolytic solution, time, and current have been shown by Faraday's law:

$$w=itM/eF \qquad \text{eq. 2.7}$$

Where w: amount of electrode material dissolved (in grams of M per square centimeter)

i: current (A)

t: time (s)

M: molecular weight of metals (g/mol)

e: number of electrons

F: Faraday's constant (96500 C/mol)

Literature sources report a wide range of current densities applied between 1 to

100 mA/cm^2 depending on the case study (Kabdaşlı et al., 2012). However, the current density is suggested to be in the range of 20-25 A/m^2 for preventing the maintenance when EC operates in long time. The current efficiency is the proportion of current consumed in producing a target product and the total current consumed.

- *Electrode material*

Electrode type is one of the important parameters to get the maximum efficiency of EC and performance of the electrochemical reactor. The anode type influences not only the cation introduced in the bulk solution but also the current efficiency (CE). The electrode materials have been used in EC including Al, Ag, As, Ba, Ca, Cd, Cr, Cs, Fe, Mg, Na, Si, Sr, and Zn. In general, polyvalent metal electrodes (aluminum or iron) gain more benefits than monovalent metal electrodes due to the coagulating properties of multivalent ions. They can deal with the combined task of electrocoagulation and electroflotation as they are anodically soluble. The dimensionally stable anodes such as SnO_2, PbO_2, graphite, nickel, etc., and boron-doped diamond (BDD) electrodes have the advantages of chemical resistance and high efficiency in the treatment of cyanide-bearing wastewaters. Materials that show a poor current efficiency, for instance graphite, PbO_2, Al, etc., also give a lower treatment efficiency.

- *Electrode gap*

The electrode gap (Figure 2.10) is also one of the important parameters in EC. The effect of electrode gap is defined as following:

- Effect the reactions in the electrolysis reactor: During electrolysis, the concentration of the solution at the cathode is more concentrated due to the different mobility of the ions present in the wastewater; however, it can be reduced by agitation of the bulk solution.
- Increases electrical resistance when the inter-electrode gap filled partially with gas during electrolysis. The vertical electrodes can improve circulation because of the gas lift. Corrugated and perforated electrodes also can release more electrolytic gases than others type.
- Save energy consumption significantly when the inter-electrode gap in the electrocoagulation reactor (ECR) is small. Narrower gaps improve mass transfer characteristics and decrease Ohmic loss. When a product gas is present, a decreasing in gap results in an increased electrolyte resistance.

➢ Arrangement of electrode

The electrode can be arranged in several types of EC system such as series or parallel arrangement and the direction of flow in electrode can be vertical or horizontal. However, the electrode can be monopolar or bipolar as shown in Figure 2.8. In monopolar system, all anodes and cathodes are connected to the power source, so each anode had positive charge while cathode had negative charge. For bipolar system, the

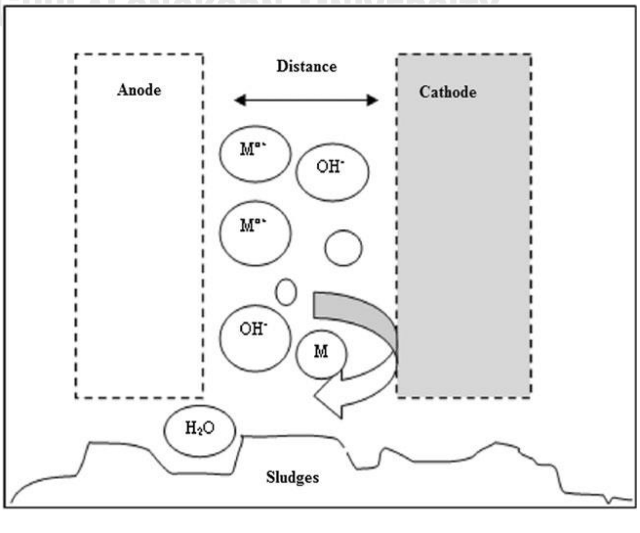

Figure 2.10. Distance between two electrodes (E. Butler et al., 2011)

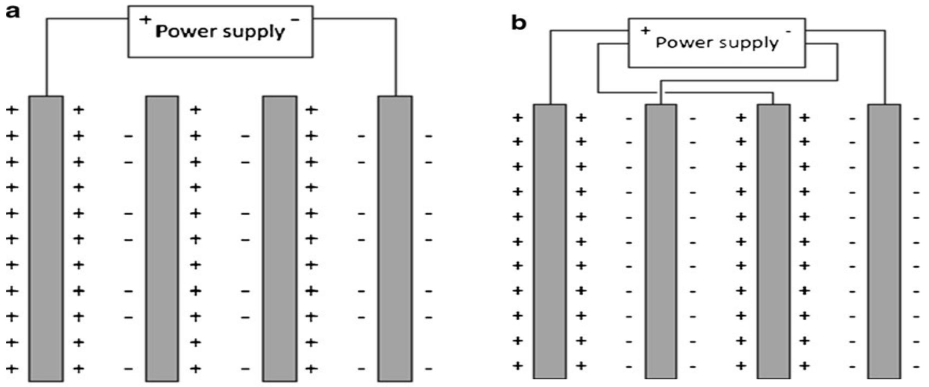

Figure 2.11. Bipolar (a) and Monopolar (b) arrangements of electrodes in electrochemical reactor (Sahu et al., 2014a)

outermost electrodes (anode and cathode) are connected to the power source and the inner electrodes do not get the current from the source directly but they are passed by current from the outermost electrode, thus polarizing them. The side of the electrode facing the anode is negatively polarized and opposite side is positive.

If U is the cell voltage (V) and I is the cell current, so the equation of voltage and current for parallel and series connection are shown below (Jiang et al., 2002):

In parallel connection:

$$U = U_i \qquad \text{eq. 2.8} \qquad \text{and} \qquad I = \sum_{i=1}^{n} I_i \qquad \text{eq. 2.9}$$

In series connection:

$$U = \sum_{i=1}^{n} U_i \qquad \text{eq. 2.10} \qquad \text{and} \qquad I = I_i \qquad \text{eq. 2.11}$$

- *Effects of conductivity and pH*

The conductivity of the solution has a great effect to the cell voltage. The greater ionic strength causes an increase in current density in the same cell voltage, or the cell voltage decreases with increasing effluent conductivity at constant current density.

pH affects to the conductivity of the solution, speciation of hydroxides, dissolution of the electrodes and zeta-potential of colloidal particles according to the radical of the metal ions dissolved from electrodes. Aluminum, iron, and hydroxides cause destabilization of colloids, effective coagulant species are formed in acidic, neutral, and slightly alkaline pH. In highly alkaline pH, $Al(OH)_4^-$ and $Fe(OH)_4^-$ ions are formed, and they have poor coagulation performance. At acidic pH, the dissolution of the iron electrodes is found significantly even without electrical current. However, the oxidation of Fe(II) to Fe(III) occurs only at pH above 5. In water, a primary hydration shell happens when all metal cations are in direct contact with water molecule surrounding, and secondary hydration shell is when more loosely held water. One of the primary hydration shells is aluminum ions Al^{3+} which consists of six water in octahedral coordination ($Al(H_2O)_6^{3+}$) (Duan and Gregory, 2003). The water molecule can be polarized and lost one or more protons when metal ion owes to high charge as shown in Figure 2.12. This mechanism depends on the solution pH. The losing molecule of water is replaced by hydroxyl ions, giving a lower positive charge according to omitting co-ordinated water molecules for convenience as express in $Me^{3+} \rightarrow Me(OH)^{2+} \rightarrow Me(OH)_2^{+} \rightarrow Me(OH)_3 \rightarrow Me(OH)_4^{-}$ eq. *2.12.*

$$Me^{3+} \rightarrow Me(OH)^{2+} \rightarrow Me(OH)_2^{+} \rightarrow Me(OH)_3 \rightarrow Me(OH)_4^{-} \qquad \text{eq. 2.12}$$

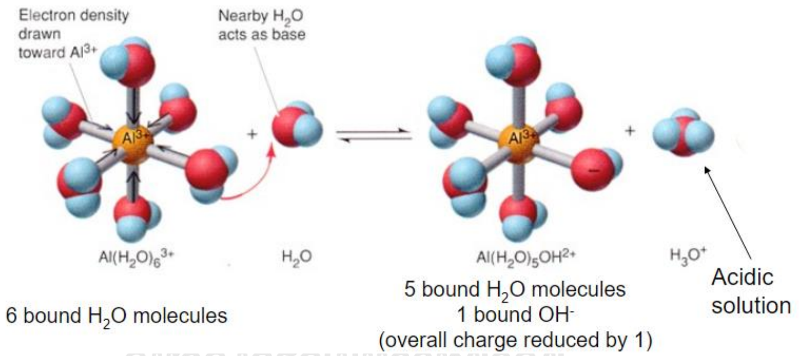

Figure 2.12. The hydrated metal ion transfer H+ to water (Silberberg, 2006)

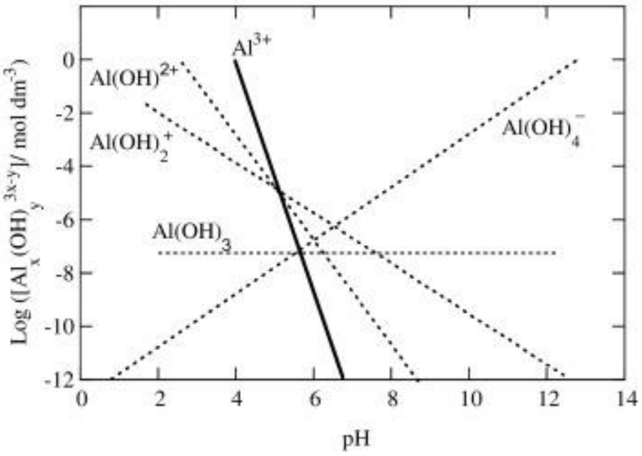

Figure 2.13. Predominance-zone diagram for aluminum species in aqueous solution in function of pH

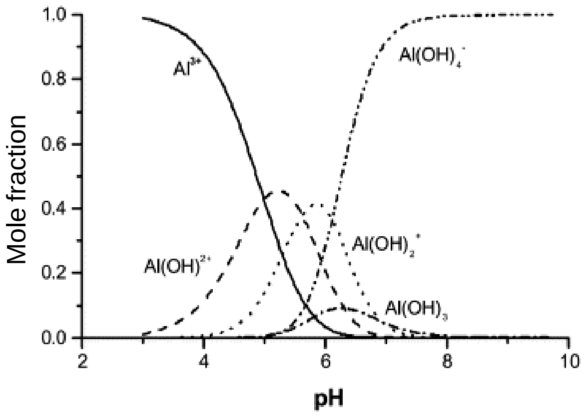

Figure 2.14. Proportions (mole fractions) of dissolved hydrolysis products in equilibrium with amorphous hydroxides (Duan and Gregory, 2003)

Predominance-zone diagram for aluminum species in aqueous solution in function of pH is shown in Figure 2.13. This is the amorphous hydroxide precipitate with various species concentration in equilibrium. The solubility of the metal is effectively when the total amount of soluble species is in equilibrium with the amorphous solid and minimum solubility at a certain pH in each case. The solubility of Al is at 1 µM when pH is approximately 6. The latter are spaced over pH 8. Al deprotonations are squeezed into less than 1 unit interval. The Proportions (mole fractions) of dissolved hydrolysis products in equilibrium with amorphous hydroxides is shown in Figure 2.14.

2.1.7 Effect of ions on EC

a. Effect of Chloride

Chloride is the main parameter that affects the EC performance. The presence of chloride ions could attribute to EC through three main reasons (Gao et al., 2010).

- Increase electrical conductivity: Chloride ions can increase the electrical conductivity of the water. Therefore, it can reduce energy consumption in EC process.
- Breakdown of insulating film on electrode: Chloride ions can be able to promote the breakdown of the insulating film through pitting corrosion when aluminum electrodes are used in EC. Aluminum electrodes often form an insulating film of alumina (Al_2O_3) on the electrode surface which affects the treatment efficiency and increases the electrical consumption.
- Indirect oxidation: chloride contained in water can lead to the formation of

active chlorine species such as chlorine, hypochlorous acid, and/ or hypochlorite on the electrode surface and in the bulk solution as shown in the equation below. These species might improve the treatment efficiency through oxidation.

$$2Cl^{-} \rightarrow Cl_2 + 2e^{-} \qquad \text{eq. 2.13}$$

$$Cl_2 + H_2O \rightarrow HOCl + H^{+}Cl^{-} \qquad \text{eq. 2.14}$$

$$HOCl \rightarrow H^{+} + OCl^{-} \qquad \text{eq. 2.15}$$

b. Effect of heavy metal

Heavy metals contained in water are generally effect to the treatment performance of EC process. Heavy metals are removed by EC through two mechanisms: (i) surface complexation and (ii) electrostatic attraction where insoluble flocs of coagulant metal hydroxide are produced independently (Daneshvar et al., 2006). In addition, other mechanisms are also possible to happen such as (iii) adsorption and (iv) direct precipitation by the formation of the pollutant metal hydroxides. The complexation mechanism (i) happens when heavy metal can act as a ligand. This complexation form bonds to the hydrous moiety of coagulant floc $Al(OH)_3$ resulting a surface complex which forms superior aggregates and coagulant precipitate. The pollutant therefore removed from aqueous phase. Heavy metal is removed through electrostatic attraction (ii) of coagulant floc. The negative charge area of coagulant attracts the heavy metal allowing their coagulant precipitate. Additionally, the (iii) adsorption can remove pollutant by the large surface areas of amorphous coagulant flocs which is able to adsorb the soluble ions or trap insoluble colloid. Furthermore, electrochemical reduction in EC also separates the heavy metal from solution by attached these species on the cathode surface which decrease the pollutant.

For iron contaminated in groundwater usually is in 2 valence state. When there is absence of oxygen, iron in solution exists in the ferrous state, and generally, when the pH is below 6.5, ferrous ion is oxidized in air according to the following reaction (D. Ghosh et al., 2008). The oxidation of ferrous is expressed in eq. 2016

$$Fe^{2+} + \tfrac{1}{4}O_2 + H^{+} \rightarrow Fe^{3+} + \tfrac{1}{2}H_2O \qquad \text{eq. 2.16}$$

Presence of chloride ion may undergo the following reactions:

- Bulk

$H_2O \leftrightarrow H^+ + OH^-$ eq. 2.17

$NaCl \leftrightarrow Na^+ + Cl^-$ eq. 2.18

$Fe^{2+} + 2Cl^- \leftrightarrow FeCl_2$ eq. 2.19

$FeCl_2 + 3OH^- \leftrightarrow Fe(OH)_3^- + 2Cl^-$ eq. 2.20

$H^+ + Cl^- \leftrightarrow HCl$ eq. 2.21

- Anode

$2Cl^- \leftrightarrow Cl_2\uparrow + 2e^-$ eq. 2.22

The reactions of iron in above equation depend on the redox potential and pH. When the pH increases, dissolved Fe(II) or Fe(III) hydrolyzes form precipitates. Between pH 7 and 14, ferrous ion hydrolyzes produce the array of mononuclear species $Fe(OH)^+$ to $Fe(OH)_4^{-2}$. The ferrous (III) is more ready than the ferrous ion (II). Ferrous ions can oxidize in a few minutes and about 90% conversion may be achieved by air increase with pH 7. The form of precipitation depends on the shape and size of the particle after coagulation happens by the adsorption on the active surfaces of the coagulants formed during the EC process. At higher pH, iron can remove by adsorption of iron hydroxide in the form of brown flocks due to the sufficient availability of coagulants. Thus, the forms of precipitation are large in size and settled down after finishing experiment. According to the factors as mention above, aluminum is selected electrode for the present day.

c. Hardness removal

In high acidity condition, the reactions below may occur in cathode (Malakootian and Yousefi, 2009b):

$HCO_3 + OH^- \rightarrow CO_3^{2-} + H_2O$ eq. 2.23

$CO_3^{2-} + Ca^{2+} \rightarrow CaCO_3$ eq. 2.24

$CO_3^{2-} + Mg^{2+} \rightarrow MgCO_3$ eq. 2.25

Through these reactions, calcium carbonate and magnesium carbonate are settle down at the cathode side.

2.1.8 Electrooxidation (EO)

a. Mechanism

Electrooxidation (EO) can fulfil either by direct oxidation on anode's surface or indirect oxidation (Anglada et al., 2009) as shown in Figure 2.15 and Figure 2.16.

- *Direct electro-oxidation process*

The oxidation of pollutants can be occurred directly on anodes by generating physically adsorbed "active oxygen"(oxygen in the oxide lattice, MO_{x+1}). This process is called anodic or direct oxidation. Anodic oxidation does not generate secondary pollutant or require complicated accessories since it does not require added chemical or oxygen. The important element in EO process is the anodic material.

The mechanism of direct oxidation of pollutants HA two main steps:

1) The pollutants diffuse from the bulk solution to the anode surface
2) Pollutants oxidize at the anode surface

At the electrode surface, the relationship between mass transfer of the substrate and electron transfer is really important. The rate of electron transfer is determined by the electrode activity and current density. During anodic oxidation of organic pollutants, two different ways were happened:

- Electrochemical conversion: Organic compounds are only partially oxidized. Therefore, a subsequent treatment may be required.

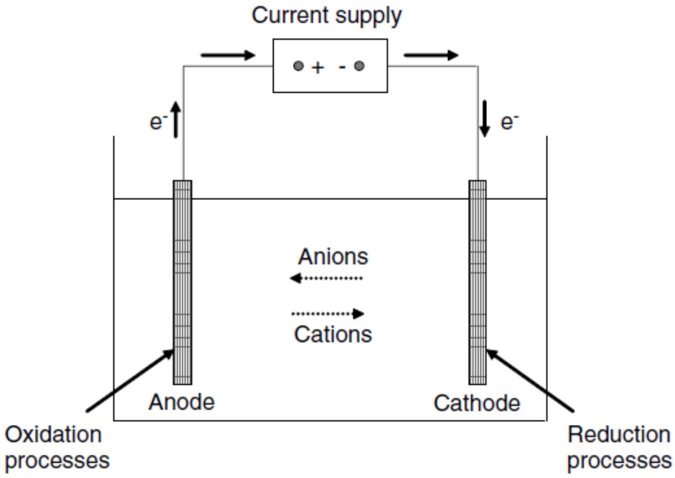

Figure 2.15. Conceptual diagram of electrochemical reactor (Anglada et al., 2009)

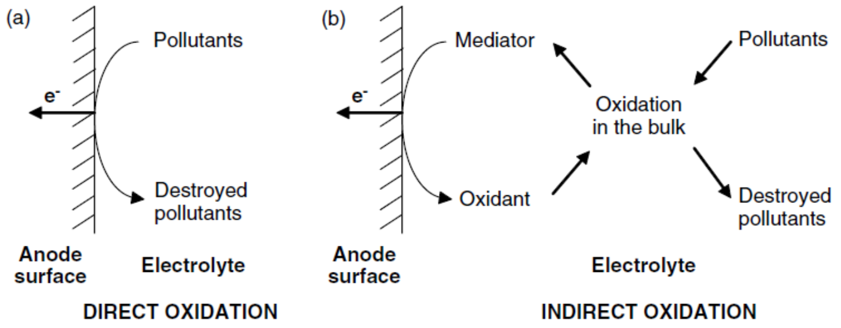

Figure 2.16. Mechanism of direct and indirect EO (Anglada et al., 2009)

$R \rightarrow RO + e^-$ eq. 2.26

- Electrochemical combustion: Organic compounds are transformed into water, carbon dioxide and other inorganic components.

$R \rightarrow CO_2 + H_2O + salts + e^-$ eq. 2.27

➢ *Indirect electro-oxidation process*

The organic pollutants can be destroyed by chlorine, hypochlorous acid and hypochlorite or hydrogen peroxide/ozone formed at electrode (Särkkä, Bhatnagar, et al., 2015). The contaminants can be degraded by electrochemically generated hydrogen peroxide. Sometimes, ammonia oxidation is taken place through this mechanism.

$2Cl^- \rightarrow Cl_2 + 2e^-$ eq. 2.28

$Cl_2 + H_2O \rightarrow HOCl + H^+ + Cl^-$ eq. 2.29

$HOCl \rightarrow H^+ + OCl^-$ eq. 2.30

$H_2O \rightarrow OH^- + H^+ + e^-$ eq. 2.31

$2OH^- \rightarrow H_2O_2$ eq. 2.32

$H_2O_2 \rightarrow O_2 + 2H^+ + 2e^-$ eq. 2.33

$O_2 + O \rightarrow O_3$ eq. 2.34

In indirect oxidation, active chlorine species from chloride ions anodically destroy pollutant. Sometimes, the metal ions are oxidized on an anode from a stable state to a reactive high valence state which in turn attack pollutants directly and may also produce hydroxyl free radicals to promote degradation. It is called mediated electro-oxidation.

b. Electrooxidation material

The choice of electrode material is very important in EO process. Traditionally, the anode electrode makes from lead and lead dioxide, dimensionally stable anode (DSA), graphite, and boron-doped diamond (BDD) (Särkkä, Bhatnagar, et al., 2015). The electrode material must have the following properties:

- High electrical conductivity
- High physical (resistance to erosion) and chemical stability
- Low cost/ life ration
- Catalytic activity and selectivity

In order to select the electrode material, the competition between the oxidation of organics at the anode and the side reaction of oxygen evolution must be considered.

$$2H_2O \rightarrow O_2 + 4H^+ + 4e^- \qquad \text{eq. 2.35}$$

At approximately 1.2 V, the oxidation of water to oxygen occurs versus normal hydrogen electrode (NHE). The potential of oxygen evolution of different anode, V versus normal hydrogen electrode are shown in Table 2.6. The advantages and disadvantage of these electrode materials are shown in Table 2.7.

2.1.9 Chemical reactor

Chemical reactions mostly exist everywhere in the environment and chemical reactor is a device to let chemical reaction happen under controlled conditions for specified products. The derived mathematical models are employed to consider the quality of mixing and mode of operation in order to understand the reaction. This ideal reactions

Table 2.6. Potential of oxygen evolution of different anodes, V versus NHE (Anglada et al., 2009)

Anode	Potential (V)	Conditions
Pt	1.3	0.5 mol L^{-1} H_2SO_4
Pt	1.6	0.5 mol L^{-1} H_2SO_4
IrO2	1.6	0.5 mol L^{-1} H_2SO_4
Graphite	1.7	0.5 mol L^{-1} H_2SO_4
PbO_2	1.9	1 mol L^{-1} H_2SO_4
SnO_2	1.9	0.5 mol L^{-1} H_2SO_4
TiO_2	2.2	1 mol L^{-1} H_2SO_4
Si/BDD	2.3	0.5 mol L^{-1} H_2SO_4
Ti/BDD	2.7	0.5 mol L^{-1} H_2SO_4

Table 2.7. Comparison of electrode performance in EO process (Särkkä, Bhatnagar, et al., 2015)

Electrode	Advantages	Disadvantages
Ti	Stable	Passive, expensive
Pt	Inert, low oxygen. evolution over potential	Expensive
PbO_2	Good current efficiency, cheap, effective in oxidizing pollutants, high oxygen evolution over potential, easy to prepare	Corrosive, toxic Pb^{2+}-ions could be released
DSA electrodes	Supports indirect oxidation, good current efficiency, high oxygen, evolution over potential, lower cost, higher availability	Short lifespan, lack of electrochemical stability
BDD	Inert under tough conditions, high oxygen evolution overpotential and electrochemical stability, good current efficiency, high corrosion stability, good conductivity	Very expensive

are simplified models for the real reaction. They can be classified according to the mode of operation such as discontinuous versus continuous, and quality of mixing such as perfect mixing versus no mixing. The three resulting ideal reactors are (Caccavale et al., 2011):

- Batch reactor (BR)
- Continuous stirred tank reactor (CSTR)
- Plug flow reactor (PFR)

Batch reactor is a discontinuous stirred reactor corresponding a closed thermodynamic system, whereas Plug flow and continuous stirred tank reactor are the continue reactors and open systems.

a. <u>The rate of chemical reactions</u>

The chemical reaction rate is the speed that chemical process. The quantities of reactants and products could be determined by using stoichiometry of mass conservation of single elements. The reaction rate (R) of conversion A and B can be written by using equation 2.36.

$$A + B \rightarrow \text{products} \qquad \text{eq. 2.36}$$

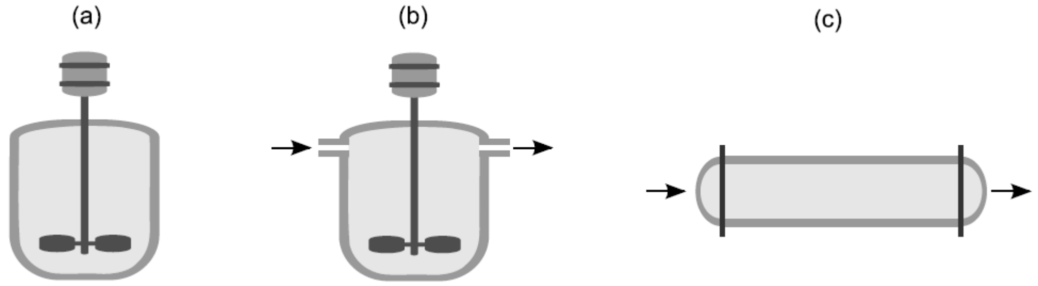

Figure 2.17. Ideal reactors: (a) Batch reactor, (b) Continuous stirred tank reactor (CSTR), and (C) Plug flow reactor

Can be expressed as

$$R=k_c\left(T_r\right)C_A^{nA}C_B^{nB}=k_0\exp\left(-\frac{E_a}{RT_r}\right)C_A^{nA}C_B^{nB} \qquad \text{eq. 2.37}$$

Where C_A and C_B are the molar concentrations of reactants, n_A and n_B are the orders of reaction ($n=n_A + n_B$ being the overall reaction order), k_c (T_r) is the rate constant, k_0 is the preexponential factor, E_a is the activation energy, R is the universal gas constant, and T_r is the absolute reaction temperature. The simple reaction orders are explained by the frequency of collision of two molecules namely the schemes where third body stands for any molecule with constant concentration. However, any collision involves more than two molecules must be neglected.

b. The ideal batch reactor

The ideal batch reactor is analyzed by means of mathematical modeling that consists of mass and energy balances. They provide a set of ordinary differential equation that in most cases, have to be solved numerically. However, analytical integration is still possible in isothermal systems and with reference to simple reaction schemes and rate expressions. Therefore, when basic kinetic schemes are considered, some general assessments of the reactor behavior can be formulated.

- *Conservation mass*

The conservation mass balance can be written for a component of the reacting system in the reactor. Let $N_i = V_rC_i$ denote the molar quantity of ith species, where Vr is the volume of the reactor. Assuming a single reaction with rate R, the rate of change of the molar quantity, $\dot{N}i = dNi/dt$ [moles time^{-1}], must be equal to the rate of reaction taken with the proper algebraic sign.

$$N_i = v_i R V_r \qquad \text{eq. 2.38}$$

Where, v_i is the stoichiometric coefficient of i^{th} component, taken positive if it is a product and negative if the component is a reactant. Since the reaction rate is a function of concentration, the accumulation term is

$$N_i = V_r C_i + C_i V_r \qquad \text{eq. 2.39}$$

If the volume of reaction is constant, so

$$\dot{C}_i = \nu_i R \qquad \text{eq. 2.40}$$

When multiple reactions occur simultaneously, the right-hand side of (2.47) is replaced by a sum of reaction terms

$$\dot{C}_i = \sum_{j=1}^{N_R} v_{i,j} R_j \qquad \text{eq. 2.41}$$

Where, $v_{i,j}$ is the stoichiometric coefficient of component i in reaction j (taken negatively if component i is a reactant in reaction j, positive if it is a product, and null if it is not involved); and N_R is the total number of reactions. The most classical basic reaction schemes encountered in chemical engineering are shown in Table 2.8, together with the explicit expressions of the isothermal concentration profiles as a function of time.

c. <u>Conservation of energy</u>

The conservation of energy is an essential element of realism into the model. The form of the equation of energy quantitatively describes the thermal effects of producing when the potential energy stored in chemical bonds is transformed by an exothermal chemical reactor into sensible heat. In batch reactor, the accumulation of internal energy is the different between the heat produced by reaction and heat exchanged with the surrounding.

$$\text{Stored Energy} = \text{Generated heat} - \text{Exchanged heat} \qquad \text{eq. 2.42}$$

The stored energy (left-hand side), first term, is related to the total mass m of reaction solution, to the overall constant volume specific heat capacity c_{vr} [energy mass^{-1}

Table 2.8. Simple chemical reaction scheme

No.	Model	Kinetic scheme	Integrated BR model equation
1	Zero-order	$A \xrightarrow{k_{c0}} P$	$C_A = C_{A0} - k_{c0}t$
2	First order	$A \xrightarrow{k_{c1}} P$	$C_A = C_{A0}\exp\left(-k_{c1}t\right)$
3	Second order	$A \xrightarrow{k_{c2}} P$	$C_A = \dfrac{C_{A0}}{1+k_{c2}t}$
4	Equilibrium	$A \xrightarrow{kcB} B$	$C_A = \dfrac{C_{A0}}{1+k_{eq}}\left[1-\exp(-(k_{cA}+k_{cB})t)\right]$
5	Parallel	$A \xrightarrow{k_{cP1}} P_1$ $A \xrightarrow{k_{cP2}} P_2$	$C_A = C_{A0}\exp\left(-(k_{cP1}+k_{cP2})t\right)$ $C_A = C_{A0}\dfrac{k_{cP1}}{k_{cP1}+k_{cP2}}\left[1-\exp(-(k_{cP1}+k_{cP2})t\right]$
6	Series	$A \xrightarrow{kcI} I \xrightarrow{kcP} P$	$C_A = C_{A0}\exp\left(-k_{cI}t\right)$ $C_I = C_{A0}\dfrac{k_{cI}}{k_{cP}-k_{cI}}\left[\exp(-k_{cI}t)-\exp(-k_{cP}t)\right]$
7	Multiple series	$A \rightarrow \ldots \rightarrow P$	
8	Series-parallel	$A \xrightarrow{kcI} I \xrightarrow{kcP} P$ $A \xrightarrow{kcS} P$	$C_A = C_{A0}\exp(-(k_{cI}+k_{cS})t)$ $C_I = C_{A0}\dfrac{k_{cI}}{k_{cP}-k_{cS}-k_{cI}}\begin{bmatrix}\exp(-(k_{cI}+k_{cS})t)\\ -\exp(-k_{cP}t)\end{bmatrix}$

temperature^{-1}], and to the rate of change reactor temperature Tr. The right-hand side, second term, depends on the modes of heat exchange between the reactor and a heat exchange medium or the surroundings. The heat generated by the chemical reaction is given by the product of the specific molar energy change because of reaction, ΔE_R, and the number of moles converted in the reactor per unit time, RV_r.

According to Newton's law of heat exchange, the heat exchanged by the reactor is

$$mc_r\dot{T}_r = (-\Delta H_R^o)RV_r - US(T_r - T_j) \qquad \text{eq. 2.43}$$

Where, U the overall coefficient of heat exchange, S the heat exchange surface, and Tr-Tj the temperature difference between the reactor and the coolant.

2.1.10 Design of experiment (DOE)

Design of experiment (DOE) is a very useful method to determine the relationship between factors affecting a process and the output of the process. It can analyze the relationship of cause-and-effect. The input information is required to manage the optimal output. DOE can be analyzed in many software programs. The advantages of using DOE are:

- Minimize or reduce the amount of experiments
- Vary all factors in simultaneousness of an experimental activities
- Suitable strategy for an experiment

To understand the basic DOE concepts, knowledge of some statistical tools and experimentation concepts are needed (Sundararajan, 2016).

a. <u>Concept of DOE</u>

The terms of controllable and uncontrollable input factors, responses, hypothesis testing, blocking, replication an interaction are commonly used in the methodology of DOE. The relationship of input and output is shown in Figure 2.18.

- Controllable input factors or x factors: input parameters that can be modified in the process or experiment.
- Uncontrollable input factors: parameters that cannot be changed. Thus, these factors need to understand how they may affect the response.
- Responses or output measurements: the process outcome elements that gave the desired effect.
- Hypothesis test: determination the significant factors using statistical methods. The two hypothesis statements are null and alternative. The null hypothesis is valid if the status quo is true and the alternative hypothesis is true if the status quo is not valid. Based on a probability, it tests with the level of significance.

  Blocking and replication: an experimental technique to avoid any unwanted variation in the experimental process is called blocking. In the experiment, the replicated experiment is needed in order to get an estimate of the amount of random error that could be part of the process.
- Interaction: interaction is a situation in which the simultaneous influence of two

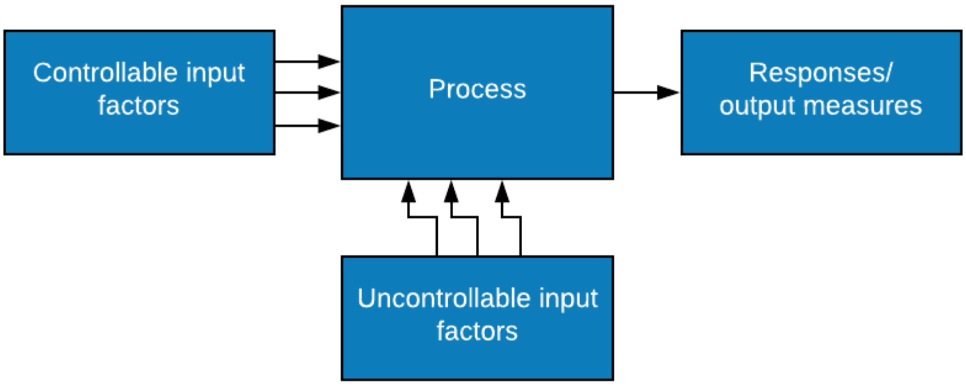

Figure 2.18. Process factors and responses

variables on a third is not additive when an experiment has three or more variables.

The methods of design of experiment of Full factorial, Response surface, and Taguchi are explained briefly below (Montgomery, 2001):

b. <u>Full factorial design</u>

A full factorial design of the experiment is an experiment consisted of two or more factors, each factor with a discrete possible level. These experimental units take all possible combinations of all levels across all such factors. The effect of each factor on the response variable, as well as on the effects of interactions between factors on the response variable is allowed to study using this method. Common input factors set is at two level each. If there are k factors each at 2 levels, a full factorial design has run. In this case, if 4 factors at two levels, it would take $2^4=16$ trial runs (Athreya and Venkatesh, 2012). If y is the response, ß is determined a parameter, x is the variable of a factor, and ϵ is the random error. The regression model represents the two-factor factorial experiment is:

$$y=\beta_o+\beta_1x_1+\beta_2x_2+\beta_{12}x_{12}+\in \qquad \text{eq. 2.44}$$

- ➢ *Two-factor factorial design*

These two factors include factor A (a level) and factor B (b level) with n replicate(s). In two-factor factorial design, y_{ijk} is the response when factor A presents i^th^ level (i=1, 2, 3,..., a) and factor B presents j^th^ level (j= 1, 2, 3,...,b) with k^th^ replicate(s) (k=1, 2, …, n). The randomized design of two-factor design is designed as shown in Table 2.9.

The effect model of the factorial experiment is written:

$$y_{ijk}=\mu+\tau_i+\beta_j+(\tau\beta)_{ij}+\in_{ijk}\begin{cases}i=1,2,3,...,a\\j=1,2,3,...,b\\k=1,2,...,n\end{cases}\qquad \text{eq. 2.45}$$

Whereas μ is an overall mean effect, τ_i is the effect of factor A-ith level, β_j is the effect of factor B-jth level, $(\tau\beta)_{ij}$ is the effect of interaction between τ_i and β_j, and ϵ_{ijk} is random error item.

- *Two-level (2^k) Factorial Design*

Factorial design investigates many factors in the experiment. It studies the effect of each factor on the response. The k factor is the most essential of factorial design with only two levels which can be two values of quantitative or qualitative parameters. The complete replication 2^k ($2\times2\times2\times...\times2=2^k$) is commonly important for applying in the early part of the experiment. It can reduce the amount of experiment work.

The 2^k design contents k main effects, (k | 2) two-factor interactions, (k | 3) three-factor interaction, and one k-factor interaction.

- *Single Replicate of 2^k Factorial Design*

Single-replicate of 2^k factorial design is generally selected for apply in screening experiment. Single replicate of design can be called unreplicated factorial. The data analyzing is real high-order interaction and inappropriate to use error mean square by pooling interactions. To solve this problem, Daniel recommends examining a normal probability plot for the estimate of the effect.

- *One-half Fraction of 2k Factorial Design*

One-half fraction of 2k factorial design is a design when the experiment cannot be run in full. For example, the experiment of 3 factors with 2 levels will be run in 2^3=8 experiment. However, the one-half fraction of 2k factorial design needs only 2^{3-1}=4 experiment. If supposing four combination experiments of a, b, c, and abc are selected as one-half fraction, the principle and alternative of fraction are shown in Figure 2.19.

Table 2.9. General experiment design for a two-factor factorial method

		Factor B					
		1	2	.	.	.	b
Factor A	1	y111, y112,..., y11n	y121, y122,..., y12n				y1b1, y1b2,..., y1bn
	2	y211, y212,..., y21n	y221, y222,..., y22n				y2b1, y2b2,..., y2bn
	.						
	.						
	.						
	a	ya11, ya12,..., ya1n	ya21, ya22,..., ya2n				yab1, yab2,..., yabn

c. Response Surface Methodology and Design

Response surface methodology (RSM) is very important to optimize the response of the experiment when several variables influent to the modelling and analysis of the problem. For example, in one experiment has the level of temperature (x_1) and pressure (x_2). It can provide the maximum yield (y) of the process that can be written as a function of factor's level of temperature and pressure by equation 2.57 where ϵ is an error in response y. The surface of the expected response E (y) and response surface η is shown in equation 2.58. The graph of response surface with the contours plot for better visualize is shown in Figure 2.20.

$$y=f\left(x_1,x_2\right)+\in \quad \text{eq. 2.46}$$

$$\eta=f\left(x_1,x_2\right) \quad \text{eq. 2.47}$$

The first-order model of RSM in equation 2.59 is constructed for determine the low-order polynomial which is well linear function, when the relationship between variations and the response are unknown. The second-order model in equation 2.60 is applied when the degree of polynomial is higher and it is in curvature.

$$y=\beta_o+\beta_1x_1+\beta_2x_2+...+\beta_kx_k+\in \quad \text{eq. 2.48}$$

$$y=\beta_o+\sum_{i=1}^{k}\beta_ix_i+\sum_{i=1}^{k}\beta_{ii}x_{ii}^2+\sum_{i<1}\beta_{ij}x_ix_j+\in \quad \text{eq. 2.49}$$

- Central Composite Design

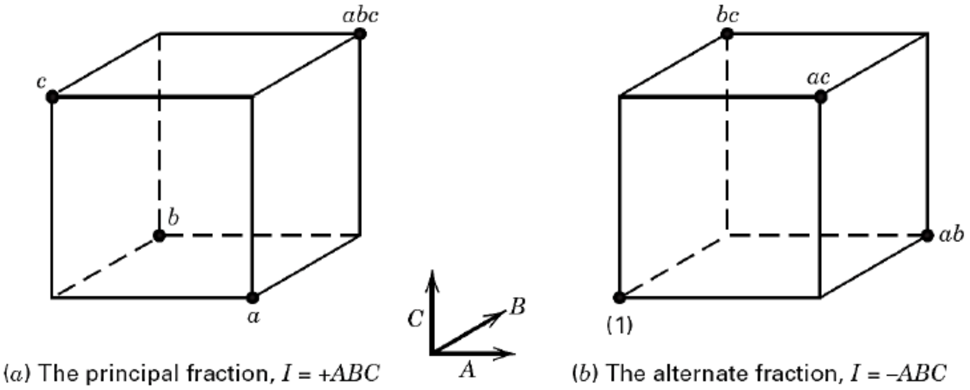

Figure 2.19. The 2 one-half fraction of factorial design 2^3

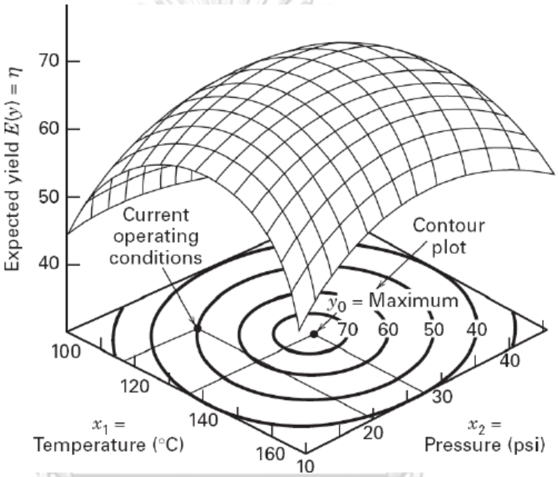

Figure 2.20. Contour plote of respond surface

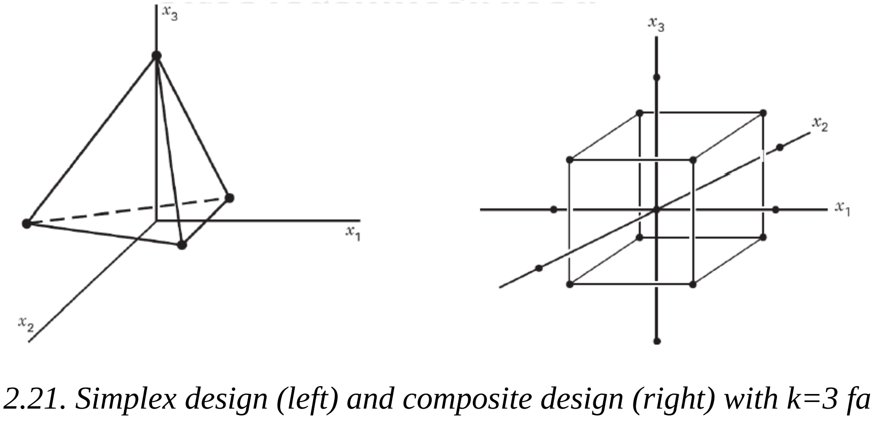

Figure 2.21. Simplex design (left) and composite design (right) with k=3 factors.

In RSM, the second-order rotatable design, central composite design (CCD), or Box-Wilson design is applied for response surface design fitted to second-order model. The central composite design and simplex design of two parameters including the distance of axial runs from design center (α) and amount of center points (nC) are illustrated in

Figure 2.21 with k=3 factors. The ratability essentially predicts in interested zone for second-order model.

- Box-Behnken Design

Box-Benhnken design is used for fitting response which has three level designs. This method combines 2 factorials with incomplete block designs. The advantage of this design is very efficient result in terms of the number of required runs either rotatable or nearly rotatable as shown in Figure 2.22.

Box-Behnken design is a spherical design in which all points lying on sphere radius and does not contain any points at the vertices of the cubic region created by the upper and lower limits for each variable.

d. <u>Taguchi method</u>

Full factorial design requires a large number of experiments, so it takes time and laborious. Taguchi method can overcome this problem by reducing the number of experiments. Taguchi design was developed by Genichi Taguchi in Japan to improve the implementation of off-line total quality control. The concept of this method is to find the controllable factor and uncontrollable factor to make the problem less sensitive to the variations called Taguchi robust parameter design problem. Control variables are factors that can be controlled while noise variables are factors that cannot control except during experiments in the lab. Taguchi based on mixed levels, highly fractional factorial designs, and other orthogonal designs. The design chosen for controllable variables is called inner array and the design was chosen for noise variables is called outer array. The crossed array combines the inner and the outer arrays which are the list of all

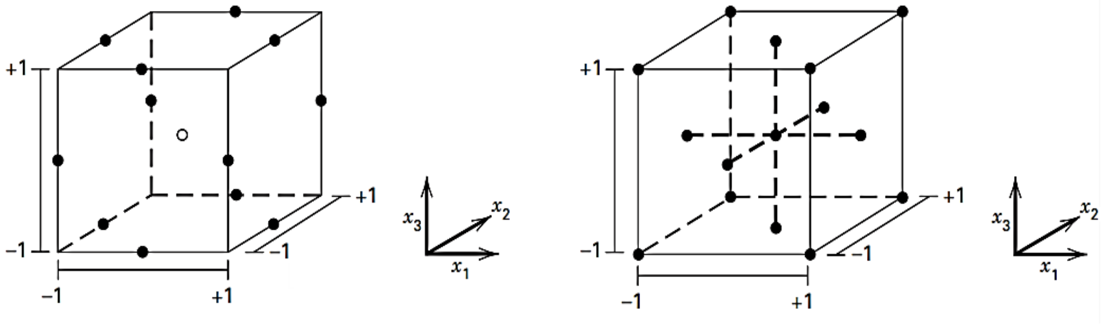

Figure 2.22. Three factors design by Box-Behnken (left) and Central Composite Design (right)

samples. This combination means that the full set of experiments of the outer array is performed for each sample in the inner array. The crucial for a robust solution in the cross array is inform the information about the interaction between the controllable variables and the noise variables.

For example, in one experiment have five factors, three controllable factors (k_{in}=3) and two uncontrollable factors (k_{out}=2) with two levels for inner and outer arrays. To simplicity, the full factorial design was used even though they are never taken into consideration by the Taguchi method, so the inner array is 2^3 and the outer array is 2^2 as shown in graphic in Figure 2.23.

Using L^{kin} and L^{kout} full factorial designs, the equivalent in Taguchi method is L^{kin}+L^{kout}. The outcome in terms of number and distribution of the sample would not be so different from some fractional factorial over the whole number of parameters k_{in}+ko_{ut} when using fractional factorial designs or other orthogonal designs. However, the stress is on the distinction between controllable variables and noise variables. The design of a set sample for each sample in the inner array helps us to estimate the mean value and the standard deviation, or other statistical value for design noise. Then, the objective is to improve the average performance of the problem with low standard deviation.

In fact, Taguchi does not consider the mean response variable and standard deviation. Taguchi measures more than sixty different performance to be maximized called signal-to-noise (SN). The well-known signal-to-noise is present below where E is the expected value. From a list of published orthogonal arrays, the inner and the outer arrays are to be chosen.

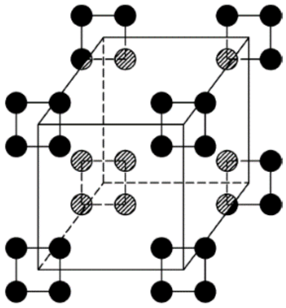

Figure 2.23. Example of Taguchi DOE for inner array kin = 3 with 23 full factorial, outer array kout = 2 with 22 full factorial

- Normal the best: to be used when a target value is sought for the response variable.

$$SN_{ntb}=-10\log_{10}\left(E^{2}\left[y_{i}\right]\right)/\left(E\left[y_{i}-E\left[y_{i}\right]^{2}\right]\right) \qquad \text{eq. 2.50}$$

- Larger the best: to be used when the response variable is to be maximized.

$$SN_{ltb}=-10\log_{10}E\left[1/y_{i}^{2}\right] \qquad \text{eq. 2.51}$$

- Smaller the best: to be used when the response variable is to be minimized.

$$SN_{stb}=-10\log_{10}E\left[y_{i}^{2}\right] \qquad \text{eq. 2.52}$$

Taguchi orthogonal arrays are in the literature with letter L, or LP for the four-level ones, followed by their sample size. Depending on the number of parameters and on the numbers of level are summarized in Table 2.10 .

The brief comparisons between the application of full factorial and Taguchi screening design are presented in Table 2.7. The steps involved in Taguchi method are:

- Identify the main function and its side effects
- Identify the noise factors, testing condition and quality characteristics
- Identify the objective function to be optimized
- Identify the control factors and their levels
- Select a suitable Orthogonal Array and construction the Matrix
- Conduct the Matrix experiment
- Examine the data and predict the optimum control factor levels and its performance
- Conduct the verification experiment

The formula of η called signal-to-noise (SN) is (W.-J. Chou et al., 2003):

$$\eta = -10\ \log(\text{mean square quality of characteristic}) \qquad \text{eq. 2.53}$$

Where the mean square quality of the characteristic property for the smaller-the-better type is $(\text{property})^2$ and for the larger-the-better type is $(1/\text{property})^2$. The array is used to design the number of parameters and level fraction.

The Taguchi orthogonal arrays are in the literature with the letter L individually, or LP

Table 2.10. The number of parameter and levels in Taguchi orthogonal arrays

Number of variables	Number of levels			
	1	2	3	4
2, 3	L4	L9	LP16	L25
4	L8	L9	LP16	L25
5	L8	L18	LP16	L25
6	L8	L18	LP32	L25
7	L8	L18	LP32	L50
8	L12	L18	LP32	L50
9, 10	L12	L27	LP32	L50
11	L12	L27	N./A	L50
12	L16	L27	N./A	L50
13	L16	L27	N./A	N./A
14, 15	L16	L36	N./A	N./A
From 16 to 23	L32	L36	N./A	N./A
From 24 to 31	L32	N./A	N./A	N./A

for the four-level ones, followed by their sample size. Array is used depending on the number of the parameter and levels that are summarized in Table 2.10.

2.2 Literature review

2.2.1 Electrocoagulation

a. Electrocoagulation in water treatment

Innovative EC is an effective method to treat raw water sources to produce potable water. The coagulant formation and particle destabilization are occurred in this system through electrolytic cells in the turbulent flow in which iron or ferric hydroxide is produced. Then, particles could be separated from the water by flocculation stage with the formation of large particles. EC process was efficiency in heavy metals removal from contaminated stream, leachate from mining, and landfill sites (Mills, 2000). EC process also was applied in portable water treatment in the USA by Vik et al. (1984). This research proved that EC was an effective process comparing to a conventional water treatment process as following reasons:

- The chemical transported to the solution in EC was lower than chemical treatment.
- Electrocoagulator had enough long lifetime of electrodes.
- EC was simple in maintenance and operation.
- The amount of sludge was less than conventional treatment

Jiang et al. (2002) studied about the electrocoagulation-flotation for water treatment in laboratory in the UK. The results showed that the up-flow electrocoagulator configuration performed better than a horizontal flow configuration in both bipolar and monopolar electrode arrangements were used in terms of dissolved organic carbon, color, and UV 254 removal. The up-flow arrangement allowed more collisions to occur between the gas bubbles and the resulting Al-contaminant flocs which enhance the overall flotation performance.

b. Electrocoagulation in turbidity removal

Electrocoagulation had been investigated by many research to remove turbidity in water/wastewater.

Han et al. (2002) compared the conventional chemical coagulation and bath electrocoagulation in terms of turbidity removal. The result showed that Electrocoagulation was more efficient than conventional coagulation in turbidity removal. The application of the electrocoagulation/flotation process also was investigated to remove the turbidity and Humic acid (HA) using Fe and Al electrodes (Seid-Mohammadi et al., 2015). As a result, Fe and Al electrodes considered as the best electrode for turbidity and HA removal, respectively. W.-L. Chou et al. (2009) explored the feasibility of reducing COD and turbidity from real oxide chemical mechanical polishing (oxide-CMP) wastewater using iron electrode and evaluated the specific energy consumption. The outcome of the experiment was that COD and turbidity decreased more than 90 and 98%, respectively under the optimum electrolyte concentration and voltage.

c. Calcium removal

Malakootian et al. (2010) conducted a research by using iron-rod electrodes for hardness removal from drinking water. The water sample was taken from water distribution network of Anar City located in northwestern part of Kerman Proven, Iran. The effects of parameters for EC are electrode type, initial pH, electric potential, electrode spacing, and operating time. The result showed that hardness was successfully removed 97.4% in the condition of pH 10, voltage of 12 V and reaction time of 60 min. Khairi et al. (2011) removed hardness from drinking water using electrochemical cell. The operating parameters of electrode type (Al cathodes and graphite anodes), initial pH (7-8), electric potential (10-28.5 V), electrode spacing (2-4 cm) and operating time were studied. The 85% of hardness was removed at pH of 7.5, detention time of 1 hours and electrical voltage of 28.5V. Brahmi et al. (2016) used aluminum electrodes to reduce non-carbonate hardness in Tunisian Phosphate Mining process water. The overall removal rate of hardness is 83.8% at optimal conditions of pH 7, NaCl of 4g/L, current density 22.2 mA/cm^2, electrode spacing 2 cm, a stirring speed of 450 revolutions per minute, and a treatment time of 30 min.

In overall, electrocoagulation (EC) process has attracted a great deal of attention in removal hardness from water. Most of the researchers showed that hardness can be removed more than 80% from water (Malakootian and Yousefi, 2009b; Zhao et al., 2014)

d. Heavy metal removal

Electrocoagulation has been applied to remove the heavy metal contained in water/wastewater. Al Aji et al. (2012) conducted the research on electrocoagulation using monopolar iron electrodes to remove copper (Cu), nickel (Ni), zinc (Zn) and manganese (Mn) from a model wastewater. The results indicated that more than 96% of heavy metal except for Mn (72.6%) was removed using 25 mA/cm2 of current density with total energy consumption of 49 kWh/m^3, and high pH values are more suitable for metal removal. M Kobya et al. (2011) removed arsenic from drinking water by the electrocoagulation using Fe and Al electrodes. The research outcomes were Arsenic could be removed more effectively using Aluminum electrode comparing to iron electrode. The optimum operating condition was 12.5 min operating time and pH 6.5 for Fe electrode (93.5%) and 15 min and pH 7 for Al electrodes (95.7%) at 2.5 Am^{-2}, orderly. Electrocoagulation was able to remove arsenic concentration less than 10 μg L^{-1} with Fe and Al electrodes. The pseudo-second-order adsorption model was fit to the adsorption of arsenic over the electrochemically produced hydroxides and metal oxide complexes.

The removal of heavy metal ions, namely Cu^{2+}, Cr^{3+}, Ni^{2+}, and Zn^{2+}, from metal plating wastewater using electrocoagulation technique was studied by Al-Shannag et al. (2015). The results showed that at a current density of 4 mA/cm2, retention time 45 min and pH of 9.56, over 97% of heavy metals were removed from the wastewater. This treatment required a low amount of energy. Pseudo-first-order model with current-dependent parameters was applied to demonstrate the removal of such heavy metal ions.

2.2.2 Electrooxidation (EO) in natural organic matter removal

Manea et al. (2014) studied the electrochemical oxidation and reduction process using boron-doped diamond (BDD) electrode for drinking water treatment. The result was shown that BDD electrode is a suitable material for NOM and NC removal in forms of nitrite and ammonium presented in drinking water sources. However, nitrate formed as oxidation product for drinking water source characterized by high content of nitrate in BDD-based electro-oxidation. Therefore, BDD-based electrode was not an efficient method for nitrate removal since it consumed high energy to remove nitrite. Tran and Drogui (2013) researched about electrochemical removal of microcystin-LR from aqueous solution in the presence of natural organic pollutants (humic acid). In MC-LR degradation efficiency, current density and the type of anode material are the main parameters. The degradation was mainly attributed to the direct anodic oxidation. The results showed that the color caused by the presence of NOM could be removed by up to 81% using BDD electrode with sodium chloride due to the generation of active chlorine which is a powerful oxidizing agent. MC-LR was decomposition exhibited first-order reaction behaviors.

a. Electrode material for Electrooxidation

Development of electrode material was a hot topic in electrochemical process. The problems of electrode were polarization, corrosion, and passivation (Shestakova and Sillanpää, 2017). Polarization of electrode was occurred due to poor mass transfer and accumulation of gas at electrode surface. Corrosion was happened when pollutant was oxidize at the anode surface and some corrosive product such as chlorine gas.

Passivation of electrode was caused by polymeric and oligomeric compounds forming during electrode reaction. Therefore, following researches were studied or developed the electrode material. Motheo and Pinhedo (2000) evaluated the possibilities of electrochemical methods in the degradation of humic substances. Dimensionally stable anodes (DSA) type with the following compositions: $Ti/Ir_{0.3}\ Ti_{0.7}\ O_2$; $Ti/Ru_{0.3}Ti_{0.7}\ O_2$; and $Ti/Ir_{0.2}\ Ru_{0.2}\ Ti_{0.6}\ O_2$ were used. The results showed that the electrolysis efficiency is depended on the composition of electrode material. $Ti/Ru_{0.3}Ti_{0.7}O_2$ electrode presents the best performance considering the elimination of most of the electro-oxidation products. Tang et al. (2014) improved the HA removal by preparing $Ni\text{-}Sb\text{-}SnO_2/Ti$ oxide electrodes. This research indicated that these electrodes could produce ozone with high efficiency in an aqueous medium at room temperature comparing to DSA electrodes. Ozone was known as a disinfectant for HA degradation.

The conductive diamond anode was employed for azoic dye removal in Electrooxidation since it could obtain high current density efficiency and complete mineralization of organic (Cañizares et al., 2006). The result of this work could conclude that the efficiency of azoic dyes did not depend on the molecule by only on concentration range in the conductive diamond electrolyte.

b. Effect of chloride

Chloride in form of sodium chloride in the electrolyte is very essential in electrochemical performance since it can improve the conductivity and oxidation in the process.

Subramaniam and Halim (2014) analyzed the effect of Electrochemical Oxidation on biodegradability and toxicity of Batik Industry Wastewater. The optimal concentration of chloride was evaluated in terms of COD and color removal in EO process. The result showed that chloride was an indirect electrochemical oxidation (chlorine or hypochlorite) for pollutant removal. Sodium chloride higher than 2.5 M had a major effect on color and COD removal with pH 13, electrode spacing 1 cm, and current density 200 mA.

2.2.3 Research gap

Different researches have been done to remove turbidity and natural organic from water using different treatment methods. In some case, combinations of two or more processes are achieved to treat these contaminants. The best method to treat these contaminants is electrochemical since it does not contain secondary pollutant as the conventional method. However, the ions contained in water such as iron, chloride, and hardness also affected the treatment performance of electrocoagulation/flotation in turbidity removal. The literature has showed that the amount of chloride in water can improve the conductivity of water (Arroyo et al., 2009). Mehmet Kobya et al. (2003) researched about the effects of relevant wastewater characteristics such as conductivity and pH, and important process variables such as current density and operating time on the chemical oxygen demand (COD) and turbidity removal. For the effects of dissolved ions and natural organic matter on electrocoagulation of As(III) in groundwater were conducted by You and Han (2016). Additionally, the optimal condition of electrode configuration was very crucial in EC process. Many researchers evaluated EC performance in term of electrode material, configuration, reactor types, and conductivity in water (Bazrafshan et al., 2008; Essadki et al., 2009; Gao et al., 2010; Mahvi et al., 2011). However, the effect of ion contaminations in water on turbidity and

Table 2.11. Summary of literature and future study

Literature review	Condition/ Treatment existing	Gaps and Future study
Electrocoagulation	turbidity and NOM synthetic water were removed individually in EC process.	
	The effects of ion contaminations and operating condition such as electrode arrangement, configuration, current density, and pH were crucial in EC performance.	Electro Coagulation and Oxidation were evaluated in synthetic water containing both turbidity and NOM.
Electrooxidation	Most of HA treatment in EO studies, the synthetic water contained only HA.	Effects of operating conditions and ion contaminations in groundwater was analyzed.
	Adding chloride could improve indirect oxidation of dye and COD.	Novel Conductivity carbon coated on graphite electrode was assessed.
Electrode-coated for EO	Develop electrode material such as conductive diamond, Ni-Sb-SnO_2/Ti oxide, and $Ti/Ru_{0.3}Ti_{0.7}O_2$ could improve treatment process.	

NOM removal on Electrocoagulation was partially studied.

Therefore, the effect of operating conditions and ions contamination including iron and calcium to the combination of Electro Coagulation and Oxidation in turbidity and natural organic compound removal was a topic of this present study.

CHAPTER 3

MATERIAL AND METHODS

The objective of this research was to investigate the effect of operating conditions and ion contaminations to Electro Coagulation and Oxidation in turbidity and NOM removal. This chapter was classified into six main parts as shown in Figure 3.1 and briefly detailed as follows:

- Turbidity and NOM were synthesized by using bentonite clay and humic acid, orderly. The characteristic of these two pollutants was then analyzed. Calcium chloride and ferrous sulfate were synthesized for calcium and ferrous in solution, respectively. The operating conditions were initial pH and current density.
- Gas flowrate, electrode loss, and treatment efficiency were evaluated the optimal electrode configuration and arrangement. Chemical coagulation was compared to Electrocoagulation process in terms of treatment efficiency and chemical dose.
- Kinetic study was determined the optimal time and current density
- The effects of individual ferrous, calcium, initial pH, and current density were studied.
- The effect of co-existing ion contaminations and operating condition was analyzed. Design of Experiment (DOE) methodology of Minitab computer software was employed to design the experiment. Response Surface Design has analyzed the effect and model prediction in terms of turbidity and HA removal. Settling test was examined to design the settling process.
- The treatment of EC effluent which contained NOM was EO. Electrode material was studied. The effect of chloride in indirect EO was studied by varying different concentration of chloride into EO system. Design criteria was proposed to treat these pollutants.

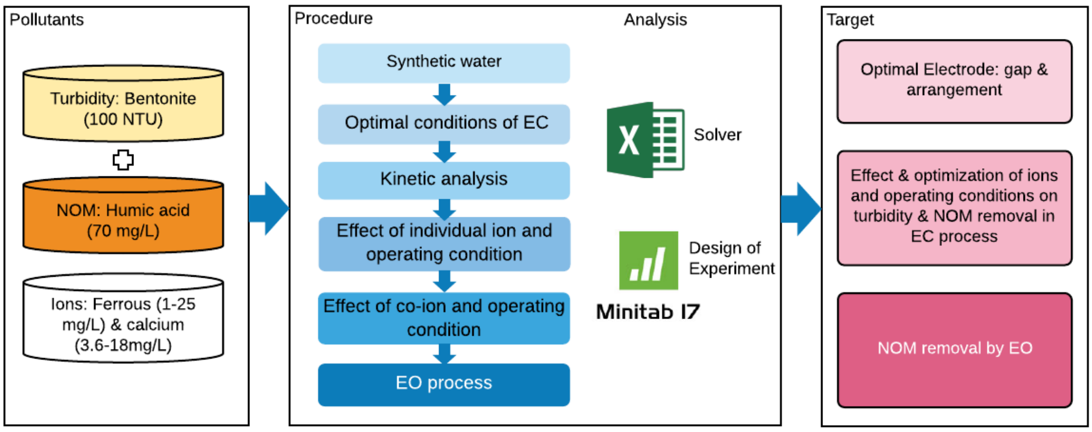

Figure 3.1. Methodology overview framework

3.1 Experimental set-up

EC was operated in a batch column which was suitable for laboratory scale application. The system consisted of 4 liter clear acrylic cylindrical tank with 13 cm inner diameter and 40 cm height. The electrodes employed in this study were placed at 3 cm from the bottom of the column by using electrode supporter. DC power supply (maximum current of 5 A and 100 V) was connected to the electrode for transferring current. The cone was connected to the top of the reactor for measuring gas flowrate using soap film meter. The experimental set up as shown in Figure 3.2.

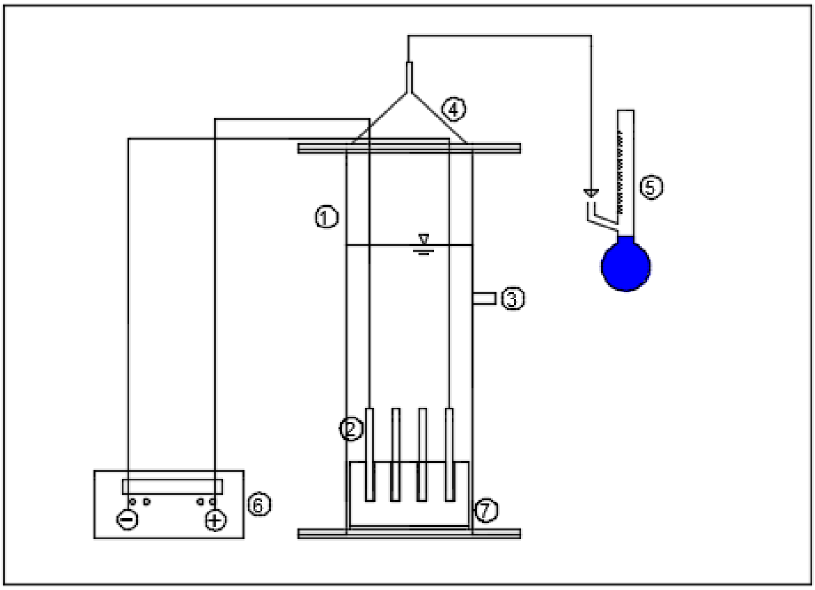

Figure 3.2. Schematic diagram of the batch EC reactor system: (1) Acrylic reactor, (2) electrode, (3) effluent, (4) cone, (5) Soap film meter, (6) DC power supply, (7) electrode supporter

3.2 Material and equipment

This section was involved with three main parts including apparatus, reagents, and analytical parameters.

3.2.1 Apparatus

The apparatus employed for EC and EO process, and equipment for analyzing parameters in synthetic water were:

- Reactor: clear acrylic reactor had 13 cm inner diameter and 40 cm height. The freeboard of the reactor was 8 cm. The effluent was sampled at the middle of the column.
- Electrode: the electrode plate was made from aluminum for EC process, and graphite, aluminum and conductive carbon for EO process. Their dimensions were 2 mm thickness, 5 cm width, and 20 cm length.
- Electrode supporter: it was used to prevent electrode collapse while operating and had an important function in varying inner electrode gaps.
- DC power supply: regulated DC power supply single channel MCH-K10050 made in Malaysia was supplied with electric energy to an electric load. The output voltage was in between 0 to 100 V and output amp was in between 0 to 5A.
- Soap film meter: manual soap film meter which soap bubble was functioned as gas flowrate detector was employed.
- pH meter: pH meter model METTLER-TOLEDO FiveEasy Plus was used to observe the pH while experimenting.
- Conductivity meter: Mettler Toledo, FiveEasy Conductivity was employed to measure the conductivity.
- Turbidimeter: Portable turbidimeter model HANNA- HI 98703 was used to measure the water turbidity. The unit measured the scattered light at an angle of 90° and be able to test both colored and colorless liquids. The meter was supplied complete with AMCO-AEPA-1 primary turbidity standards used for calibration and performance verification. The accuracy is ±2% of reading plus 0.02 NTU. The detection limit was varied from 0.01 to 1000 NTU.

- Jar test: Jar test model Twister JR D-Series Multi-positions with 6 paddles (6D) was used for operating in Jar test. The dimensions (W, L, H) of this model were 235 x 1125 x 400 mm. The roller size (L x H) was 75 length x 25 mm axial.
- Stopwatch
- Filter syringe: Filter Syringe Nylon had pore size 0.45 micron with 25 mm diameter.
- DO probe meter: SDL150 DO meter could measure oxygen in air from 0 to 100% (accuracy ± 0.7% O_2) and temperature ranged from 0 to 50ºC.
- Ferrous analyzed equipment:
  - Genesys 10S UV-Vis Spectrophotometer: the container type is single cell holder and automated 6-cell changer standard. The photometric accuracy instrument is ±0.005 A at 1.0 A. The wavelength ranges from 190 to 1100 nm and it repeats ±0.5 nm.
  - Separatory funnels: 125-mL, Squibb form, with ground-glass or TFE stopcocks and stoppers.

- Chloride measurement set with Material Number(s) 51344706, DX237-Cl Chloride half-cell. The measurement range is 5×10^{-5} to 1 mol/L and 1.8 to 35500 mg/L. The temperature measured range from 0°C to 80 ºC with the optimal pH from 2 to 12.
  - Mettler Toledo ISE meter
  - perfectION^{TM} combined chloride ion selective electrode
  - Chloride Ion Selective Electrode Fill Solution
  - Pipette for fill solution, and Polishing Strips
  - The additional equipment: ISE (Ion Selective Electrode) Amplifier, Magnetic stir plate, pipettes, computer.

- Calcium measurement set model DX240-Ca Calcium half-cell, material number 51340600 is a product from perfectION^{TM} Combination Chloride Electrode: Measurement range from 1.0 to 10^{-6} mol/L. Optimal pH range from 2 to 12 and temperature range from 0 °C to 50 ºC.
  - Mettler Toledo ISE meter

- Calcium Ion-Selective Electrode model
- Calcium Ion-Selective Electrode fill solution
- pipette for fill solution
- Additional equipment as Chloride measurement

➢ Batch settling column with 40 cm height was employed for batch settling test. 4 sampling ports were provided equally intervals in height (5 cm).

3.2.2 Reagents

Chemical substances were required to synthesis water and analyzed some parameters. All chemical reagents were bought from S-Corp Innovation Co., Ltd. Only Humic acid and bentonite were bought from P.M.M Co., Ltd.

➢ Synthetic water
  a. Hardness: Calcium chloride ($CaCl_3$), reagent grade
  b. Iron: Ferrous ($FeSO_4 . 7H_2O$), reagent grade
  c. Turbidity: bentonite, agricultural grade
  d. Natural organic matter: humic acids (HA), agricultural grade, 70% purity.
  e. Chloride: Sodium chloride (NaCl), reagent grade

➢ Chloride test chemical reagent
  a. Deionized or distilled water
  b. Ionic Strength Adjuster (ISA)
  c. Filling Solution, 1 M KNO_3
  d. Chloride Standard, 0.1 M NaCl
  e. Chloride Standard Solution
  f. Chloride Standard Solution, 100 ppm Cl^-

➢ Ferrous test chemical reagent
  a. Hydrochloric acid, HCl
  b. Hydroxylamine solution
  c. Ammonium acetate buffer solution
  d. Sodium acetate solution
  e. Phenanthroline solution
  f. Potassium permanganate $KMnO_4$
  g. Standard iron solutions
  h. Diisopropyl or isopropyl ether

➢ Calcium test chemical reagents:
  a. Deionized or distilled water
  b. Ionic Strength Adjuster (ISE)
  c. Calcium Chloride solution 0.1 M $CaCl_2$
  g. Calcium Chloride solution 1000 ppm Ca^{2+}
  d. Calcium Chloride solution 100 ppm Ca^{2+} as $CaCO_3$

3.3 Analytical parameters

Analytical parameter is very essential for the experiments. In this research, the parameters required to analyze were briefly detailed in Table 3.1.

a. Ratio of gas flowrate to electrode loss

Gas flow rate was measured by using soap film meter. It was determined by the ratio of generated gas volume (ΔV) to time (Δt) as expressed in eq. 3.1. Electrode loss was calculated by the different weight (m) between before and after treatment operation as shown in eq.3.2. Therefore, the ratio of gas flow rate to electrode loss (Qg/Loss) was calculated.

$$Qg = \Delta V/\Delta t \qquad \text{eq. 3.1}$$

$$\text{Electrode loss (Loss)} = m_{before} - m_{after} \qquad \text{eq. 3.2}$$

b. Natural organic matter

NOM was synthesized by humic acid. HA, hydrophobic NOM, was measured by using Ultraviolet (UV) absorbance of UV- vis spectrophotometer at 293 nm using a quartz cell after filtrating through 0.45 micron pore filter syringe with 25 mm diameter (Asgharian et al., 2017). If R is the treatment efficiency of NOM, abs_i and abs_f are the initial and final absorbance of HA, respectively, the removal efficiency therefore could be measured by using the following equation:

Table 3.1. Summary analytical parameters for the experiment

Parameter	Method	References
Gas flow rate	Soap film meter	(Vepsäläinen et al., 2012)
NOM (Humic acid)	UV spectrophotometer, 293nm	(Asgharian et al., 2017)
Turbidity	Nephelometric Turbidity Unit (NTU)	(Seid-Mohammadi et al., 2015)
Ferrous concentration	Phenanthroline Method	(American Public Health Association et al., 1915)
Calcium concentration	Calcium ion selective electrode (ISE)	(Durst, 1969)
Chloride concentration	Chloride ion selective electrode (ISE)	

$$R\%=\frac{abs_{i}\text{-abs}_{f}}{abs_{i}}\times 100 \qquad \text{eq. 3.3}$$

The standard curve of HA concentration (mg/L) with UV absorbance (nm) was also useful for determining the concentration of HA while experimenting.

c. Turbidity

The concentration of turbidity was measured using portable turbidimeter model HANNA-HI98703 in duplicate for accuracy. The calibration was taken every week. The removal efficiency was calculated by using eq. 3.4 where R is the removal efficiency (%), Tub_i and Tub_f are the initial and final turbidity, respectively.

$$R\%=\frac{Tub_{i}\text{-Tub}_{f}}{Tub_{i}}\times 100 \qquad \text{eq. 3.4}$$

d. Chloride

The concentration of chloride was measured by using Ion Selective Electrode (ISE) method (Freiser, 2012). Chloride electrodes measure free chloride ions in aqueous solutions accurately. ISEs are not ion-specific. All are sensitive to some other ions to some extent. The ability of an ion-selective electrode to distinguish between different ions in the same solution is expressed as the Selectivity Coefficient. The calibration linear of chloride concentration (mol/L) in logarithm scale was plotted with potential voltage (V) in experiments. Verify calibration was required every two hours by placing electrodes in the standard solution. If the value has changed, recalibration was made.

e. Calcium

The concentration of calcium was also analyzed using calcium ion selective electrode (ISE) method. Thus, the calibration linear of calcium concentration (mol/L) in logarithm scale was plot with potential voltage (V). Verify calibration was required in every two hours by placing electrodes in the standard solution. If the value has changed, recalibrated.

f. Iron

Phenanthroline Method followed standard method (American Public Health Association et al., 1915) was employed to measure the concentration of ferrous in water. The standard curve of iron concentration with absorbance was plotted for measuring ferrous containing in water.

3.4 Design of experiment (DOE)

The main part in this research was to evaluate the effect and optimization of ferrous, calcium, initial pH, and current density in terms of turbidity and HA removal. Moreover, the predicted model of these terms were also analyzed. Thus, the design of experiment (DOE) was very useful to identify conditions of experiment and determine the relationship between factors affecting the process and the output of that process. This information was required to manage the process inputs to optimize the outputs.

In this study, Minitab 17 software was selected for design the experimental condition using DOE methodology. Minitab has two windows visible (session window and worksheet) and one window minimizes (project manager). The DOE in Minitab provides five different types of design including Screening, Factorial, Response Surface, Mixture, and Taguchi. The process of Design was dealt with two main parts: screening and optimization as shown in Figure 3.3. 2^k factorial design and central composite design of response surface methodology (CCD-RSM) were chosen for experimental design and analysis in the processes of factor screening and factor optimization, respectively. The Analysis of Variance (ANOVA) was also used as the processed functions to complete both design and statistical analysis of the experiment. The level of confidence was 95%. With four factors including initial pH, current density (J), calcium, and ferrous ion in 3 levels were designed by using half central composite design (CCD). The relationship between the independent variables and the responses were calculated by the second-order polynomial equation and fitted to the experimental data of all responses (Ahn, 2016) as expressed in eq. 3.5.

$$Y = \beta_o + \sum_{i=1}^{k} \beta_i + \sum_{i=1}^{k} \beta_{ii} x_i^2 + \sum_{i=1}^{k-1} \sum_{i<j=2}^{k} \beta_{ij} x_i x_j + \varepsilon \qquad \text{eq. 3.5}$$

where, y is the predicted response of the model, k is the number of factor, β_o is a constant, β_i is a linear coefficient, β_{ii} is squared coefficient, and β_{ij} is the interaction coefficient, x_i and x_j are the independent variables, and ε is noise or error of the model prediction.

Table 3.2. Investigated factors and its level

Factor	Unit	Levels		
J	mA/cm^2	1.0	2.5	4.0
pH	-	5	7	9
Ca^{2+}	mg/L	3.6	10.8	18.0
Fe^{2+}	mg/L	1	13	25

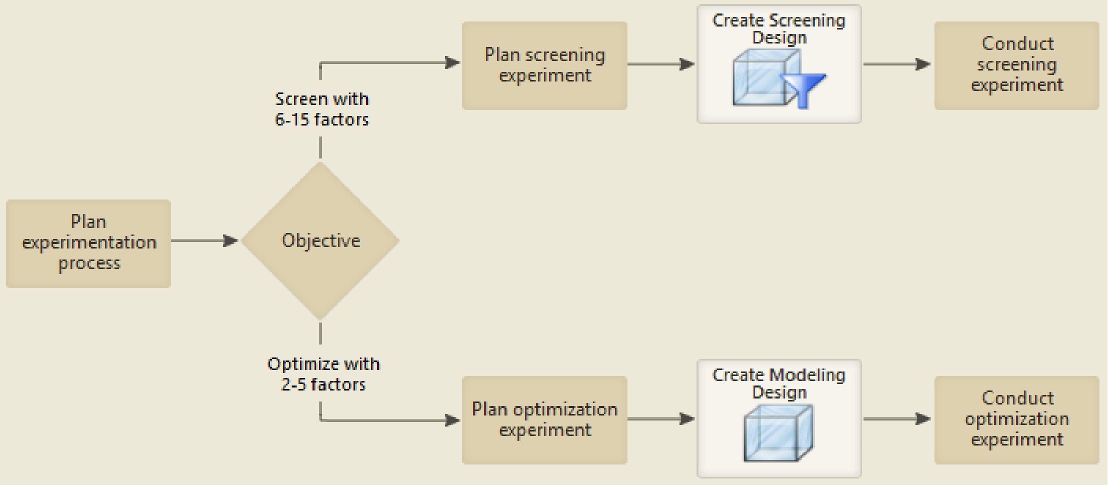

Figure 3.3. Plan and create experiments of Design of Experiment (DOE)

3.5 Experimental procedure

As mentioned, two main different processes in series of work including EC performance on Turbidity and HA removal, and on EO performance in terms of HA removal were investigated. The overall experimental processes and analytical methods for answering the scopes of this study were shown in Figure 3.4 and described as follows:

- Synthetic water preparation
- Optimal condition of electrode configuration and arrangement for EC process
- Kinetic study and treatment efficiency of EC process
- Effect of individual ion contamination and operating condition on turbidity and NOM removal in EC process
- Effect of co-existing ions and operating conditions on turbidity and NOM removal
- Electrode material, kinetic and effect of chloride on HA removal, and propositions of design criteria

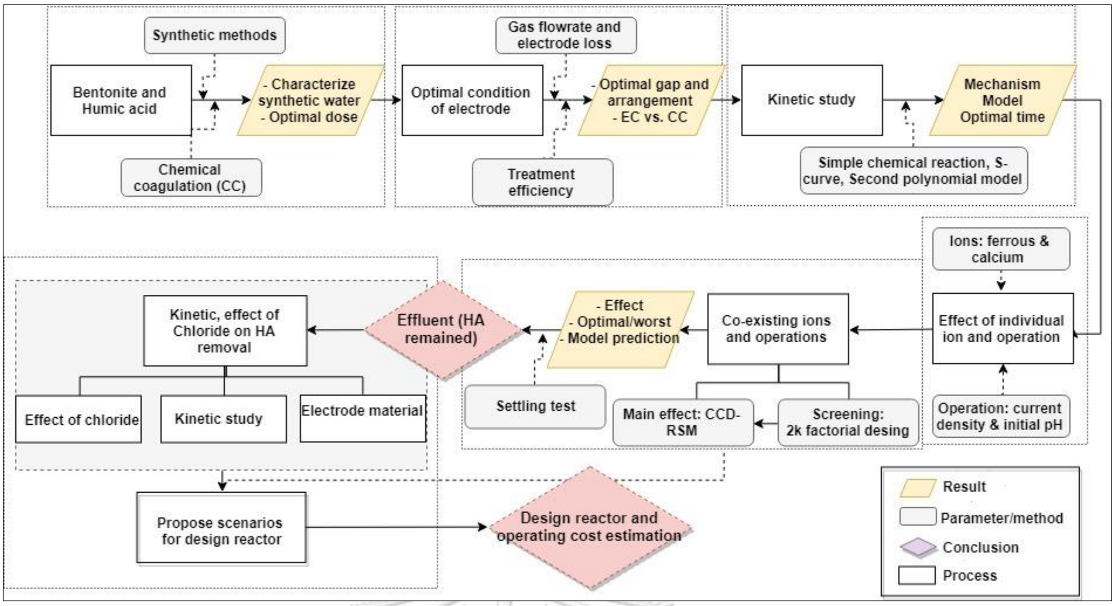

Figure 3.4. Flowchart of experimental procedure

3.5.1 Synthetic water preparation and chemical coagulation

a. <u>Synthetic water preparation</u>

Turbidity and NOM were the main parameters to be analyzed in this work. The variations of the substance concentration were based on the literature review: concentration of turbidity (Irvine et al., 2011), and NOM (Rodrigues et al., 2009). Table 3.3. shows the concentration of turbidity and HA concentrations. Calcium, ferrous, and initial pH were also investigated. Therefore, the way to synthesize these parameters were described in Table 3.3.

- *Turbidity*

Synthetic turbid water was prepared by adding bentonite directly into tap water. Bentonite suspension was re-suspensed by using rapid mechanical agitation (300 rpm) for 5 minutes in a jar test apparatus (Twister JR D-Series). Then, it was following slow mixing at 40 rpm in 30 minutes to obtained a uniform dispersion of bentonite particles

Table 3.3. The variations of substance concentration contained in water

Parameter	Unit	Concentration
Turbidity	NTU	100
NOM	mg/L	50

(Al-Sameraiy, 2012). After that, the turbidity was measured along the time using portable turbidimeter for finding a suitable time that the turbidity was not steeply change. Therefore, high concentrated bentonite was employed as a stock solution for creating turbid water.

- *Natural organic matter*

Humic acid is a hydrophobic acid and also the major fraction of natural organic matter since it has highly functionalized carbon-rich polydisperse polyelectrolytes (Matilainen and Sillanpää, 2010). In this study, Humic acid (HA), agricultural grade was synthesized since most of humic acid in surface or groundwater came from humic acid fertilizer that has been used in agricultural sector. HA was mixed with tap water at the calculated amount. In order to get 50 mg/L of NOM, HA was synthesized at concentration 70 mg/L.

- *Calcium ion*

Synthetic calcium was prepared by adding $CaCl_2$ in calculated amount. The concentration of $CaCl_2$ was measured in mg/L of calcium.

- *Iron ion*

In underground strata, far from the oxidizing effect of oxygen in air, conditions usually favor the reduction of the natural ferric iron deposits to the ferrous state. Since the ferrous salts are highly soluble, groundwater supplies frequently carry significant concentrations, and as this ferrous iron is in true solution. Thus, in order to synthesizing iron in groundwater, El Azher et al. (2008) reduced initial dissolved oxygen (DO) in water (DO < 1 mg/L) by using nitrogen gas. In our case, the reduction of initial oxygen was less than 0.5 mg/L before adding ferrous ion to prevent oxidizing ferrous to ferric. $FeSO_4.7H_2O$ was synthesized and its concentration was measured by standard method of Phenanthroline.

b. Chemical coagulation

A jar test is vital in most water treatment plant systems. It provides the empirical chemistry for coagulant dose, chemical requirements for pH control, and sludge production. It also provides some useful empirical information about mixing requirements, floc formation, sludge thickening, and settling efficiency (Mac Berthouex and Brown, 2017).

Jar test was employed for chemical coagulation. The objective of doing Jar test was to determine the optimal chemical dose in the removal efficiency of turbidity and absorbance. Alum ($Al_2(SO_4)_3$. $18H_2O$) was used to remove turbidity and HA from synthetic water. The rapid mixing of 100 rpm was in 1 minutes and followed by slow mixing 40 rpm in 40 minutes; then, kept it settle down 30 minutes (Black et al., 1957).

3.5.2 Optimal conditions of electrode for treatment performance

This part was to screen the optimal conditions of electrode gap, arrangement and current density for treatment performance. It was divided into two main parts including (i) optimal conditions of electrode gap and current density in terms of gas flow rate generation and electrode loss, and (ii) removal efficiency of turbidity and HA. Finally, the comparison of this optimal condition to conventional coagulation was evaluated.

a. Analyze electrode configuration

The optimal condition of current density and electrode gap was evaluated in terms of gas flow rate and electrode loss ratio. Gas flow rate may help in flotation process while electrode loss was an obstacle in EC process. Therefore, the highest ratio was chosen in this study.

Aluminum electrodes each having dimension, 20 cm x 5 cm x 0.2 cm, with fully submerged active surface area of 100 cm^2 was employed. All inter-electrode distance was varied from 1 cm, 1.5 cm, to 2 cm. The current density varied from 1.5 to 2.5 mA/cm^2. The constant current during EC was maintained by appropriately adjusting the impressed cell voltage from a regulated DC power supply Model MCH-K10050. All experiment was conducted at room temperature. The electrode arrangement and current density were summarized as shown in Table 3.4. This experiment was operated with tap water. It was evaluated by the ratio of gas flow rate to electrode corrosive. Gas flow rate was measured by using soap film meter at 4 min, 9 min, and 14 min and total loss of electrode corrosive was measured after 15 min operating.

The experiment was divided into two main different tests:

- *Monopolar-parallel arrangement*

In monopolar arrangement, all anodes and cathodes were connected to DC supply. Electrodes are arranged in 4 plates of monopolar-parallel as shown in Figure 3.5. Electrode gap and current density were varied as shown in Figure 3.5. By using full factorial design, 9 experiments were tested for monopolar-parallel.

- *Bipolar-series arrangement*

For bipolar arrangement, the outer electrodes were connected to a power source, and the current passes through the inner electrode as shown in Figure 3.5. The opposite side of the anode was negative charge and the opposite side of the cathode was a positive charge. Therefore, the inner sacrificial electrode has two opposite charges of each plate. The amounts of the electrode for bipolar were 4 plates. Here, 9 experiments were run.

b. <u>Optimize electrode arrangement</u>

The electrode arrangements were optimized in terms of treatment efficiency by using their optimal gap and current density from the previous part. Three conditions of synthetic waters including bentonite, HA, and HA-bentonite removal were evaluated for this part as shown in Table 3.5.

c. <u>Comparison of EC to chemical coagulation (CC)</u>

Table 3.4. Parameters for analyzing the optimal condition of mono- and bipolar

No	Parameters	Factor level		
1	Electrode at cathode	Aluminum		Aluminum
3	Gaps (cm)	1	1.5	2
4	Arrangement	Monopolar-parallel		Bipolar-serial
5	Current (mA/cm^2)	1.5	2	2.5

Table 3.5. Three conditions of synthetic water

No	Synthetic water		Unit	concentration
1	HA		mg/L	70
2	Bentontie		NTU	100
3	HA-bentonite	HA	mg/L	70
		Bentonite	NTU	100

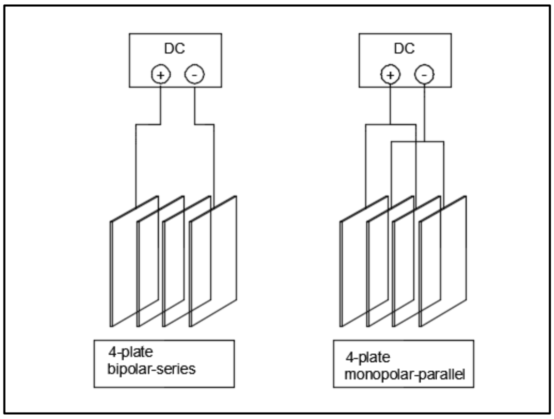

Figure 3.5. Electrode arrangement: bipolar and monopolar

The optimal condition of EC (gap, current density, and arrangement) was operated to compare with chemical coagulation in terms of removal efficiency and chemical dose.

3.6.3 Kinetic and treatment efficiency of EC performance

By applying the optimal condition of electrode gap and arrangement, EC was operated with three conditions of synthetic water again to figure out the optimal time and current density as shown in Table 3.5. Current density was varied larger than previous part (from 1 to 4 mA/cm^2). Sigmoid function, Chemical reaction rate, and second polynomial equation were employed for turbidity and NOM removal in order to figure out the fitted model. The mathematical model was already expressed in eq. 3.5 (Design of Experiment section). Turbidity and absorbance were measured in every 5 min of 40 min operation.

- *Sigmoid function (S-curve)*

Nonlinear regression, S-curve equation or Sigmoid function, was expressed in eq. 3.6. This equation was studied since the turbidity removal in EC process followed three stages: lag, reactive, and steady stage.

$$Y = \frac{100}{1 + e^{-k(x-x_{50})}} \qquad \text{eq. 3.6}$$

where, Y: output

k: Steepness of the curve

x: input

x_{50}: input factor that provide 50% of the output

In this study, S-curve was derived as expressed in eq. 3.7 where η is a removal efficiency, η_{Final} is the final turbidity removal which EC could achieved, k is a steepness, and t_{50} is a treatment time that the efficiency could reach 50%.

$$\eta = \frac{\eta_{stable}}{1+e^{-k(t-t_{50})}} \qquad \text{eq. 3.7}$$

- *Simple reaction rate*

The simple chemical reaction rate was expressed in eq. 3.8 where [C] is the concentration of substance in water (mg/L), k is the equilibrium rate constant ($[mg/L]^{1-n}\ t^{-1}$), and n is the order rate.

$$-\frac{d[C]}{dt} = k[C]^n \qquad \text{eq. 3.8}$$

3.6.4 Effect of individual ion and operating condition on EC process

This section aimed to investigate the effect of individual ion and operating condition on EC in terms of turbidity and NOM removal in HA-bentonite synthetic water. It was divided into four main parts: (i) current density, (ii) initial pH, (iii) ferrous ion, and (iv) calcium ion.

For initial pH, calcium, and ferrous studies, EC was operated with current density 1 mA/cm^2 and initial pH 7 in HA-bentonite synthetic water. The effect of current density was analyzed at natural pH of synthetic water. Current density 1, 2, 3, and 4 were taken. The summary condition was shown in Table 3.6.

3.6.5 Effect of co-existing ions and operating conditions

In order to study the effect of co-existing ions and operating conditions, four steps were taken including screening, main effect, model prediction, and settling test.

Table 3.6. Summary conditions for individual ion and operation

Effect	Level				Constant
Current density	1 mA/cm^2	2 mA/cm^2	3 mA/cm^2	4 mA/cm^2	Natural pH of synthetic water
Initial pH	5	7		9	J= 1 mA/cm^2
Ferrous	1 mg/L	13 mg/L		25 mg/L	pH= 7
Calcium	3.6 mg/L	10.8 mg/L		18 mg/L	J= 1 mA/cm^2

a. Screening parameters

The screening was taken to analyze (i) the effect of bentonite to HA removal and (ii) screening effect factors including current density, initial pH, ferrous, and calcium on turbidity and HA removal.

- Effect of bentonite on HA removal

Different concentrations of bentonite with 70 mg/L of HA was studied to analyze its effect on HA removal. Bentonite was varied from 0 to 200 NTU.

- Effect of ions and operating conditions

2^k factorial design was analyzed the parameters whether they were significant effect or not on treatment performance in EC process.

b. Effect and optimization

The main parameters were evaluated the effect of these co-terms on the removal efficiency (turbidity and absorbance) and find out the optimal and worst conditions of co-ions and operating conditions for EC by using response surface methodology.

The ions contained in water were ferrous, calcium, turbidity, and HA. The current density and initial pH were operating conditions. All levels of each parameter were shown in Table 3.7 The turbidity, HA, and initial pH were observed along the time. The total experiments were 3^4=81 experiments. Therefore, central composite design in response surface methodology was conducted to design the experiment.

c. Model prediction

Model predictions of turbidity and absorbance were found out in terms of initial pH, current density, calcium and ferrous in HA-bentonite synthetic water. To analyze this model, four steps were taken as following:

- Model adequacy checking: Normal residual plots and residual vs. order of the data were analyzed to verify the data quality.
- Full quadratic model: The second polynomial equation was proposed to predict these models by using Minitab 17.

- ➢ Model adjusting: Since the full quadratic model was too long with some unnecessary terms, model shortening; therefore, was done by illuminating insignificant factors analyzed by ANOVA.
- ➢ Model validation: After predicting the model, these models were validated with overfit data. In this step, the observed data value from individual ion and operating condition was employed.

Quality of model was analyzed by standard distance (S), R-square (R^2), and R-square adjust (R^2(adj)).

- S: measure in the response variable unit. It expresses the standard distance that data values fall from the regression line. For a given understanding, the lower S is, the better the equation predicts the response. If xi and yi are the coordinates for a feature I, (X, Y) represents the mean center for the feature, and n is equal to the number of features, the distance standard S is express in eq. 3.5.

$$S=\sqrt{\frac{\sum_{i=1}^{n}(\text{x-X})^2}{\text{n}}+\frac{\sum_{i=1}^{n}(\text{y-X})^2}{\text{n}}} \qquad \text{eq. 3.9}$$

- R-square: represent the amount of variation in the observed response which can be explained by the predictor(s). The best square R is high when additional predictors are added. Therefore, Square R gives better advantages when comparing the same sizes of predictors.
- R-square adjust: describe modified R^2 value when it was adjusted for the number of terms in the model. Adding some unnecessary terms, R^2 is artificially high, but R^2(adj) may get smaller. R^2(adj) is useful for comparing different numbers of predictors. If n is the number of measurements and p is the number of parameters or variables, therefore, R^2(adj) is expressed in eq. 3.6.

$$R^2(\text{adj})=1-\left[\left(1\text{-}R^2\right)\times\left(\text{n-1}\right)/\left(\text{n-p-1}\right)\right] \qquad \text{eq. 3.10}$$

d. <u>Settling test</u>

After EC process, settling test was studied to improve some degree of purification by settling down sludge from EC treatment. Settling test was conducted in 4 L of acrylic

Table 3.7. Level of ions concentration and operating condition

Parameters	Unit	Levels		
Initial pH	-	5	7	9
Calcium	mg/L	3.6	10.8	18
Ferrous	mg/L	1	13	25
Current density	mA/cm^2	1	2.5	4

batch reactor as shown in Appendix 7. Samples were sampling at 5, 10, 15, and 20 mm depth from the top of surface water. The process of settling test were:

- The effluent of EC was remixed to make sure that the concentration of turbidity/ flocs were uniform in the tank. The mixing was done slowly around 30 round per min to prevent sludge breaking down or going up.
- Turbidity of 4 ports was measured in every 3 min until it was stable

3.6.6 Electrooxidation process

Electrooxidation was proposed to treat remained NOM from EC effluent as shown in Figure 3.6. This part was processed into 4 main parts including (i) Electrode material, (ii) kinetic analyze, (iii) effect of chloride on HA removal, and (iv) proposition of design criteria and operating cost estimation. The effluent of EC was synthesized for EO experiments.

a. Electrode material and arrangement for EO process

Electrode material is very important in enhancing kinetic of electrode and saving energy in EO process. This section aimed to study the electrode material for improving

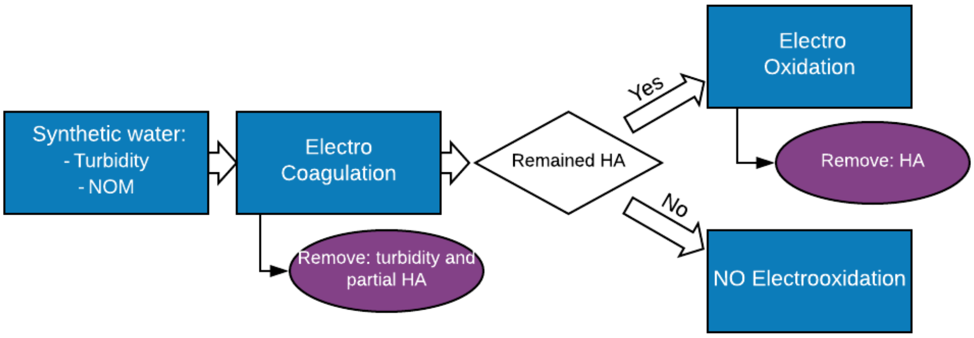

Figure 3.6. The roles of Electro Coagulation and Oxidation in turbidity and NOM removal

treatment efficiency of remained NOM in EO process. The electrode materials for (i) cathode and (ii) anode side were evaluated.

- Cathode

At cathode side, the electrode was produced the hydrogen gas to attach the pollutant to the surface of water. Graphite and aluminum cathodes were compared their performance with the effluent of EC synthetic water in terms of absorbance removal. The graphite electrode was shown in Appendix 7. The operating conditions of EO were gap 1.5 cm, current density 2.5 mA/cm^2, and graphite anode as shown in Table 3.8. The electrode arrangement was in monopolar since the electrode material of cathode were compared. It was noted that cathode and anode electrodes in bipolar were not able to compare since each electrode had both positive and negative charges.

- Electrode arrangement

After comparing electrode material for cathode side, electrode arrangement was evaluated in terms of treatment efficiency of HA.

- Anode

The comparison of graphite and conductive carbon coated onto graphite for anode were analyzed with current density 2.5 mA/cm^2 as summarized in Table 3.8.

PELCO® Conductive Carbon Glue is a conductive bond between samples and substrates which uses a graphite filter to create it. It can reduce electromagnetic or radio frequency interference and resist with large temperature change and marine environmental conditions without cracking. The processes of coating were:

Table 3.8. Electrode materials and operating conditions for EO performance

Parameters		Levels	
Current density		2.5 mA/cm^2	
Gap		1.5 cm	
Cathode study	Anode	Graphite	
	Cathode	Graphite	Aluminum
Anode study	Anode	Aluminum	
	Cathode	Graphite	Graphite coated

- Apply the conductive carbon glue on the surface of graphite
- Let it dry for 5 min at room temperature
- Recoat and cure it 24 hr at room temperature

b. Kinetic study

In order to study the kinetic of EO, current density was varied from 2.5 to 7 mA/cm^2 to figure out the optimal time and current density for HA removal from the effluent of EC by employing the best electrode materials. Finally, the chemical reaction rate was analyzed to determine the chemical reaction rate.

c. Effect of chloride on HA removal

Chloride ions could improve treatment performance in EO process by producing indirect oxidation and improving conductivity. Therefore, the effect of chloride ion on HA removal was investigated. By using optimal current density, different concentration of chloride varied from 0 to 500 mg/L Cl^- was added into wastewater.

d. Proposition of treatment process for turbidity and HA removal

The optimal conditions for EC and EO processes in turbidity and HA removal were selected to design the continuous reactors. Here, three scenarios of reactor design were proposed for HA and turbidity removal in wastewater contained turbidity, calcium, ferrous, and humic acid.

- Scenario 1: wastewater was treated in EC reactor only
- Scenario 2: EC reactor followed by sedimentation tank was proposed to remove this pollutant
- Scenario 3: EC reactor, EO reactor, and sedimentation tank were operated orderly to treat these pollutants.

Therefore, these three scenario were evaluated in terms of removal efficiency (under WHO standard). The operating cost was estimated in terms of energy consumption and electrode loss for the selected scenario.

CHAPTER 4

RESULTS AND DISCUSSION

This chapter represented the experimental and analytical results covering on three main objectives of this study including (i) optimize the treatment condition of EC process, (ii) study the effect of ion contaminations on EC performance, and (iii) HA removal by EO process. The results were divided into six main parts as following:

- Analyze the characteristic of synthetic water and conventional coagulation
- Optimize of EC electrode for improving treatment performance
    - \+ Analyze electrode gap in terms of gas flowrate and electrode loss
    - \+ Optimize electrode arrangement
    - \+ Compare EC to conventional coagulation
- Study the kinetic of EC process
    - \+ Mechanism of HA and bentonite removal in EC process
    - \+ Model prediction and validation
- Analyze the effect of individual ion and operating condition on EC performance
- Effect of co-ions and operating conditions on EC performance
    - \+ Effect and optimization of operating condition (initial pH and current density) and ion contaminations (calcium and ferrous)
    - \+ Model prediction by using second polynomial equation
- Examine EO process for HA removal
    - \+ Electrode material
    - \+ Kinetic of EO
    - \+ Effect of chloride on HA removal
    - \+ Propose continuous reactor design

4.1 Synthetic water characteristic and conventional treatment

This part was divided into two main parts: (i) analyze the characteristic of synthetic water and (ii) determine alum dose for treating these pollutants by chemical coagulation.

4.1.1 Synthetic water characteristic

Three types of synthetic water including HA, bentonite, and HA-bentonite were analyzed in EC and EO process. Therefore, their characteristics were initially analyzed. Turbidity and absorbance were measured along the time by gravity.

a. Bentonite

Bentonite is a colloidal clay and highly plasticity which causes the turbidity in water due to the repulsive force of particle (Abuzaid et al., 1998). In this study, bentonite in calcium base was employed and the chemical component was summarized in Table 4.1. This bentonite powder was prepared by mixing it into tap water using rapid mixing in 300 rpm for 5 minutes, followed by slow mixing 40 rpm in 30 minutes for well dispersing particle in water (Al-Sameraiy, 2012). However, this turbid water was not stable due to the different size distribution of bentonite. Thus, the duration for stabilizing turbidity was studied. Different initial concentrations of bentonite (849 NTU, 523 NTU, and 195 NTU) were measured along the time as expressed in Figure 4.1. The results showed that turbidity was almost stable after 30 minutes gravity settling. Finally, the supernatant of bentonite after settling down 30 minutes was synthesized as a turbid stock solution. Additionally, the characteristic of turbid water 100 NTU was shown in Table 4.2. It has noticed that the total suspended solids was round 218 mg/L and had DOC similar to tap water.

Table 4.1 showed the characteristic of bentonite which this study focused. The components of bentonite are SiO_2, Al_2O_3, and Fe_2O_3. Bentonite was in calcium base, so slightly high concentration of calcium in synthetic water.

Table 4.1. The componant analyze of bentonite from manufacture

Components (calcium base)	Value (%)
Chemical compositions	
SiO_2	70
Al_2O_3	14
Fe_2O_3	1.9
Physical performance	
Passing rate (200 mesh=74 micron)	95

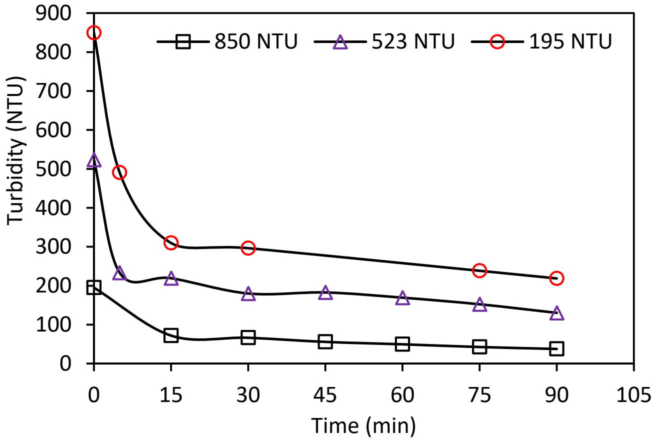

Figure 4.1. Evaluation of bentonite as turbidity with different initial concentration

b. Natural organic matter

Humic acid, agricultural grade, 70% purity was studied. It created dark brown color and high suspended solid. It was a mixture of 65% weak aliphatic (carbon chains) and 35% aromatic (carbon rings) organic acids with molecular size from 10,000 to 100,000 (Pettit, 2004). HA was measured by using UV-vis spectrophotometer at 293 nm. Since standard curve of HA and absorbance was in linear relationship (Figure 4.3), the HA removal was therefore measured in terms of absorbance. The characteristic of 70 mg/L of HA was illustrated in Table 4.2. The solution was slightly in base condition and had high suspended solid. Therefore, HA studied here had high colloidal particle and low in DOC. Figure 4.2 showed the absorbance of HA agricultural and technical grade along

Table 4.2. Physicochemical characteristics of synthetic water

Parameters	Turbidity (NTU)	Ca^{2+} (mg/L)	Cl^- (mg/L)	Conductivity (μS/cm)	pH (-)	DOC (mg C/L)	TSS (mg/L)
Tap water	1.1 ± 0.60	24.6±0.30	15.30±0.28	290 ± 10	7.27 ± 0.20	2.47	-
Bentonite (100 NTU)	100.3 ± 0.96	30.45±1.45	17.20±1.79	303 ± 13	7.18 ± 0.09	2.94	217.72 ±13.92
HA (70 mg/L)	26.4 ± 1.62	25.90±2.4	17.10±0.26	309 ± 12	7.42 ± 0.07	6.73	54.66 ±1.53
HA-Bentonite	109±5	30.85±0.47	20.90±0.85	313±11	7.24±0.1	6.65	267.33± 18.58

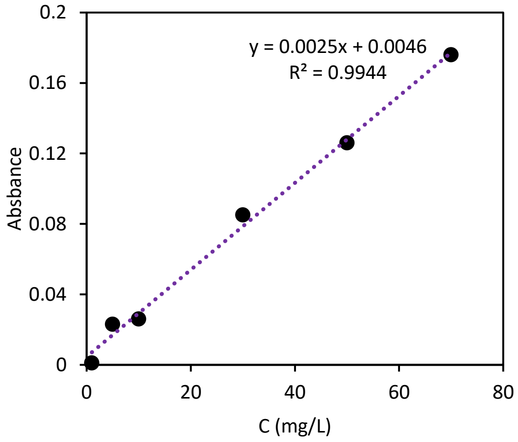

Figure 4.3. Standard curve of HA

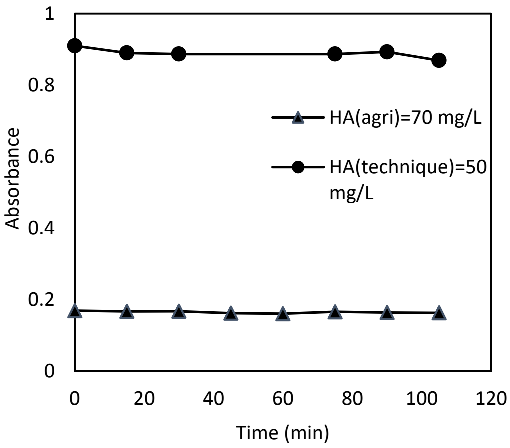

Figure 4.2. Absorbance of HA agricultural versue techincal grade

the time. It noticed that both absorbance of HA agricultural and technical grades did not decreased by gravity sedimentation and the absorbance of HA technical grade was higher than HA agricultural grade's.

c. HA-Bentonite

HA-Bentonite was synthesized by directly mixing 70 mg/L of HA into 100 NTU turbid which was synthesized by using bentonite stock solution. HA-bentonite was measured along the time as shown in Figure 4.4. The result showed HA-Bentonite was reminded around 30 NTU after keeping it settle down about 90 min by gravity as shown in Figure 4.4. However, the absorbance was not decreased. It could conclude that HA has two forms: soluble measuring by absorbance and insoluble which was able to attach bentonite to settle down. HA looks like fibers or bundles of fibers at acidic or neutral pH, so it could trap bentonite to settle down resulting in turbidity reduction Zhang et al. (2017). The composition of HA has a large number of aromatic rings linked to alkali chains of variable length, resulting in a flexible skeleton that can help bridges between bentonite and HA. HA polymer readily bind clay minerals to form stable organic clay complexes (Pettit, 2004; Zhang et al., 2017). However, even HA could improve bentonite removal, but it still took long time to settle down. Therefore, electrocoagulation was still required to treat this pollutant (HA-Bentonite). The characteristic of HA-Bentonite was also shown in Table 4.2. The dissolved organic carbon (DOC) was similar to HA synthetic water.

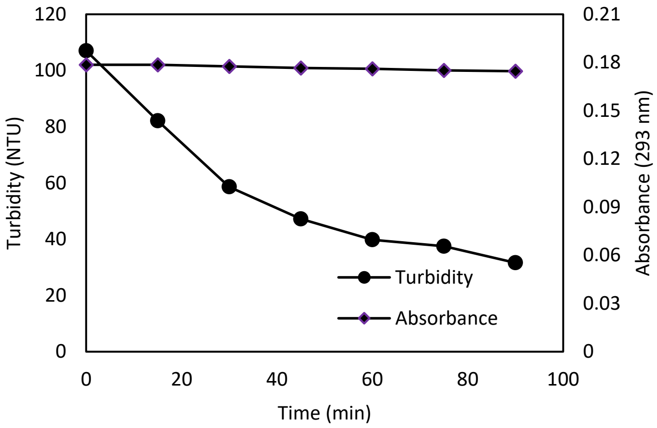

Figure 4.4. Turbidity and HA(absorbance) removal by gravity settling

4.1.2 Chemical coagulation (Jar test)

Chemical coagulation plays an important role to remove colloid and fine dispersion substance from water treatment. The objective of CC in this study was to determine the optimal alum dose for Bentonite, HA, and HA-Bentonite removal for comparing with EC process.

a. Bentonite

The result in Figure 4.5 (a) showed the treatment efficiency and pH evolution of bentonite through different chemical dosages. After adding alum 10 mg/L, the removal rapidly increased to 95 % and continually increased to 99% when 30 mg/L of alum was consumed. Increasing higher dose, the removal efficiency was very slightly increased and generated large volume of sludge. Therefore, the required optimal alum dosages were 30-40 mg/L for 100 NTU of Bentonite removal. The flocs formed of alum has been noticed that it was easily to break-up under little agitation which made it was difficult to separate. Moreover, the residual sulfate concentration from alum has a high specific conductivity in treated water (Vik et al., 1984) and conventional treatment may need to add alkalinity in the system.

b. Humic acid

Humic acid was gradually removed more than 99% after adding alum 70 mg/L and its turbidity was also decreased as shown in Figure 4.5 (a). The pH evolution after adding alum from 0 to 100 mg/L was in good range for floc formation. Generally, HA was removed by adsorptions mechanism of oxides rather than destabilization in Chemical

Coagulation (CC) (O'melia et al., 1999). The optimal dose required was about 70 to 80 mg/L.

c. <u>HA-Bentonite</u>

Figure 4.5 (c) showed the turbidity and HA removal from synthetic water contained both pollutants. The optimal dose required to removal HA and turbidity in HA-bentonite synthetic water was about 90 to 100 mg/L with final pH 6.3. Therefore, this pH range was able to form the flocs.

4.2 Optimization of EC electrode for improving treatment performance

The optimal electrode conditions for improving treatment performance was the objective of this part. To optimize condition of EC electrode in this section, two steps were examined: (i) Analyze electrode gap and current density in terms of the ratio of gas flowrate to electrode loss and (ii) Optimize electrode arrangement in terms of treatment performance (bentonite, HA, and HA-bentonite).

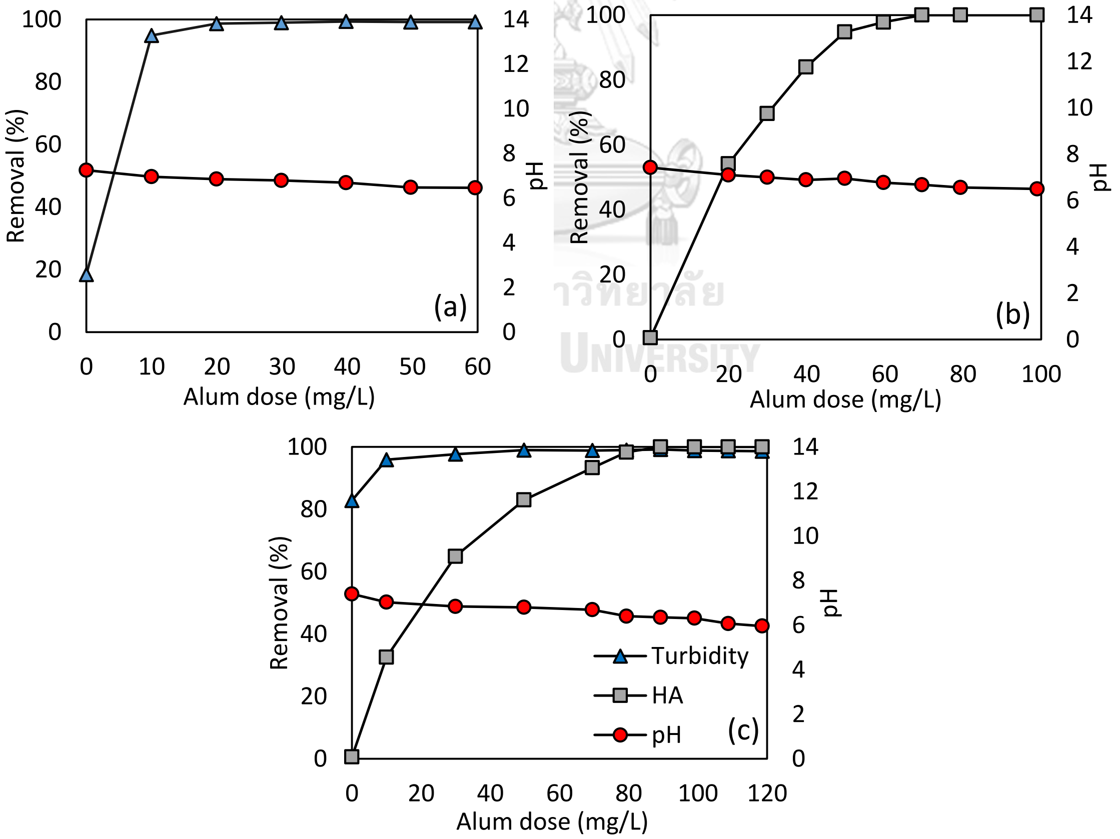

Figure 4.5. Chemical coagulant consumption in (a) Bentonite, (b) HA, and (c) HA-bentonite removal by Jar test

4.2.1 Analyze electrode configuration

Electrode gap and current density are very important in EC process. Current density defined the energy consumption and reaction rate (Hossain et al., 2013). For electrode gap, too short gap could make polarize reversion and too far related to Ohmic drop and high energy consumption (Karichappan et al., 2014). Therefore, this part was to optimize electrode gap and current density in terms of the ratio of gas flowrate and electrode loss (Qg/Loss) since improving gas flowrate could increase mixing and floating and high electrode corrosive was the disadvantage of EC process.

The electrode gaps: 1.0, 1.5, and 2.0 cm and current density: 1.5, 2.0, and 2.5 mA/cm^2 were studied at different operation times: 4 min, 9 min, and 14 min by using tap water. The generated gases from the system were hydrogen and a certain amount of oxygen which were generated from cathode and probably released from the anode side, respectively (Eq. 4.1 to 4.4). In overall of monopolar and bipolar arrangements (Figure 4.6), the Qg/Loss increased along the operating time since the partial current was lost for heating the electrodes at the beginning, so only the remaining amount could be used for electrolysis. Therefore, only limited amount of hydrogen gas was released. After a while, the electrodes could transfer electron well, amount of released hydrogen gas was increase more into the solution.

In bipolar and monopolar arrangement, 1.5 mA/cm^2 of current density with 2 cm and 1.5 cm of electrode gap were obtained as the optimal EC configuration as they could generate high gas flowrate with a small amount of electrode loss, respectively.

In anode:

$$\mathrm{Al} + \mathrm{Al}^{3+}_{(aq)} + 3e^{-} \qquad \textit{eq. 4.1}$$

$$2\mathrm{H_2O} \rightarrow 4\mathrm{H}^{+}_{(g)} + \mathrm{O}_{2(g)} + 4e^{-} \qquad \textit{eq. 4.2}$$

In cathode:

$$\mathrm{Al}^{3+}_{(aq)} + 3e^{-} \rightarrow \mathrm{Al}_{(s)} \qquad \textit{eq. 4.3}$$

$$2\mathrm{H_2O} + 2e^{-} \rightarrow \mathrm{H}_{2(g)} + 2\mathrm{OH}^{-} \qquad \textit{eq. 4.4}$$

4.2.2 Optimize electrode arrangement

The optimal condition of EC configuration from the previous results was examined with 100 NTU of Bentonite, 70 mg/L HA, and simultaneous of both pollutants with the same

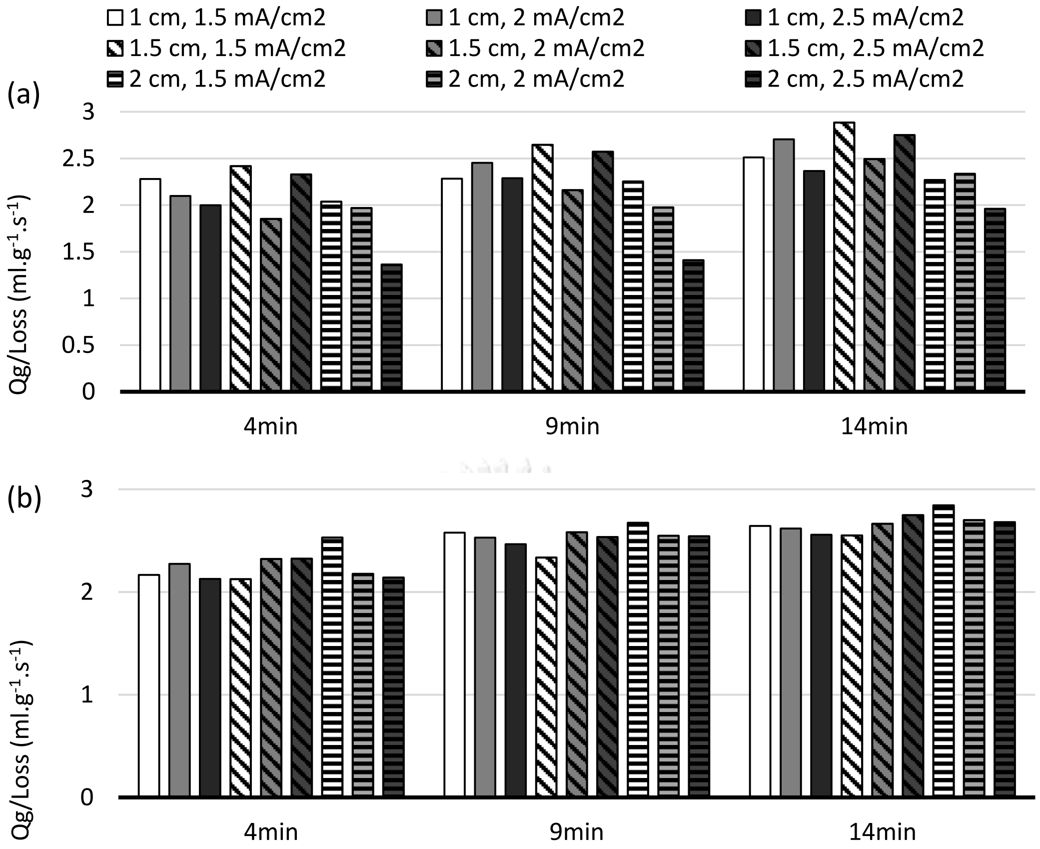

Figure 4.6. Qg/Loss performance with electrode gaps and current densities: (a) monopolar, and (b) bipolar

concentration as individual study. The results were summarized in Figure 4.7. It showed that bipolar arrangement was better than the monopolar in terms of treatment efficiency. This might attribute to the arrangement of circuit. Monopolar is a parallel connection and bipolar is a series connection. Therefore, the current pass through each electrode of bipolar was higher than monopolar two time, so dissolution of electrode material (coagulant) of bipolar was higher than monopolar (Faraday's law and and more generated bubble gas (Akbal and Camcı, 2011). Similarly, previous studies also confirm that bipolar had higher treatment efficiency than monopolar in natural organic matter removal (M Alimohammadi et al., 2017; Asselin et al., 2008; Jiang et al., 2002). At 20 minutes treatment, bipolar could improve Bentonite, HA, and HA-Bentonite about 38%, 49%, 11% of turbidity and 32% of HA, respectively, greater than monopolar arrangement as expressed in Table 4.3. Therefore, bipolar arrangement of the electrodes was finally selected.

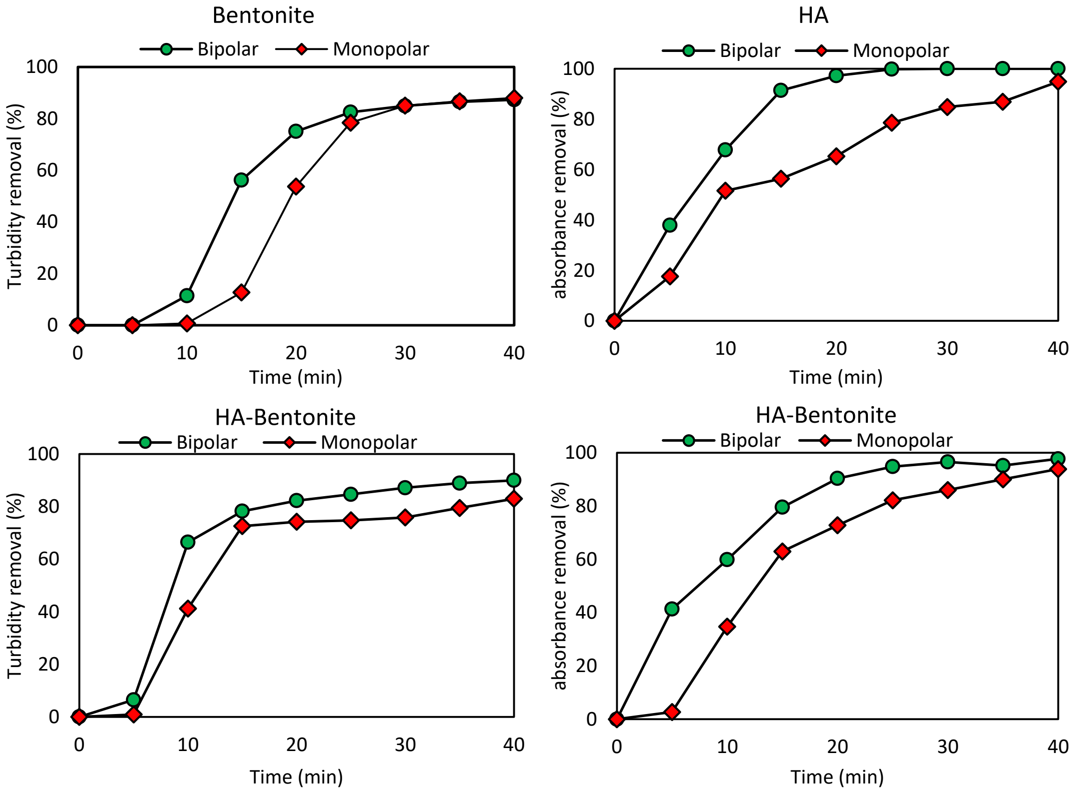

Figure 4.7. Removal efficiency of mono- and bipolar

4.2.3 Compare chemical coagulation and EC

As mentioned, the required optimal alum dosages were 30-40 mg/L, 70-80 mg/L, and 90-100 mg/L for bentonite, HA, and HA-bentonite synthetic water, orderly. Table 4.3 noticed that the chemical release from the electrode material of EC for treating bentonite, HA, and HA bentonite were similar.

Table 4.3. The removal efficiency of Mono-and Bipolar after 20 min EC treatment

Pollutants		% Removal ± SD		Mean improvement of Bipolar over Monopolar (ΔP) (%)
		Monopolar (M)	Bipolar (B)	
Bentonite		54.40 ± 0.62	75.02 ± 0.24	37.90
HA		65.27 ± 2.03	97.20 ± 1.25	48.92
HA-Bentonite	Turbidity	74.23 ± 0.40	82.27 ± 0.10	10.83
	HA	71.78 ± 3.19	94.79 ± 3.19	32.06

Note: $\Delta P = \frac{\%B - \%M}{\%M} \times 100$

Bentonite removal by chemical coagulation (CC) of Jar test was slightly higher than EC process but required alum dose around two times lower than EC process. Therefore, Jar test was better in bentonite removal in terms of treatment efficiency and chemical dosage.

For HA removal, the alum dose and electrode loss (aluminum) were similar with same removal efficiency of absorbance, but the turbidity removal from Jar test was higher than EC.

On the other hand, when the water contained both HA and Bentonite, CC could remove turbidity better than EC around 10% while the absorbance removal was similar. However, CC consumed chemical dose around 1.5 time higher than EC process since EC could produce hydrogen gas while CC was not. In sum, EC was better employed when the water contained both pollutant. Moreover, the flocs formed of alum had been noticed that it was easily broken-up under little agitation. Therefore, it is difficult to separate while EC could produce more compact sludge. In addition, the residual sulfate concentration from alum has a higher specific conductivity in treated water while EC can reduce the conductivity from water (Tchamango et al., 2016; Vik et al., 1984). This might explain that the anions (Chloride, nitrate, sulfate) in solution could attach Al^{3+}, some cations (Calcium, Magnesium) in solution also could adsorb on the flocs of aluminum hydroxide, and formation of polymer formation of Al^{3+} such as $Al_n(OH)_{3n}$ (Lekhlif et al., 2014). Therefore, the conductivity was decreased in EC process. Moreover, CC treatment may need to be added alkalinity in the system while EC does not.

Therefore, electrocoagulation process was investigated in this study due to the

Table 4.4. Comparison of chemical coagulation to EC process

Types	Chemical consumption		% Removal	
	mg/L		Absorbance	Turbidity
Bentonite	Alum	30.00	-	98.96
	EC (electrode loss)	69.47	-	94.73
HA	Alum	70.00	<99.4	-
	EC (electrode loss)	66.85	<99.4	-
HA+ Bentonite	Alum	90.00	98.99	98.33
	EC (electrode loss)	59.88	<99.4	89.48

convenient operation, low electrode loss, no chemical added, compressed system, and little-compacted sludge. Tchamango et al. (2016) also recommended to use EC since its effluent was able to recycling.

4.2.4 Summary

The optimal condition of electrode configuration and arrangement was at gap 2 cm, current density 1.5 mA/cm^2, and bipolar arrangement. EC was better performed than CC process in HA-bentonite synthetic water, while bentonite synthetic was preferable to treat by CC. The current density was required to optimize again in the next section.

4.2 Kinetic study of electrocoagulation

This section was divided into two parts including mechanism study and model prediction. By using the optimal gap and arrangement from the previous part, the kinetic was carried out in terms of synthetic water containing bentonite, HA, and HA-bentonite by varying current density from 1 mA/cm^2 to 4 mA/cm^2 to seek out the optimal time and current density.

4.3.1 Bentonite and HA removal

a. Bentonite removal

The removal of turbidity was divided into three stages called lag, reactive, and stable stages as shown in Figure 4.8 (a) (Chawaloesphosiya et al., 2015). At the beginning, the hydrogen gas generated from cathode side and aluminum ions from anode side was released in small amount due to electric losing for heating electrodes. It might be able to destabilize the particle, but it was not able to form sweep flocs for settling down. Moreover, the polymerization of aluminium hydroxide also created turbidity (Adjeroud et al., 2015). Therefore, the turbidity was increased or similar to the initial concentration, called lag stage. After a while, more aluminum precipitates attached the particles to form flocs resulting in the destabilization and it raised upward by hydrogen gas, called reactive stage. After the removal efficiency reached the limitation of EC, it became steady stage. This mechanism is summarized in Figure 4.9 (a). Merzouk et al. (2009) investigated the removal of turbidity and heavy metal using EC process. The removal of turbidity was also followed this three stages. Moreover, Figure 4.8 also showed that higher current density could improve the treatment performance (SEID et al., 2015). The optimal current density was found at 3 mA/cm^2 with 20 min treatment as illustrated in Figure 4.8 (a).

b. <u>HA removal</u>

Figure 4.8 (b) showed the absorbance removal in EC process with variation of current density. The treatment performance of HA 70 mg/L was improved with the increasing

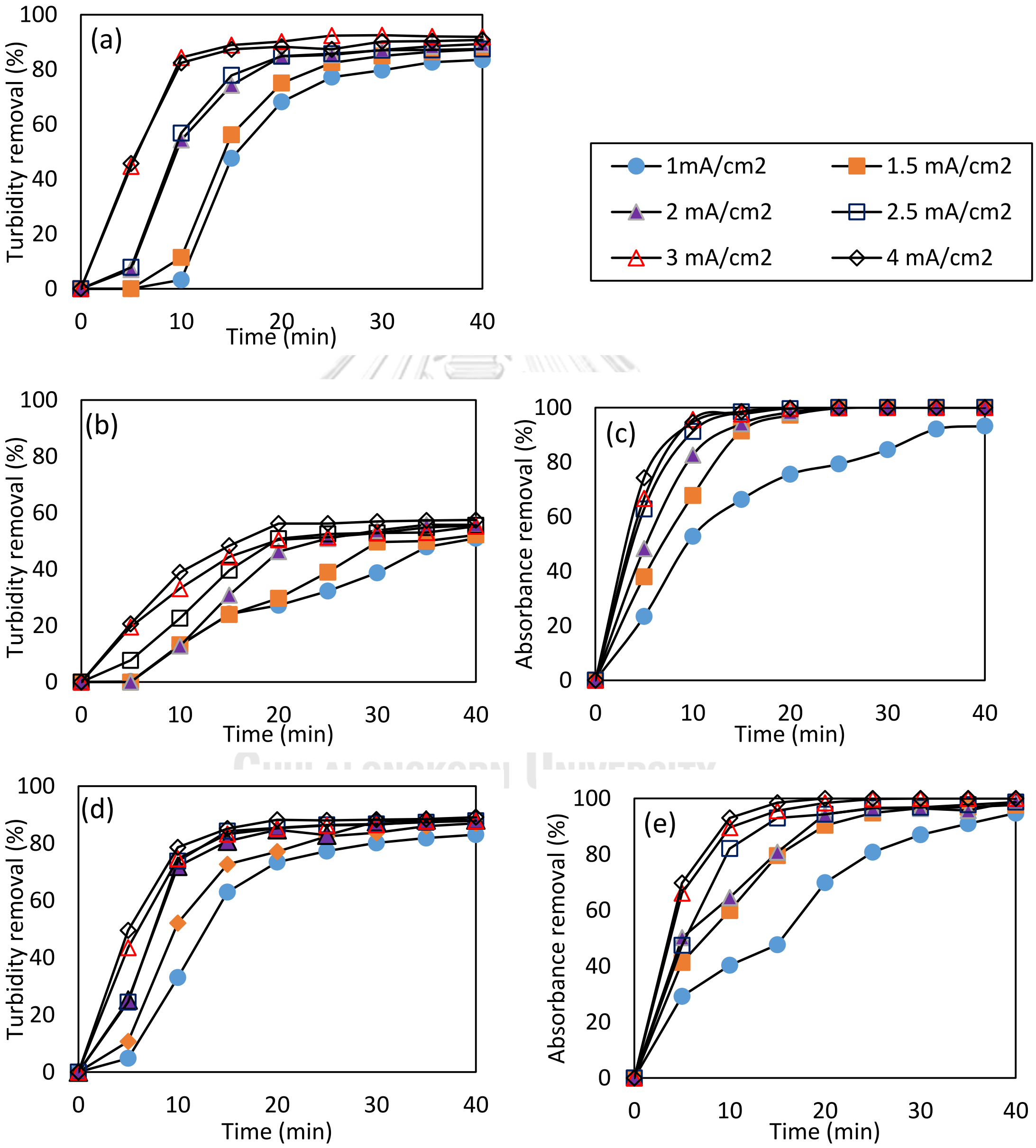

Figure 4.8. The kinetic of (a) bentonite, (b) turbidity of HA, (c) absorbance of HA, (d) turbidity of HA-bentonite, and (e) absorbance of HA-bentonite removal at different current density in EC process.

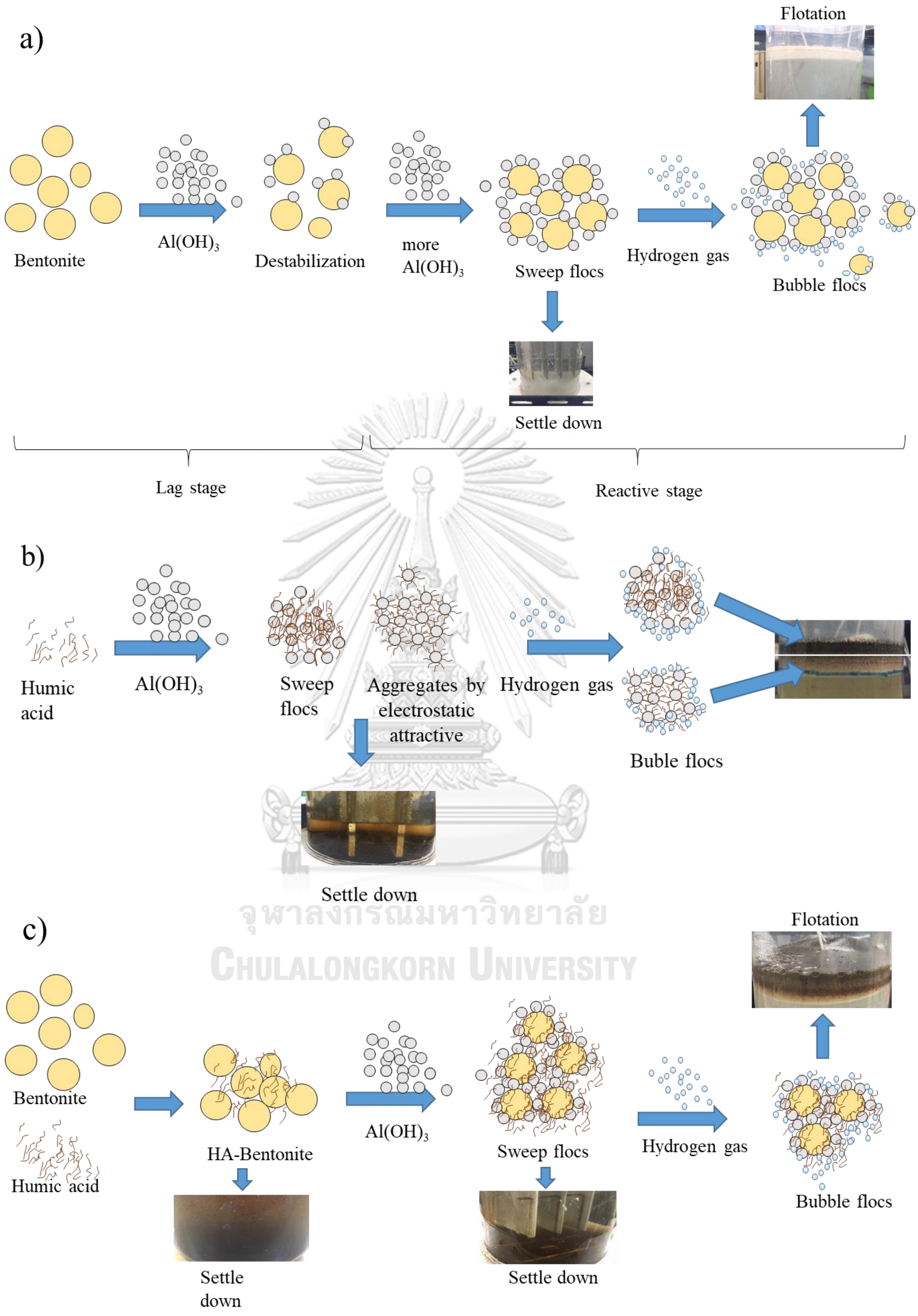

Figure 4.9. Mechanism of (a) Bentonite, (b) humic acid, and (c) HA-Bentonite removal in Eectrocoagulation process.

]

of reaction time. HA can be removed either electrostatic attraction mechanism and surface complexation during the precipitation of aluminium hydroxides (Mahmood Alimohammadi et al., 2014). Some research stated that HA removed by adsorption, sweeping flocculation, and charge neutralization mechanism that made it was removed faster than bentonite as shown in Figure 4.9 (b) (SEID et al., 2015). Then, it was able settle down or attached with hydrogen gas to float to the surface of water. The suspended colloid HA might be removed by destabilization of aluminium ion as bentonite (Asselin et al., 2008). The optimal current density and time were 3 mA/cm^2 and 20 minutes, respectively.

c. <u>HA-bentonite removal</u>

Absorbance and turbidity graphs (Figure 4.8) of HA-Bentonite synthesis are similar to HA's and Bentonite's, respectively. At the beginning stage, turbidity was removed faster than synthetic water containing only Bentonite because of HA colloid as shown an example in Figure 4.10 (a) at current density 1.5 mA/cm2. HA could produce bridges for Bentonite to form flocs because its composition has numerous of aromatic rings linked by alkyl chains of variable lengths as shown in Figure 4.9 (c). At acidic or neutral pH, the structure of HA forms fibre or bundles of fibre (Zhang et al., 2017). After 20 minutes of treatment, the removal efficiency of HA-Bentonite was similar to synthetic water contained only Bentonite.

In overall, the absorbance removal of HA-Bentonite was similar to synthetic water contained only HA as shown an example in Figure 4.10 (b).

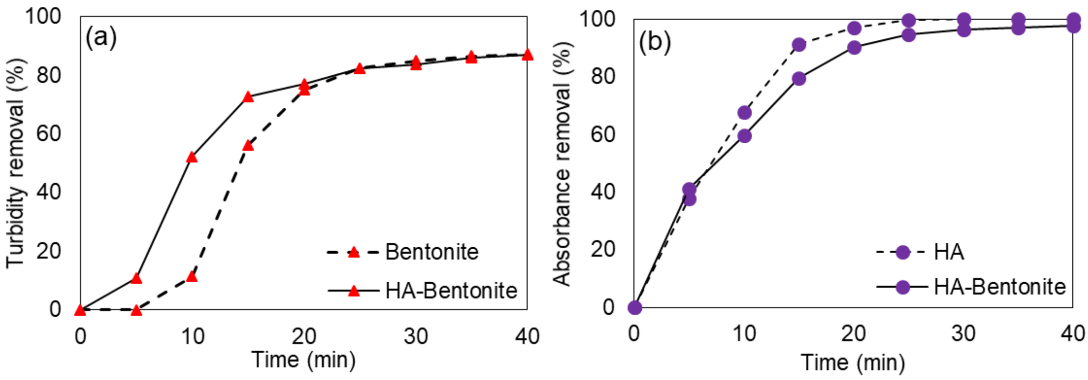

Figure 4.10. The treatment efficiency of (a) turbidity of Bentonite vs. HA-Bentonite and (b) absorbance of HA vs. HA-Bentonite with current density 1.5 mA/cm^2.

4.3.2 Model prediction

The objective of this part was to study the fitted model of bentonite, HA, and HA-bentonite removal in EC process. Three models were analyzed including chemical reaction rate, Sigmoid function, and statistical modeling.

a. Sigmoid function and chemical reaction rate

Sigmoid function and simple chemical reaction rate (zero-, first-, and second-order) were compared for considering the better fitted model for turbidity removal which was evaluated by R-square. Sigmoid function was employed since turbidity removal had three stage as S-curve. If [C] is the concentration (mg/L), [C_o] is the initial concentration (mg/L), k is the equilibrium rate constant ($[mg/L]^{1-n}$ t^{-1}), η is the removal efficiency (%), t is operation time (min), and K is the steepness coefficient (1/min), the equation of these models are:

Zero-order: $[C] = -kt + [C_o]$

First-order: $\ln[C] = -kt + \ln[C_o]$

Second-order: $\frac{1}{[C]} = kt + \frac{1}{[C_o]}$

S-curve: $\eta = \frac{\eta_{stable}}{1+e^{-k(t-t_{50})}}$

- *Bentonite*

The results of predicted model (Sigmoid equation, zero-, first-, and second-order chemical reaction) in terms of turbidity removal in Bentonite synthetic water with different current densities were validated with observe data. Figure 4.11 showed the validation at current density 1 mA/cm^2 and the result of other current densities was similarly (not shown graph). The most fitted model was Sigmoid function with all ranged current density based on R-square. Therefore, Sigmoid equation (S-curve) was employed to predict the turbidity removal. The k value, t_{50}, and R^2 of the validation between model and observe value was summarized in Appendix 1. The result in Figure 4.12 shows the steepness coefficient (k) of 100 NTU bentonite removal in Electrocoagulation. The k value was increased when current density increased.

- *Humic acid removal*

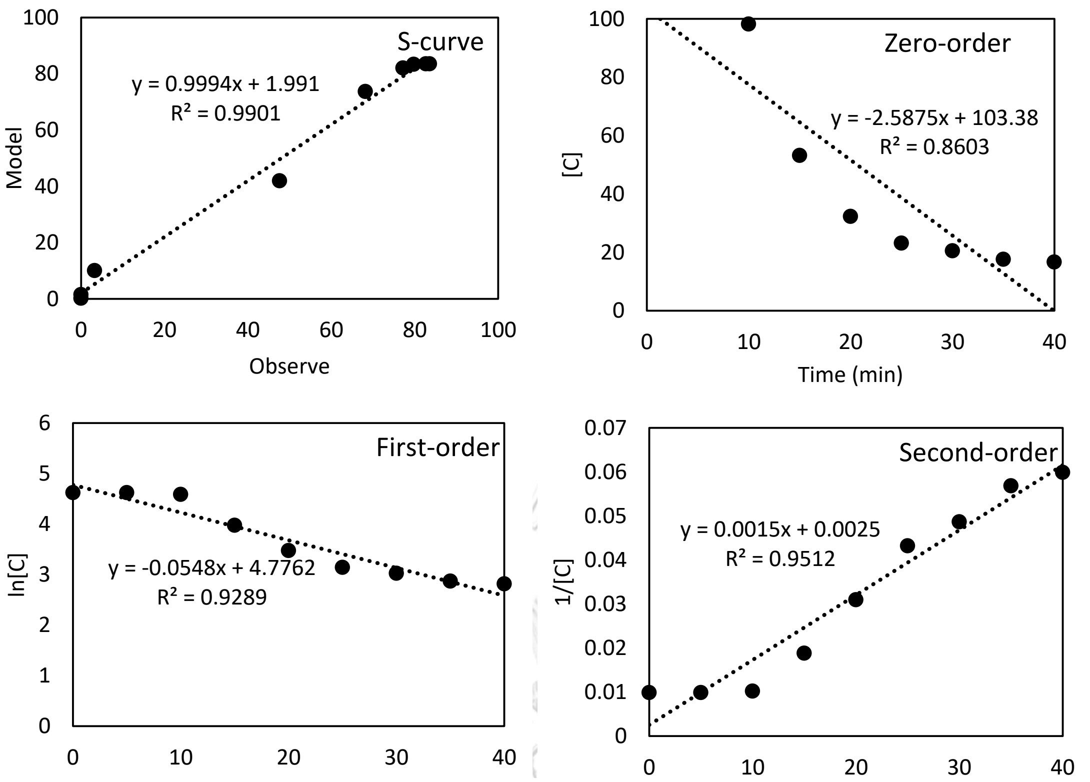

Figure 4.11. The validation of observed data to different predicted equations based on R-square

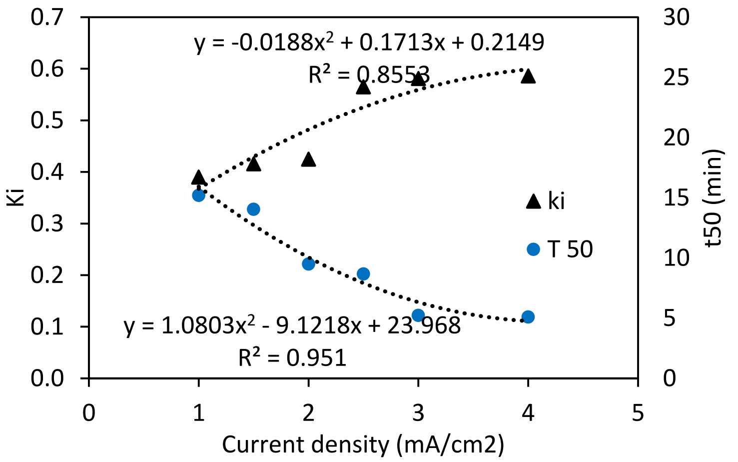

Figure 4.12. k value and t_{50} of turbidity prediction of differenct current density

The experimental results of HA removal in different current densities (1, 1.5, 2, 3, and 4 mA/cm^2) was analyzed with simple chemical reaction rate. The results showed that absorbance removal was fitted to first-order kinetic since it had the highest R^2. An example result of HA removal employed with current density 1 mA/cm^2 was shown in Figure 4.13. Therefore, the absorbance removal of HA synthetic water was predicted using first-order kinetic. All constant rates (k_i) were analyzed by using solver function in Microsoft excel as shown in Appendix 1.

The constant rate (k) was gradually increased when the current density increased as shown in Figure 4.14. It meant that increasing current density could increase the chemical reaction in system.

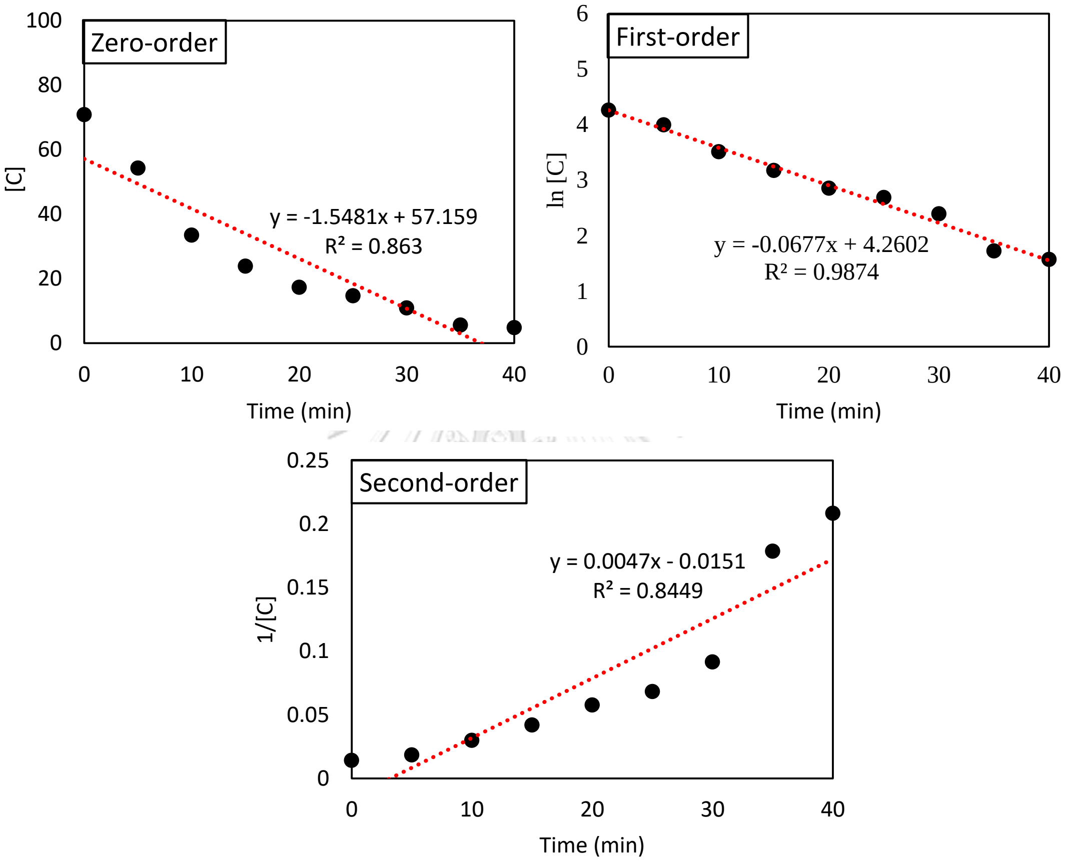

Figure 4.13. Scatter plot for the rate constant in zero, first, and second-order

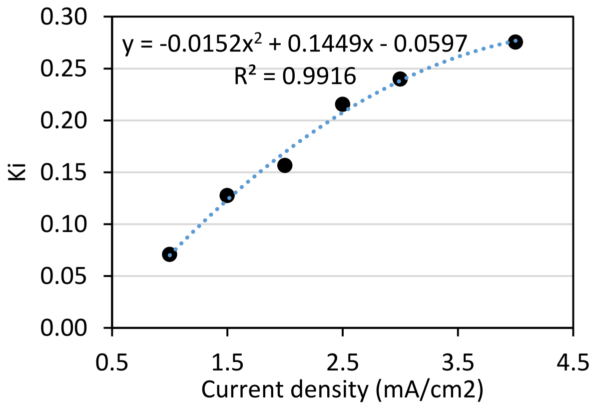

Figure 4.14. Constant rate (ki) of 1st order in HA removal in HA synthetic water

- *HA-Bentonite*

HA-bentonite was predictied in terms of turbidity and HA removal. The validation of turbidity removal prediction in Logistic function had $R^2 = 0.99$ and all graphs of validity were shown in Appendix 1. Figure 4.15 showed the relationship between current density and steepness coefficient and duration which treatment could reach 50% removal. K value was increased when the current density was increased from 1 mA/cm2 to 4 mA/cm^2. By using first-order kinetic, the graphs of HA model prediction were shown in Appendix 1. Figure 4.16 shows the function of k value with current density.

b. Statistical modeling

Statistical modelling is an another method to predict the turbidity and humic acid

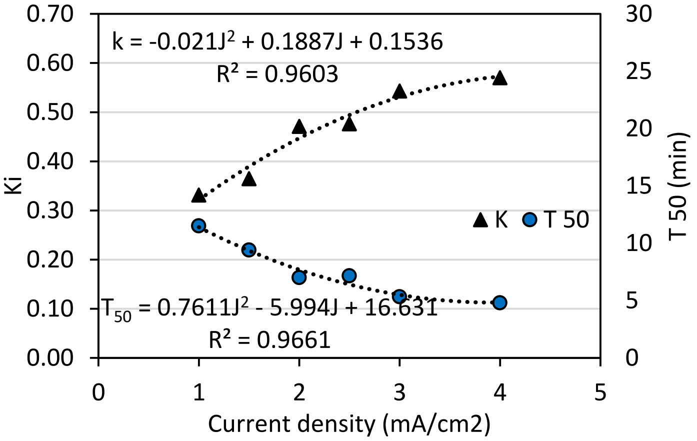

Figure 4.15. Validation of steepness coefficient and T_{50} observed data to predicted equation of HA-bentonite for turbidity removal

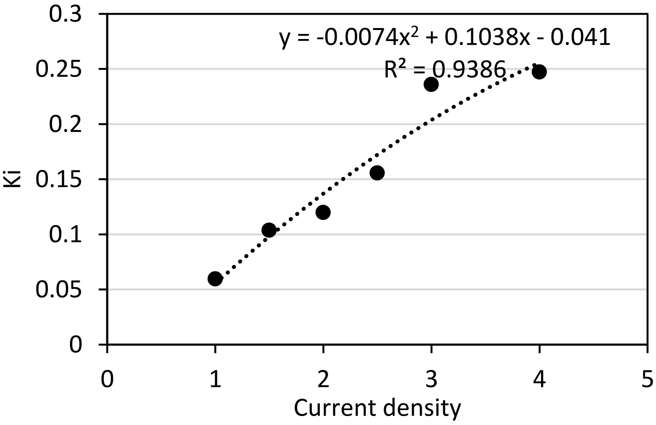

Figure 4.16. Validation of predicted constant rate (k) with ovserved data of HA in HA-bentonite synthetic water

removal in EC process. The objectives of using this mathematical equation were to figure out that the removal efficiency of bentonite and HA could be predicted with this equation or not and also evaluate its correlation to Sigmoid function and 1st order chemical reaction rate.

By using multiple regression analysis, Bentonite (R_1%), HA (R_2%), and HA-Bentonite (R_3%: turbidity and R_4%: absorbance) removal were produced in various empirical correlations with two factors including time (T: 5, 15, and 25 minutes) and current density (J: 1.0, 1.5, 2, 2.5, 3.0, and 4.0 mA/cm^2), the responses were using the second-order polynomial with multiple variables. The results were expressed in full quadratic forms as shown in eq. 4.11 to 4.14 with prediction regressions (R^2). In overall analysis of the models, the coefficients of determination R^2 were higher than 0.95.

To confirm the reliable of model prediction, the graphs of observed value versus predicted values were plotted as shown in Figure 4.17. It showed that the second-order polynomial models correlated well to the experimental results for Bentonite, HA, and HA-Bentonite removal. The red linear lines showed the percentage errors of model values to observed values. The result indicated that the model prediction of bentonite passed 10 % error and only few points were out of the range as shown in Figure 4.17(a). For HA and HA-Bentonite graphs were also similar to the one of bentonite's as shown in Figure 4.17 (b) & (c). Most of data values were in red line. Therefore, the predicted data values were in 10% of discrepancy.

Table 4.5. Empirical correlations of bentonite, HA, and HA-bentonite removal in EC process

Pollutants	Model	R-square	
Bentonite (Turbidity)	$R_1\% = -89.6 + 11.26\ T + 33.6\ J - 0.2071\ T^2 - 2.18\ J^2 - 0.716\ T.J$	0.96	Eq. 4.5
HA *(Absorbance*)	$R_2\% = -54.54 + 8.660\ T + 47.58\ J - 0.1669\ T^2 - 5.64\ J^2 - 0.617\ T.J$	*0.98*	Eq. 4.6
HA-bentonite (Absorbance)	$R_3\% = -71.03 + 11.238\ T + 29.67\ J - 0.2304\ T^2 - 2.336\ J^2 - 0.623\ T.J$	*0.99*	Eq. 4.7
HA-bentonite (Turbidity)	$R_4\% = -36.7 + 6.10\ T + 39.96\ J - 0.0981\ T^2 – 4.53\ J^2 - 0.409\ T.J$	*0.95*	Eq. 4.7

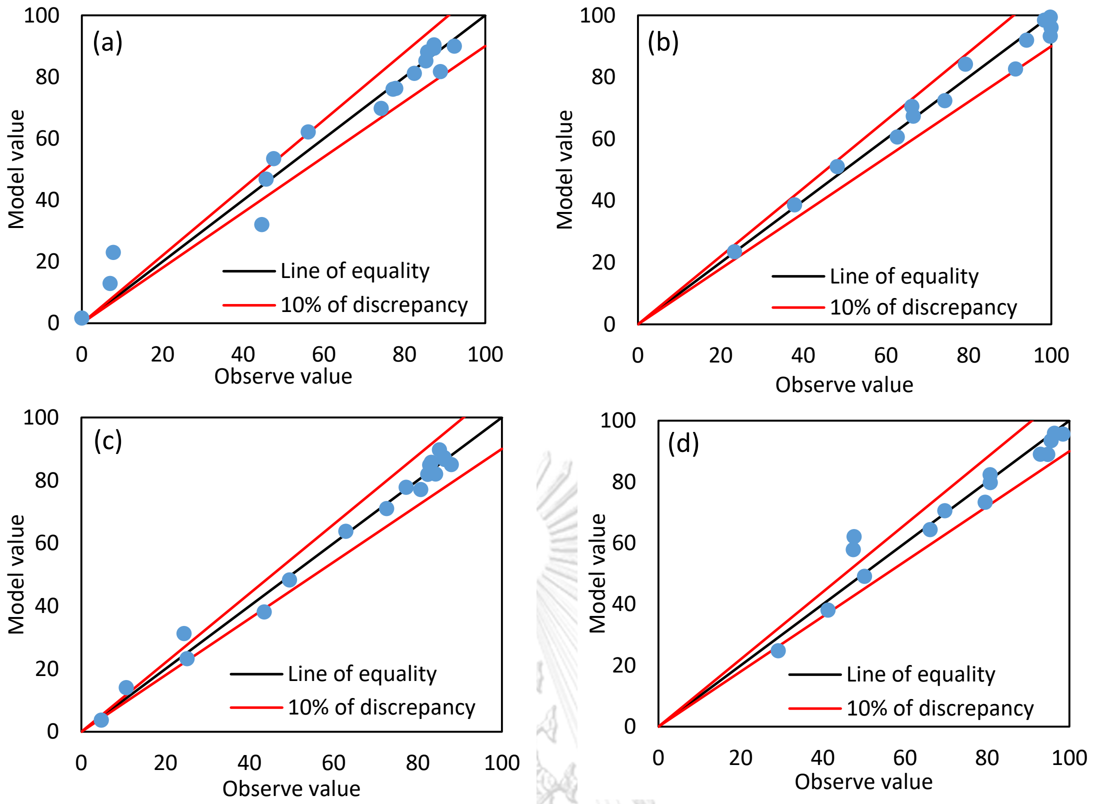

Figure 4.17. (a) turbidity removal and (b) humic acid removal in synthetic water contained 70 mg/L of HA with different concentration of bentonite

4.3.3 Summary

In summary, the kinetic of bentonite removal has three stages: lag, reactive, and stable stage following destabilization mechanism while HA can be removed faster by sweeping flocs mechanism. HA improved turbidity removal in HA-bentonite since its colloid could attach the pollutants. The optimal reaction time of these pollutants was found at 20 minutes with current density 3 mA/cm^2.

Comparing equations of Sigmoid function, chemical kinetic rate and empirical correlation, empirical correlation was the most fitted model with the highest R-square. It was able to predict both turbidity and absorbance and convenient in calculation. Therefore, the model prediction of the effect of operating conditions and ion contaminations on turbidity and absorbance removal was analysed by using second-polynomial equation at optimal reaction time.

4.4 Individual effect of ion and operating condition

The objective of this part was to analyze the mechanism of the effects of individual operating conditions (i.e., current density and pH) and ion concentrations (i.e., calcium and ferrous) in terms of turbidity and HA removal in HA-bentonite at 20 minutes treatment time. Therefore, the explanation was divided into (i) turbidity and (ii) HA removal. The effects of pH, calcium, and ferrous ions were studied at the lowest current density (1 mA/cm^2) for demonstrating their effects on turbidity and HA removal as shown in Table 4.7. However, the effect of current density was operated in EC at natural (pH 7.49±0.15) without any adjustment and any ions. The summarized conditions was demonstrated in Table 4.6.

4.4.1 Turbidity removal

a. Current density

Current density (J) is an important parameter in EC process since it controls the reaction rate and determines the coagulant dosage in the solution. High current density provides a large amount of coagulant released into an aqueous solution, so the speed of treatment is also increased. Meanwhile, some disadvantages were found such as energy consumption, electrode loss, large sludge and costs of operating (Hossain et al., 2013; Malakootian et al., 2010).

The current density was varied from 1 to 4 mA/cm^2 in synthetic water containing 70 mg/L of HA and 100 NTU of bentonite with its natural pH without any adjustment, 7.49±0.15. Because HA also caused the turbidity, the initial turbidity of this solution, therefore, was produced approximate 108.3 ± 2.7 NTU. The results in Figure 4.18 showed the turbidity removal at 20 minutes were 73.41%, 84.73%, 85.25%, and 88.24% after applying the current density 1, 2, 3, and 4 mA/cm^2, orderly. It was clarified that

Table 4.6. The conditions of individual effect analyze

Parameter	Unit	Level				Constant
Current density	mA/cm^2	1	2	3	4	Natural pH
Initial pH	-	5	7		9	J= 1 mA/cm^2
Ferrous	mg/L	0	1	13	25	pH= 7 and J= 1 mA/cm^2
Calcium	mg/L	0	3.6	10.8	18	

higher current density could increase the treatment efficiency by introducing more aluminum hydroxides and improving hydrogen gas. Thus, more precipitated aluminum attaches with the particles or colloids to form flocs resulting in destabilization at pH around 7 to 8 and they raised upward by hydrogen gas or settled down.

b. Initial pH

Initial pH is an important operating factor influencing the performance of electrocoagulation process (Ghernaout et al., 2008). The effect of initial pH on turbidity and HA removal were examined by adjusting the pH between 5 to 9 (± 0.02) using NaOH and HNO_3 and supplied 1 mA/cm^2 of current density. The results of Figure 4.18 showed that turbidity removal efficiency at 20 minutes highly increased from 80.77% to 89.97% when pH increasing from 5 to 7 and oppositely decreased to 71.72% when pH continuously increased to 9. It was clarified that turbidity was effectively removed at neutral region and slightly alkalinity as it was removed by destabilization and sweep flocs mechanism since mechanism of destabilization work at pH (6-8) (Crittenden et al., 2012).

c. Calcium ion

The effect of initial concentration of calcium was varied from 0 to 18 mg/L by adding $CaCl_2$. EC was examined at pH 7 ± 0.02 with 1 mA/cm^2 of current density.

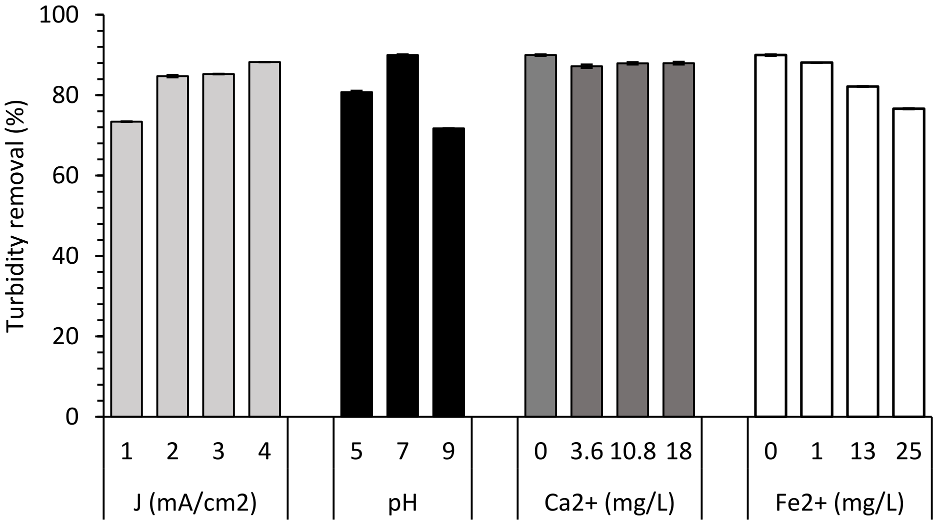

Figure 4.18. Effect of current density, initial pH, calcium and ferrous on turbidity removal

The result showed that turbidity removal were 89.97%, 87.22%, 87.91%, and 87.95%, after adding 0, 3.6, 10.8, and 18.0 mg/L of calcium (Ca^{2+}), respectively, as shown in Figure 4.18. This result showed that adding calcium ion in solution was not influent the treatment efficiency. The removal efficiencies were not statistical significant effect ($p > .05$). Generally, calcium could be removed by forming to calcium carbonate at cathode in EC process as shown in eq. 4.9 and 4.10, when the solution was in high pH (Malakootian and Yousefi, 2009a).

$$HCO_3 + OH^- \rightarrow CO_3^{2-} + H_2O \qquad \text{eq. 4.8}$$

$$CO_3^{\ 2-} + Ca^{2+} \rightarrow CaCO_3 \qquad \text{eq. 4.9}$$

d. Ferrous ion

The concentration of ferrous ion was investigated at 0, 1, 13, and 25 mg/L using ferrous sulfate ($FeSO_4.7H_2O$). The initial pH was adjusted to 7 (± .02) with 1 mA/cm^2 of current density.

Figure 4.19 showed that increasing concentration of ferrous from 0 to 25 mg/L, the turbidity removal was improved at initial stage. However, turbidity seemed like decreasing after 20 minutes treatment as shown in Figure 4.18. The turbidity removal in EC process were 89.97%, 88.11%, 82.17%, and 76.63% when ferrous concentration were 0, 1, 13, and 25 mg/L, respectively. Some researchers employed ferrous sulfate in conventional coagulant or iron electrode for EC process (Mehmet Kobya et al., 2003; Parmar et al., 2011). Ferrous works as coagulant in the solution by creating a positive

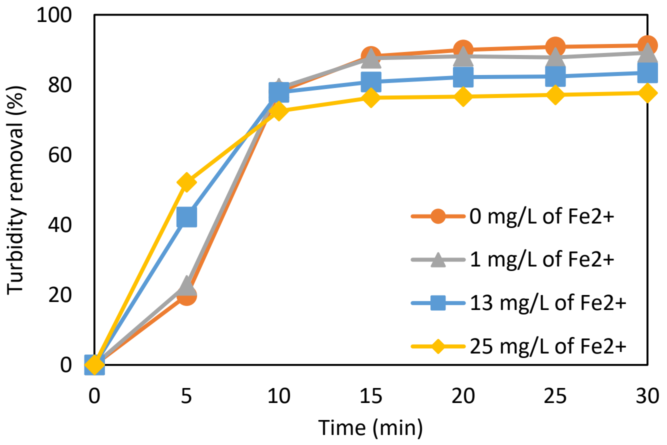

Figure 4.19. Turbidity removal at different concentrations of ferrous added

gel of hydroxide which promoted charge neutralization of negative colloid (Parmar et al., 2011). Therefore, ferrous promoted coagulation of colloidal particles at the beginning. However, when the particles were reduced, the remained insoluble form of ferric iron (Dean et al., 1972) (eq. 4.10) and aluminum hydroxide could not attach with residual particle anymore. Finally, they became the turbidity in the solution.

$$Fe^{2+}\ (aq) + 10\ H_2O\ (l) + O_2\ (g) \rightarrow 4\ Fe(OH)_3\ (s) + 8\ H^+\ (aq) \qquad \text{eq. 4.10}$$

4.4.2 Humic acid removal

a. <u>Current density</u>

The percentages of HA removal were 70%, 94%, 98%, and 100% after supplying the current density 1, 2, 3, and 4 mA/cm^2, respectively, as shown in Figure 4.20. The role of current density of HA removal was matched to turbidity removal as well.

b. <u>Initial pH</u>

The removal of HA seemed different from turbidity removal as shown in Figure 4.20. When pH value further increased, HA removal decreased. HA reached the peak value of 97.14% at pH 5 and 20 minutes treatment. The result could conclude that HA was better removed in the acidic region than neutral and alkalinity region which was opposite from turbidity removal. This may be explained by the surface charge of HA molecule and coagulation with different pH. In alkaline conditions, the functional groups of carboxylic or phenolic acids radial of HA (-COOH and –OH) increased the

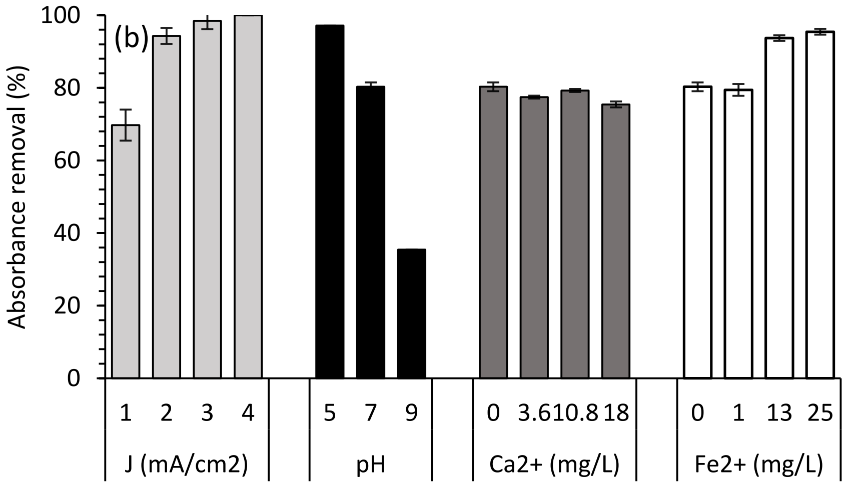

Figure 4.20. Effect of Current density (J), pH, Calcium (Ca^{2+}), and Ferrous (Fe^{2+}) on Absorbance removal

negative charge by deprotonating to –COO$^-$ and –O$^-$) which resulted more coagulants (Al^{3+}) requirement (Wang et al., 2011). Meanwhile, the hydrolysis of coagulants in alkaline region had lower positive charge. These two consequences caused the HA removal was lower in alkalinity than the base condition. Another reason is adjusting pH between 5 and 6, the formation of large insoluble bridged complexes or micro-flocs links to each other could act as nuclei for macro (flocculation) (Ashery et al., 2011). Moreover, this result was supported by Rezaei et al. (2018).

c. Calcium ion

Figure 4.20 showed that calcium existing in the solution from 0 to 18 mg/L was not effect on the HA removal. Sudoh et al. (2015) indicated that Ca^{2+} can block the surface charge of negative molecules and also functions as the bridges of two adjacent molecules. Duan et al. (2003) also reported that Ca^{2+} may compress the electrical double layer (EDL) of HA colloid particles and powdered activated carbon (PAC) in saline water. Therefore, the electrostatic repulsion between PAC and HA could be reduced. Then, van de Waals attractive forces allow having a greater beneficial effect on adsorption. This reaction also happens to the EDL of HA and bentonite too. Moreover, HA molecules may change to coiled and spherical in shape when HA molecules were affected by reducing charge in ionic strength solutions, which result in improving adsorption (Ghosh and Schnitzer, 1980) by Aluminum hydroxide. Moreover, calcium carbon forming during calcium ion removal may help HA removal by adsorption too (Bob and Walker, 2001). However, in this case study, the concentration of calcium may be low and not be able to help HA removal in EC process.

d. Ferrous ion

For absorbance removal (Figure 4.20) showed that HA removal was better when increasing ferrous concentration along the time. The HA removal in the solution were 80.29%, 79.42%, 93.71%, and 95.43% after adding respective ferrous concentration 0, 1, 13, and 25 mg/L. This increasing was started since the initial until steady stage as shown in Figure 4.21. This result was opposite from turbidity removal due to different mechanism of HA and turbidity. Adding more and more ferrous ions, the sweep flocs and adsorption mechanism of ferric hydroxide on HA could improve the treatment performance as mentioned in turbidity removal. HA-Fe complex was form and

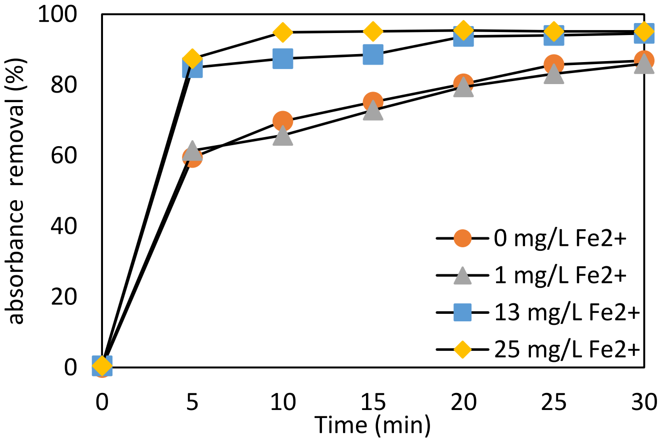

Figure 4.21. HA removal at different concentrations of ferrous

separated by flotation and sedimentation(Park and Yoon, 2009). Additionally, HA was measured by the absorbance after filtration; therefore, ferric precipitation did not affect the HA measurement as turbidity.

4.4.3 Final pH

In overall, the effects of initial pH, current density, calcium, and ferrous on final pH were shown in Figure 4.22. Only initial pH and ferrous were significant effect on pH evolution in the solution. The improvement/decrease of pH (ΔpH) values were 1.09, 0.39, -0.3 when initial pH values were 5, 7, and 9, respectively. The result indicated that pH was increased when initial pH values were in acidic and neutral condition while it was decreased when pH was in high alkalinity region. Chen et al. (2000) and Vik et al. (1984) explained the neutralized pH in EC process. The chemical reactions at anodes or in the bulk wastewater are shown following:

$$Al^{3+} - 3e^{-} = Al^{3+} \qquad \text{eq. 4.11}$$

$$Al^{3+} + 3\,H_2O = Al(OH)_3 + 3\,H^{+} \qquad \text{eq. 4.12}$$

$$2H_2O - 4\,e^{-} = O_2 + 4\,H^{+} \qquad \text{eq. 4.13}$$

$$2\,Cl^{-} - 2e^{-} = Cl_2 \qquad \text{eq. 4.14}$$

$$Cl_2 + H_2O = HOCl + H^{+} + Cl^{-} \qquad \text{eq. 4.15}$$

$$HOCl = OCl^{-} + H^{+} \qquad \text{eq. 4.16}$$

Figure 4.22 showed that pH was in range 6.09 to 8.69 when the initial pH ranged from 5 to 9. Under these conditions, hydrogen gas may produce from reaction eq. 4. 13, 4.14, 4.16, and 4. 17. A few mechanisms take place in these pH evolution.

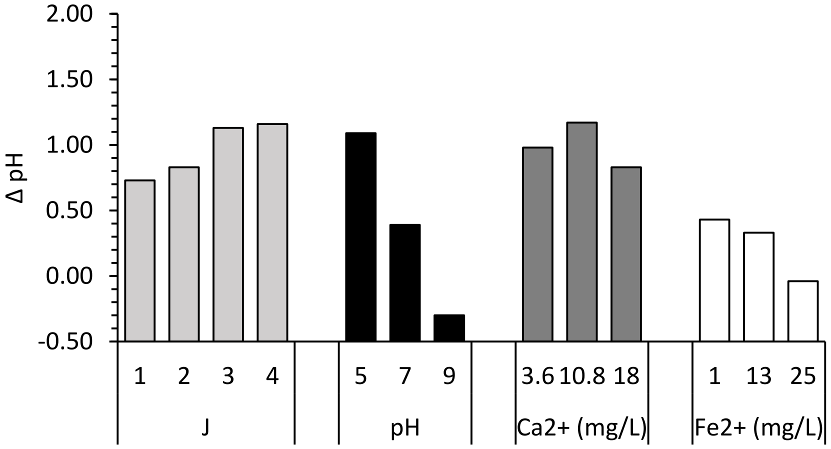

Figure 4.22. Effect of current density, pH, calcium, and ferrous on pH evolution

- Increasing pH: CO_2 was oversaturated in acidic condition. Then, it was released from wastewater owing to H_2 disturbance resulting in increasing pH. Moreover, the reaction eq. 4.13 and eq. 4.16 will shift to the left-hand side which increases the pH in the solution. Furthermore, some anions presented in solution such as chloride (Cl^-), nitrate (NO_3^-), sulfate (SO_4^{2-}), bicarbonate (HCO_3^-), etc can exchange partly with hydroxide (OH^-) in aluminum hydroxide $Al(OH)_3$ to free hydroxide (OH^-). Therefore, these hydroxides (OH^-) also cause the pH increased.
- Decreasing pH: $Al(OH)_3$ is an amphoteric metal hydroxide. Therefore, in high pH, $Al(OH)_3$ can form to $Al(OH)_4$ as expressed in eq. 4.18, leading to decrease pH in the solution. In addition, some Ca^{2+} and Mg^{2+} presented in solution can co-precipitate with $Al(OH)_3$ and form hydroxide, which also decreases the pH in EC process.

$$Al(OH)_3 \quad + \quad OH \quad = \quad Al(OH)_4 \qquad \text{eq. 4.17}$$

For the effect of ferrous ion, the results indicated that increasing ferrous concentration from 1 to 25 mg/L, final pH was reduced. As mentioned previously, ferrous roles as a coagulant in turbidity and HA removal. It was formed to ferric hydroxide ($Fe(OH)_3$) by releasing hydron cations which cause pH decreasing in solution as shown in eq. 4.11. Therefore, it consumed hydroxide molecules in the system resulting in pH reduction.

4.5 Effect of co-existing ions and operating conditions

Effect of co-existing ions and operating conditions on EC performance in HA-Bentonite removal was the main part of this study. The result of this section was dealt with three main parts including (i) screening factors for main responses, (ii) effective analysis and optimization of co-existing ions and operating conditions on turbidity and HA removal, and (iii) model prediction. The co-existing ions were calcium and ferrous, while the operating conditions were initial pH and current density with three level study as illustrated in Table 4.7. Current density, initial pH, calcium, and ferrous were independent variables. These parameters were controlled in the EC process. Voltage of DC power supply may change along the time to fix the current density constant. Initial pH was adjusted by using HNO_3 and NaOH. Ca^{2+} and Fe^{2+} were synthesized by using $CaCl_2$ and $FeSO_4.7H_2O$, respectively. Therefore, voltage, NO_3^-, Na^+, Cl^-, and SO_4^{2-} were not able to control in the system. The controllable and uncontrollable input factors in EC operation were illustrated in Table 4.8.

Table 4.7 Investigated factors and its level

Factor	Unit	Levels		
		-1	0	+1
J	mA/cm^2	1.0	2.5	4.0
pH	-	5	7	9
Ca^{2+}	mg/L	3.6	10.8	18.0
Fe^{2+}	mg/L	1	13	25

Table 4.8. Controllable and uncontrollable input factors in DOE

Controllable input factors	Uncontrollable input factors
Current density	voltage
Initial pH	NO_3^- and Na^+
Ca^{2+}	Cl^-
Fe^{2+}	SO_4^{2-}

Note: controllable input factors are parameters which can be controlled or modified in the system and uncontrollable input factors are parameters which cannot be changed. This parameters need to recognize their effect to the responses.

insignificant effect on treatment performance and analyze the effect of variation range of each parameters to the response. The respond parameters, turbidity and HA, were analyzed. This section was separated into two parts: (i) effect of bentonite concentration on HA removal and (ii) effect of ions and operating conditions.

a. Effect of Bentonite concentration on HA removal

By using the optimal current density (3 mA/cm^2) from kinetic study, bentonite concentration was varied to find out its effect on humic acid removal. Figure 4.23(a) illustrated the turbidity removal along the time. Higher initial turbidity concentration resulted better turbidity removal efficiency. However, the absorbance of HA (70 mg/L) removal was not significantly changed after varying bentonite concentration from 0 to 200 NTU at 20 minutes treatment (P-value<.05) as shown in Figure 4.23 (b). Therefore, 100 NTU of Bentonite and 70 mg/L of HA were studied for the effect of co-existing ions and operating conditions in Electrocoagulation on their removal.

b. Effect of operating conditons and ion contaminations

The four parameters including current density, initial pH, calcium, and ferrous were screened by using 2-level factorial design with 95% confidence level of a single replication. The results of screening parameters including current density, initial pH, ferrous, and calcium were analyzed in terms of turbidity and HA removal in HA-Bentonite synthetic water at 20 minute treatment. By using factorial plot of 2^k factorial design in DOE, Pareto analysis was used to screen out the insignificant factors. The Pareto analysis was determined by using eq. 4.19 (Ibarra-Taquez et al., 2017).

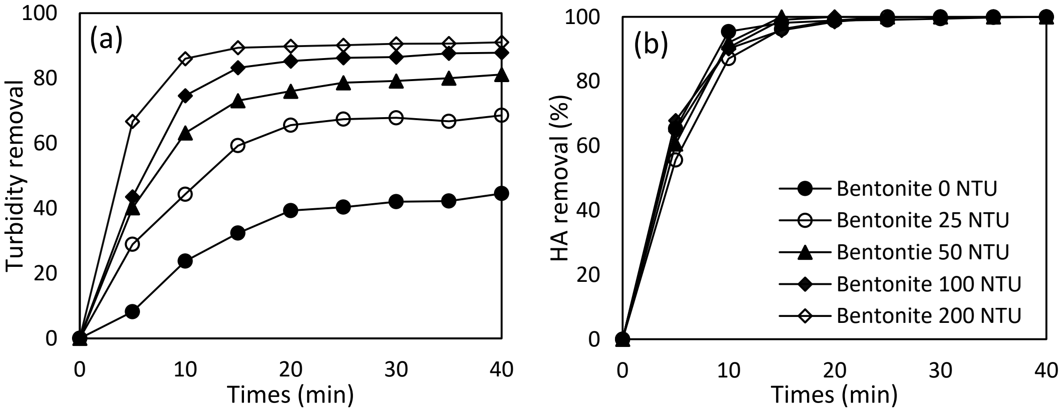

Figure 4.23. Effect of bentonite concentration on (a) turbidity removal and (b) HA removal

$$PE_i = \left(\frac{b_i^2}{\sum b_i^2} \right) \qquad \text{eq. 4.18}$$

where b_i is the value of each i factor as shown in the vertical line. The blue and white bar color of bar represented the positive and negative effect on removal efficiency, respectively, as shown in (Figure 4.24 and Figure 4.25).

- *Turbidity removal*

According to Figure 4.24, current density, initial pH, and calcium resulted the positive effect while only ferrous provided the negative effect on turbidity treatment. Three single and two interactive terms were obtained as the significant terms including (i) interception of current density and pH, (ii) interception of ferrous, calcium, and current density, (iii) pH, (iv) ferrous ion, and (v) calcium ion had standardized effect higher than 2.131. However, even current density was not significant effect, but its interception had high significant effect. Therefore, these four factors were chosen to study their effect on turbidity removal.

- *HA removal*

The results of Pareto graph (Figure 4.25) also showed that seven main and interception factors had a significant effect on humic acid removal. They were pH, current density, interception of pH and current density, interception of ferrous, current density and pH, interactive of ferrous and pH, and ferrous. However, the main factors of calcium did not have a significant effect.

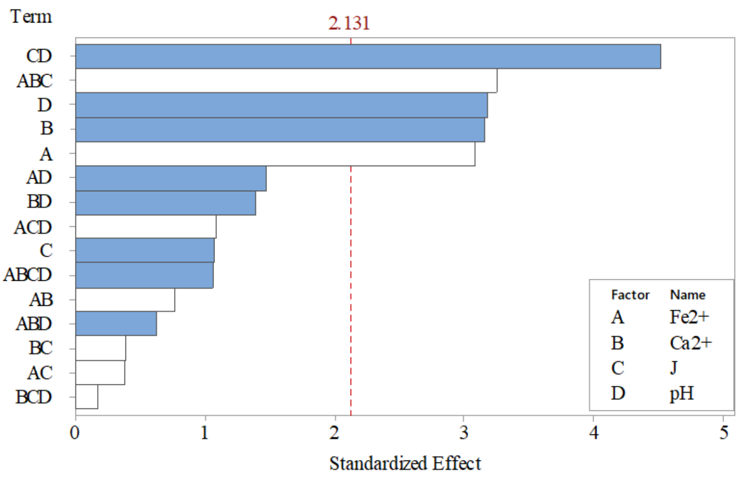

Figure 4.24. Pareto chart of the standardized effects of turbidity removal (%)

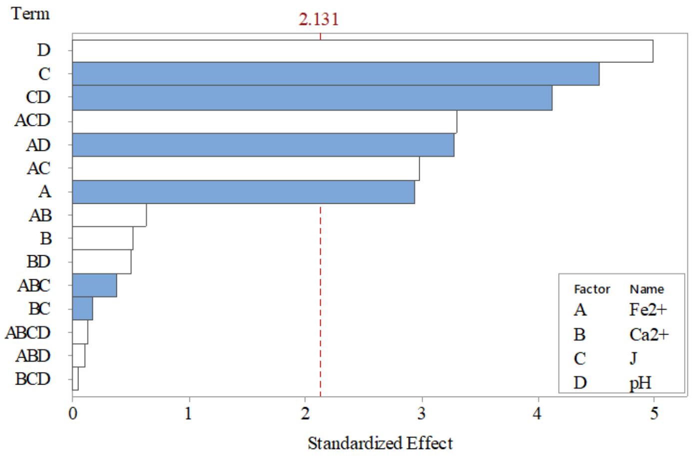

Figure 4.25. Pareto chart of standardized effect of absorbance removal(%)

In summary, only 100 NTU of bentonite and 70 mg/L of HA were selected. Four factors including current density, initial pH, calcium, and ferrous were important to study about their effectiveness on turbidity and HA removal since ferrous, calcium and pH had significant effect on turbidity while ferrous, pH, current density had significant effect on HA removal.

4.5.1 Effective analysis and optimization

Two responses including turbidity and HA (absorbance) were analyzed in this section. Design of experiment (DOE) in Minitab 17 software was employed to design the experiment by using Central Composite Design in Response Surface Methodology (CCD-RSM). The parameters were assessed in 3-level design as shown in Appendix 2. Main effects represented when the mean of the response (turbidity and HA removal efficiency) changed at the different levels of the variable. Minitab plotted the main effect graph by fitting means for each value of a variance in the model. For example, when the effect of current density on treatment performance was studied, other factors (pH, ferrous, and calcium) were meant. The evaluation of effects was done by using P-value and effect value in Minitab. VIF was also crucial to explain the correlation of each factor. If it is close to 1, it indicates that the predictors are not correlated. The regression coefficients are poorly estimated when VIF is greater than 5-10. Analysis of variance (ANOVA) was determined to evaluate the statistical effect of each factor. The results were analyzed by 95% level confidence of statistical analysis. ANOVA was observed as following effects:

- ➢ Linear effects: individual factor was effect on response.
- ➢ Squared effects: when each factor was power 2.
- ➢ Interaction effects: two different factors interact and effect on response.

a. <u>Turbidity removal</u>

The ANOVA analysis and coefficient effect table on turbidity removal were summarized in Appendix 3. The effect and P-value of each parameters were shown in Figure 4.26. In overall, linear and 2-way interaction terms had significant effect on turbidity removal. However, the squared term was not significant effect on turbidity removal since P-value less than 0.05. The effect of each parameter to turbidity removal was around 4%. Figure 4.27 showed the fitted mean of each factor on turbidity removal. The interception effects were plotted in factorial plot (Figure 4.28). The contour plot and surface plot were shown in Appendix 3. In overall, three out of four factors including ferrous, calcium, and pH had significant effect on turbidity removal. All VIF value of linear effects was 1, so all factors were not correlated.

- ➢ Current density

Based on main effect plots, Figure 4.27 described the effect of current density on turbidity removal. Current density was not significant effect. It might attribute to the very high effect of initial pH, calcium and ferrous. When the current density increased, the treatment also increased as explained in section 4.7. The optimal condition of current density was obtained at 3.4 mA/cm^2 which was higher than the kinetic study (current density 3 mA/cm^2). After increasing current density more than 3.4 mA/cm^2,

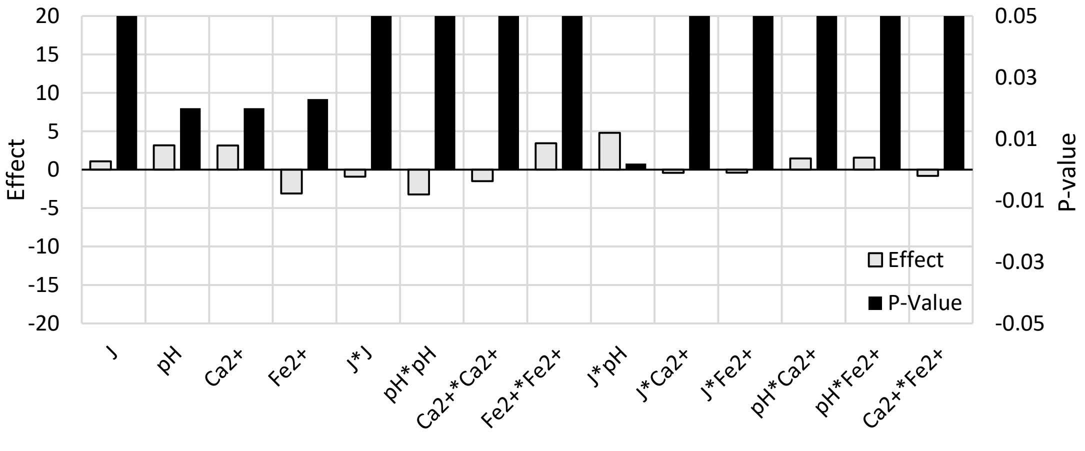

Figure 4.26. The effect and P-value of current density, initial pH, calcium, and ferrous on turbidity removal

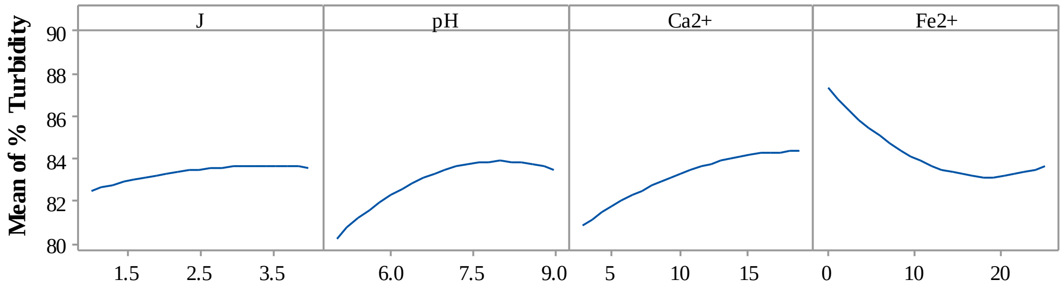

Figure 4.27. Main effect plots of the fitted mean value of turbidity removal (%).

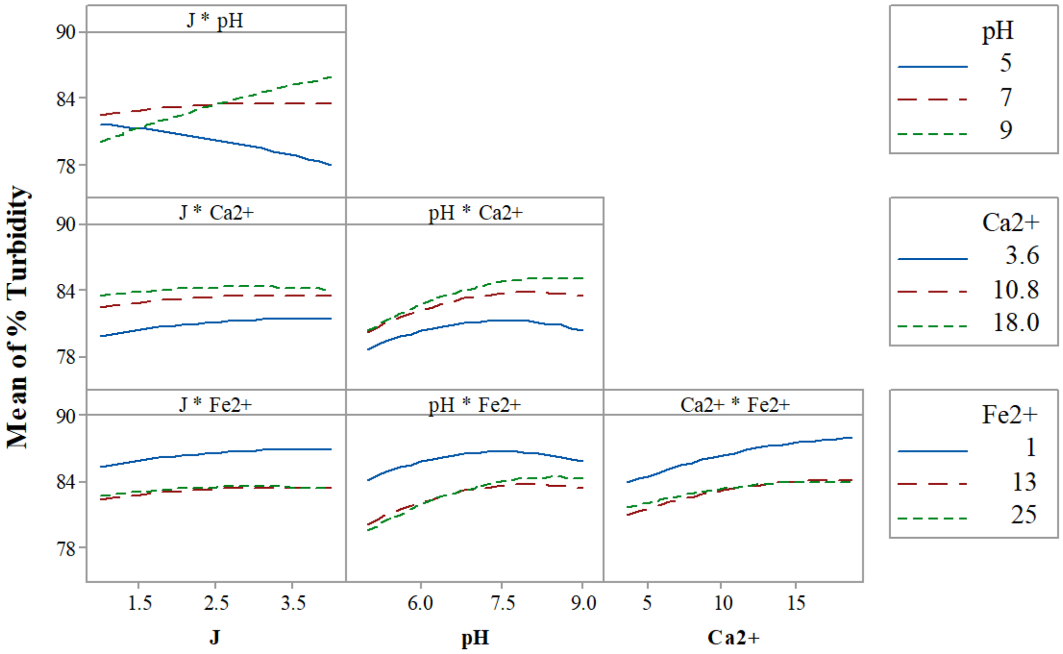

Figure 4.28. Interaction plot of turbidity removal

the turbidity removal was slightly decreased due to too much mixing and overdosing of aluminum released from electrodes which creating turbidity in the system.

Figure 4.28 showed the interception effect of current density with other parameters. The result showed that increasing current density was still improved the treatment performance for the interaction of current density with calcium and ferrous. However, the interaction of current density and initial pH, the result showed that increasing current density, the turbidity removal was decreased from 82% to 78% for pH 5. At low pH (4<pH<5.5), aluminum hydroxide and colloidal particle could not form the flocs due to high zeta potential and strong repulsive force (Mohammad and Mahdi, 2016). Therefore, this insoluble aluminum became the turbidity in the system. On the other hand, at initial pH 9, the removal efficiency was increased when current density increased since pH was decreased along the reaction time.

- Initial pH

The result of main plot showed that increasing pH from 5 to 8, the turbidity dramatically increased from 80% to 84.5%. However, the removal seemed reduced when pH up to 9 (turbidity removal 83%). Therefore, the optimal condition found at pH 8 since the basis of the precipitation charge neutralization (PCN) is around pH 8 for aluminum hydroxide (Hayden and Rubin, 1974). The interaction of ferrous and calcium was not effect on optimal pH as shown in Figure 4.28.

- Calcium

Figure 4.27 also showed the performance of calcium on turbidity removal. Calcium had significant effect on the treatment performance. Increasing calcium from 3.6 to 18 mg/L could improve the turbidity removal in EC process which was different from individual study of calcium. The different might explained by the potential of other factors when they were adding together in the solution; then, it made the effect of calcium was clearly visible.

Therefore, the optimal condition of turbidity removal was found at 18 mg/L Ca^{2+}. The interaction of ferrous was not effect on the function of calcium in turbidity removal (Figure 4.28).

- Ferrous

Adding ferrous from 1 to 25 mg/L had significant effect on turbidity removal in HA-Bentonite synthetic water. The effect of ferrous on turbidity removal still bring negative effect on turbidity removal as individual effect study in section 4.4.1. The treatment was decreased when the ferrous was increased from 1 mg/L to 18 mg/L due to insoluble form of ferric in the solution. However, when ferrous was adding more to 25 mg/L, the turbidity removal was slightly increased. The insoluble form of ferric from ferrous lower than 18 mg/L could create the turbidity. However, adding more ferrous (25 mg/L), ferric might be able to form flocs and separate through sedimentation or flotation.

Therefore, the optimal ferrous concentration in HA-bentonite synthetic water was found at 18 mg/L for turbidity removal.

b. <u>HA removal</u>

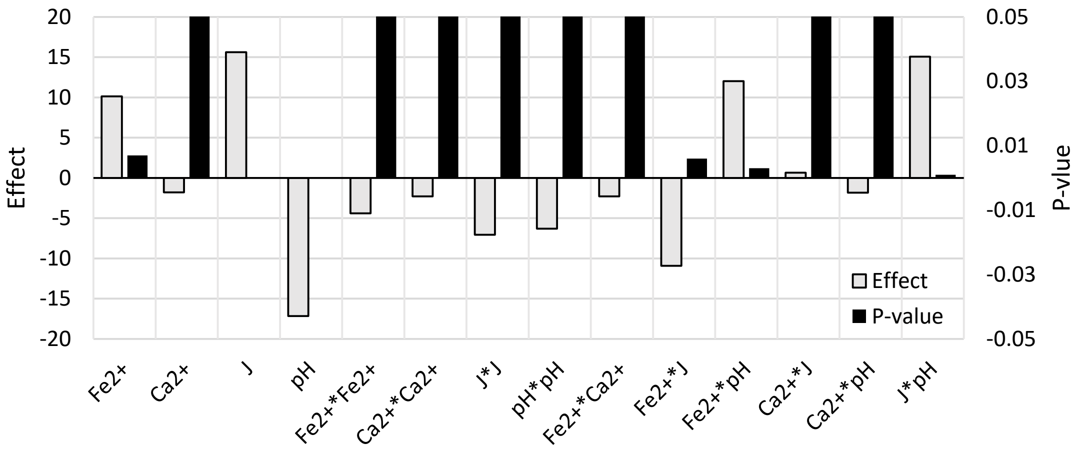

Figure 4.29. Effect and P-value of current density, initial pH, calcium, and ferrous on HA removal

Figure 4.29 showed the effect and P-value of current density, initial pH, calcium, and ferrous on HA removal in HA-bentonite synthetic water. The result showed that only calcium was not significant effect. Initial pH was the highest effect on HA removal. The main factors effects on HA were shown in Figure 4.30. The interception of factorial plot was shown in Figure 4.31 and the contour and surface plot were illustrated in Appendix 3. The graph was shown an error of the HA removal since its removal was higher than 100%. It is because of a fitted plot in respond surface design of Minitab 17.

- Current density

Based on Figure 4.30, the absorbance removal was gradually increased with current density. As mentioned in turbidity removal, the turbidity removal was slightly decreased when current density was higher than 3.4 mA/cm^2 due to too much aluminum released from the anode. However, the absorbance removal was not related to this

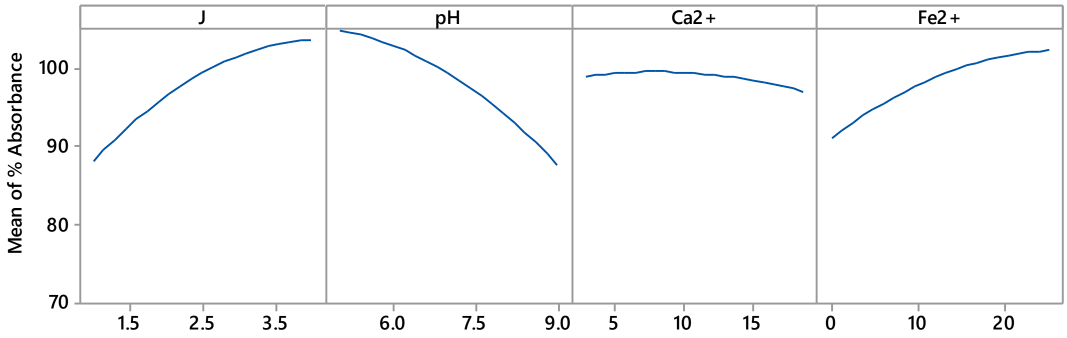

Figure 4.30. Main effects on absorbance removal

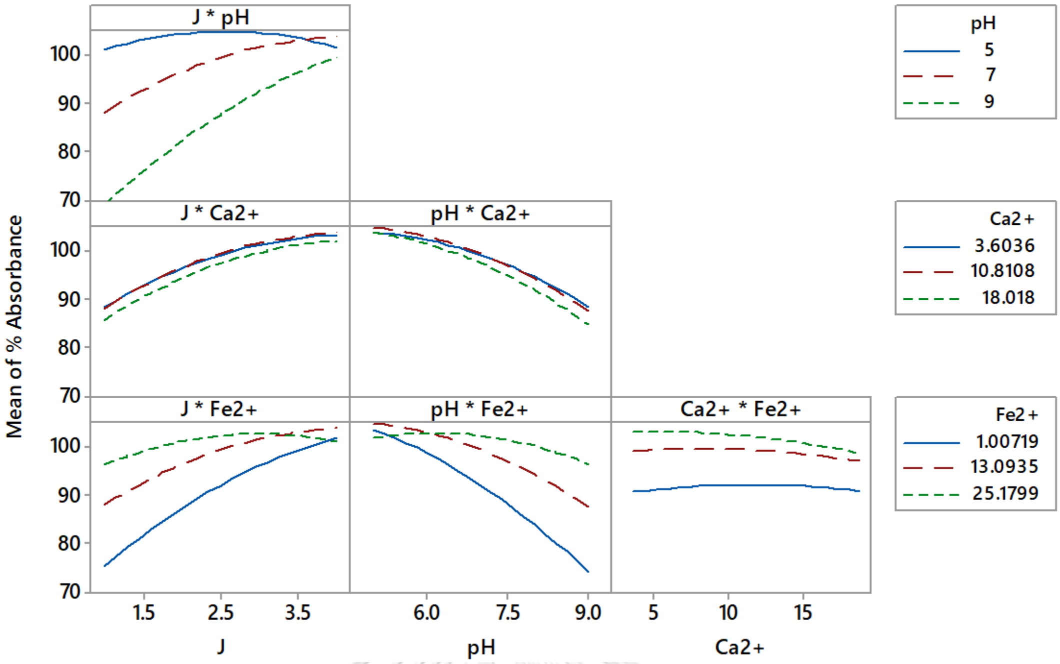

Figure 4.31. Interaction plot for HA removal

phenomenon since absorbance was measured in soluble form after filtrating through 0.45 micron. Therefore, the optimal condition was found at 4 mA/cm^2 for absorbance removal in HA-bentonite synthetic water. Figure 4.31 showed that effect of current density was not changed when ferrous, calcium, and initial pH were added. Additionally, the effect of ferrous, calcium, and initial pH were not seen when the current density was high. This was probably explained by the potential of current density on HA removal.

- Initial pH

Initial pH was significant effect on absorbance removal. Increased pH from 5 to 9, absorbance removal was dropped from 100% to 88%. This result supported that electrocoagulation process is a function of initial pH. Moreover, it indicated that initial pH value was effect to the reaction performance, where lower pH values lead to faster treatment kinetic. This result was in agreement with results obtained by other studies too (FENG et al., 2007). Bazrafshan et al. (2012) studied the effects of initial pH (3, 5, 7, and 9) on HA 20 mg/L removal by supplying voltage 50 V, various conductivity (1000 to 3000 µS/cm) and reaction time 75 min. At optimal conductivity 3000 µS/cm, the treatment efficiency was increased from 87.45% to 92.69% when pH was increased from 3 to 5 and gradually reduced to 71.9% when pH was up to 9. Wang et al. (2011)

also showed HA was highly removed at pH 5 when treatment was performed with different pH (4, 5, 6, 7, 8, and 9) by using coagulation process since HA had high negative charges while coagulant had low positive charges at alkalinity condition. Figure 4.31 also showed at pH 5, the effect of calcium and ferrous were not able to see due to the very significant effect of initial pH on absorbance removal.

- Calcium

The linear effect of calcium on HA removal was also described in Figure 4.30. Adding calcium ion from 3.6 to 8 mg/L, the removal efficiency was about 99%, but it was reduced to 96% after adding more calcium. Calcium was not significant effect on HA removal. Therefore, calcium concentration ranges in this studied may not be able to conclude that calcium ions could help or reduce the treatment efficiency of HA. Meanwhile, Tang et al. (2014) showed that adding calcium 20 mg/L reduced the treatment in HA 5 mg/L direct oxidation of electrode at high pH as it formed complexes with HA, which impeded the absorbance of HA on the surface of the electrode.

- Ferrous

When the wastewater contained ferrous ions from 1 mg/L to 25 mg/L, ferrous was significant effect on EC in HA removal. More ferrous ion contained in the solution, more positive effects on treatment were found. The removal was increased from 90 to 100 % when ferrous was added from 1 to 25 mg/L. This phenomenon had already explained when only ferrous ion was contained in HA-bentonite polluted water. Therefore, the optimal condition of ferrous contained in wastewater for HA removal was 25 mg/L.

4.5.2 Model Prediction

a. Model adequacy checking

In order to predict model, model adequacy was checked to ensure that the real system and selected model are adequate approximations and verify the data quality. The model adequacy checking included residual plots of normal probability plot and versus order using Minitab 17 were analyzed (Montgomery, 2010). The results were analyzed with same level confidence of statistical analysis in previous parts both turbidity and absorbance removal in HA-bentonite synthetic water.

- Normal probability plot: to ensure that data values are in normal distribution, other variable influents to the response, or outliers exist in the data or not.
- Residuals versus order of the data: to explain the systematic effect in the data due to data collection or time order.

➢ *Turbidity*

Figure 4.32 (a) represented the normal probability plot of turbidity removal response. It showed that the normal probability percentage versus standardized residuals had a good fit since all points roughly followed a straight line, and also confirmed that the analytical data was suit to the statistical assumptions. Figure 4.32 (b) showed the residual versus fitted value and observation order. The scatters were randomly within the range of residuals (-4, 4) across the zero line and versus order fluctuate in a random pattern around the center line. It was confirmed that all experiments were no systematic effect while doing the experiment (Gomez and Sartaj, 2014). In overall, all data for turbidity removal analyze was good in terms of statistic analyze.

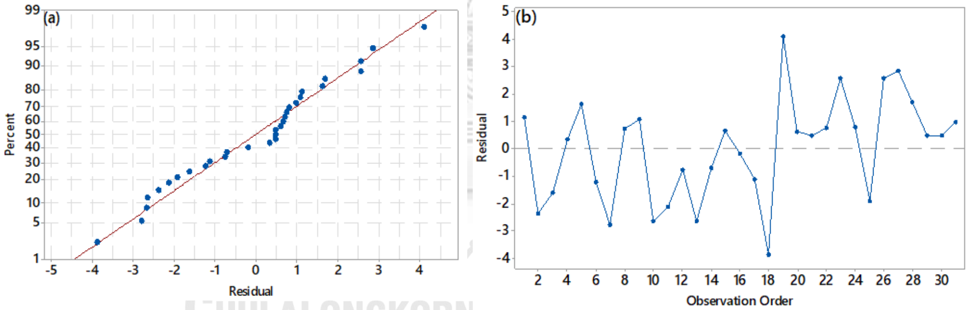

Figure 4.32. (a) Normal probability of residua, and (b) observation order versus residual plot for turbidity removal

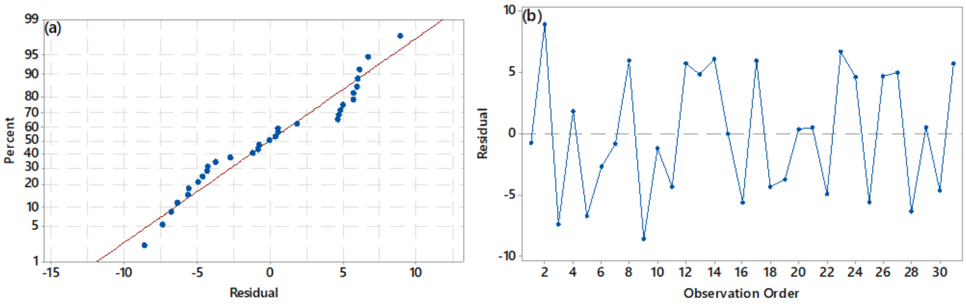

Figure 4.33. Normal probability of residual, Fitted value versus residual, and Observation order versus residual plot for absorbance removal

- *Humic acid*

Figure 4.33 showed the normal probability of residual, fitted value versus residual, and observation order versus residual plot for HA. The result showed that all data was randomly in normal distribution and no error terms correlated with another.

b. Model prediction

By using multiple regression analysis, turbidity and humic acid removal (absorbance %) at 20 min treatment were predicted by using statistical model in terms of four factors including pH, current density (J), Calcium (Ca^{2+}), and ferrous (Fe^{2+}). The 31 experiments were run following conditions of DOE. Second-order polynomial in Minitab 17 was employed by using Response surface methodology (RSM). The results were expressed in (i) full quadratic forms and (ii) model equation shortening or model adjusting. The quality of model prediction was evaluated by S value, coefficient of determination (R^2), and adjusted square R (R^2(adj)).

- *Turbidity*

1. Full quadratic form

The analysis of variance using Minitab was already shown in Appendix 3. Therefore, the model prediction of turbidity removal (%) was expressed in full quadratic forms are given by eq. 4.20. ANOVA showed that the model prediction had P-value less than 0.05. It means at least one terms in the predicted model had a significant effect on the mean responses. The linear, square, and 2-way interception of factors had a significant effect on the model prediction. Lack-of-fit was not significant effect on the model (P-value<.05). Therefore, no evidence that can conclude that the model does not adequately explain the variation in the responses.

The coefficients of determination of model prediction with observed data were R^2 ~ 0.72 and R^2(adjust) ~ 0.46 which were generated by Minitab. The R^2-value expressed that 72% of turbidity removal efficiency (%) could be confidentially explained by current density (J), initial pH, ferrous, and calcium and their interaction. Therefore, most of the terms were correlated with the response factor. Figure 4.34 showed that turbidity removal was scattered in range 74% to 91%. This might be because all data were measured at the steady stage of EC process, so most of turbidity was removed

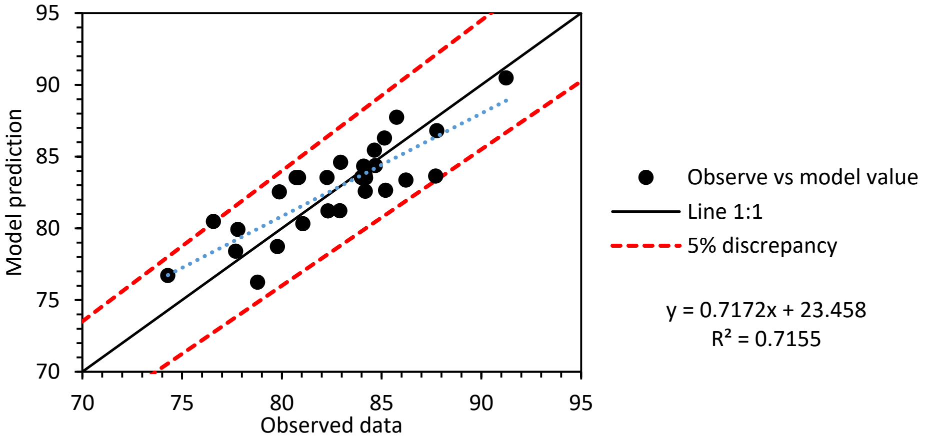

Figure 4.34. The correlation between observe and model data value of turbidity removal

over 70%. The model prediction was fitted to observed data as regression line (Line of observing vs. model) was similar to the line of equality (Line 1:1). Line of equality or line 1:1 evaluated the the error of predicted data values to the observe data values. The result of observed versue model value were around line of equality, so this predicted model was well fitted with the observed data. The regression line had slop about 72% which error 28% from Line 1:1. However, most of the predicted data passed 5% of discrepancy (red dot line). Line of discrepancy could explain the percentage of model prediction which error from the line of equality. Therefore, even this model had good R-square and most of predicted data values were around 5 % error from the observed data values.

2. Model adjusting

The full quadratic model was long with many terms which were not highly effect on the response. Moreover, it was not convenient in use. Therefore, the model adjusting was done to reduce unnecessary parameter terms. This study, the adjusted model were made based on P-value. Some parameters which had high P-value on model response were eliminated from the model. After that, Minitab were analyzed the coefficient of new model. The new model prediction was expressed in eq. 4.21. Figure 4.36 showed the adjusted model prediction which 6 terms were illuminated from full quadratic form. The result showed that all predicted responses had confidentially fit to the observed data since all values were passed 10% of discrepancy. The comparison of R-square and

Table 4.9. Evaluation of fell quadratic and adjusting model for turbidity

Model	S	R-sq	R-sq(adj)
Full quadratic	2.60	72 %	47 %
Adjusting	2.44	66 %	53 %

S value were illustrated in Table 4.9. S values of full quadratic and adjusted model were almost same. It meant the standard distance of observed data values which fall from the regression linear of both full and adjusted model was similar. The R-square of these two models were also similar and R-square (adjust) was little better than old one. It meant reducing some unnecessary terms in the model was not much effect on the response.

- *Humic acid*

1. Full quadratic

The predicted model of absorbance was expressed in eq. 4.22. Analysis of variance for predicted model was shown in Appendix 3. It illustrated that linear, square, and 2-way interaction of terms had significant effects on model prediction. By using empirical correlation of HA removal (% absorbance), the R(s)-square were R^2 ~ 88% and R^2(adjust) ~ 77%. It could conclude that most of observed data could be explained by the model. The prediction of HA was better fit than turbidity removal in HA-synthetic water. However, it had standard distance error higher than turbidity model. Figure 4.35 illustrated the validation of predicted model to observed data. The data values were in range from 42 to 100% and 48% to 104% of observed and predicted absorbance

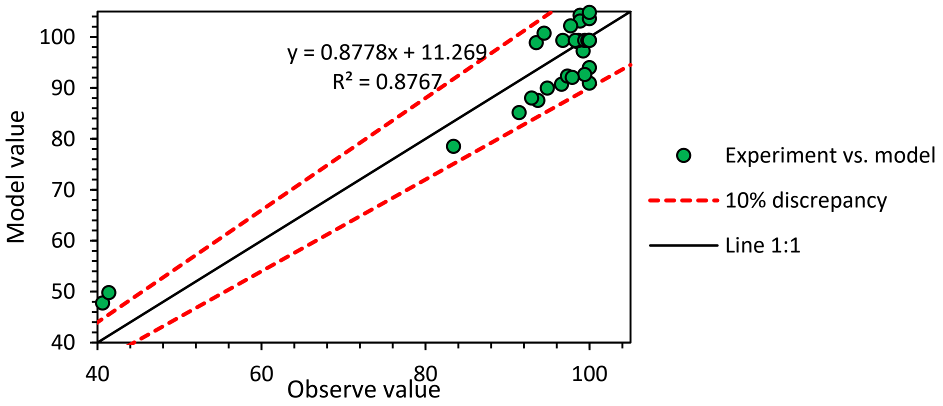

Figure 4.35. The correlation between observe and model data value of absorbance removal

removal, respectively. Therefore, few predicted values were errors since they were higher than 100%. All scatter points were around line of equality, so this model could predict the HA removal. The error of model predicted value was around 10% of discrepancy. The error of regression line to line of equality was about 12%. Therefore, this model could be able to predict the overfit data.

2. Model shortening

Table 4.10. Evaluation of R-square of full and adjusted model for HA

Model	S	R-sq	R-sq(adj)
Full quadratic	6.96	87.67%	76.88%
Adjusting	6.30	86.74%	81.06%

Terms		Predicted model	
Turbidity	Full quadratic	$\% \text{Turbidity} = 74.9 - 3.88 J + 3.48 pH + 0.281 [Ca^{2+}] - 0.585 [Fe^{2+}] - 0.200 J*J - 0.404 pH*pH - 0.0143 [Ca^{2+}]*[Ca^{2+}] + 0.0118 [Fe^{2+}]*[Fe^{2+}] + 0.800 J*pH - 0.0193 J*[Ca^{2+}] - 0.0110 J*[Fe^{2+}] + 0.0511 pH*[Ca^{2+}] + 0.0323 pH*[Fe^{2+}] - 0.00468 [Ca^{2+}]*[Fe^{2+}]$	eq. 4.19
	Adjusting	$\% \text{Turbidity} = 96.33 - 5.24 J - 2.179 pH - 0.138 [Ca^{2+}] - 0.293 [Fe^{2+}] - 0.00233 [Fe^{2+}]*[Fe^{2+}] + 0.800 J*pH + 0.0511 pH*[Ca^{2+}] + 0.0323 pH*[Fe^{2+}]$	eq. 4.20
Abs	Full quadratic	$\% \text{Absorbance} = 109.7 - 0.029 [Fe^{2+}] + 0.90 [Ca^{2+}] - 0.9 J - 2.1 pH - 0.0151 [Fe^{2+}]*[Fe^{2+}] - 0.0222 [Ca^{2+}]*[Ca^{2+}] - 1.57 J*J - 0.79 pH*pH - 0.0132 [Fe^{2+}]*[Ca^{2+}] - 0.3012 [Fe^{2+}]*J + 0.2484 [Fe^{2+}]*pH + 0.029 [Ca^{2+}]*J - 0.064 [Ca^{2+}]*pH + 2.510 J*pH$	eq. 4.21
	Adjusting	$\% \text{Absorbance} = 99.1 - 0.566 [Fe^{2+}] - 0.125 [Ca^{2+}] + 2.59 J + 2.2 pH - 2.20 J*J - 1.143 pH*pH - 0.3012 [Fe^{2+}]*J + 0.2484 [Fe^{2+}]*pH + 2.510 J*pH$	eq. 4.22

Based on Figure 4.37, model adjusting was done by reducing 6 terms which were not highly effect on the response. However, single factor could not eliminate even it was not much effect since the model would be a non-hierarchical when some linear terms were deleted. Therefore, model adjusting was given in eq. 4.23. Figure 4.35 showed the validation of adjusted model to observed data. All predicted responses were fitted to the observed data with 30% discrepancy and 13% of regression line slop was error from line of equality. All R-square values were given in Table 4.10. Through S values of these two models, adjusted model had slightly standard distance further from regression line than full quadratic form. R-square and R-square (adjust) of adjected model were orderly 87% and 81 % . It seemed this model was still good enough correlation.

c. <u>Validation of overfit data</u>

Validation was very usefull to check the validity or accuracy of model prediction. The 22 observation values in individual ions and operating condition studies were validated for co-existing study modeling. Data values were expressed in Appendix 4.

➢ *Turbidity removal*

Figure 4.36 indicated the validation of turbidity predicted model to new experimental data values. The result showed that the validated data was still in 10% of discrepancy. Therefore, this model could be predicted with overfit data in 10% error from line of equality.

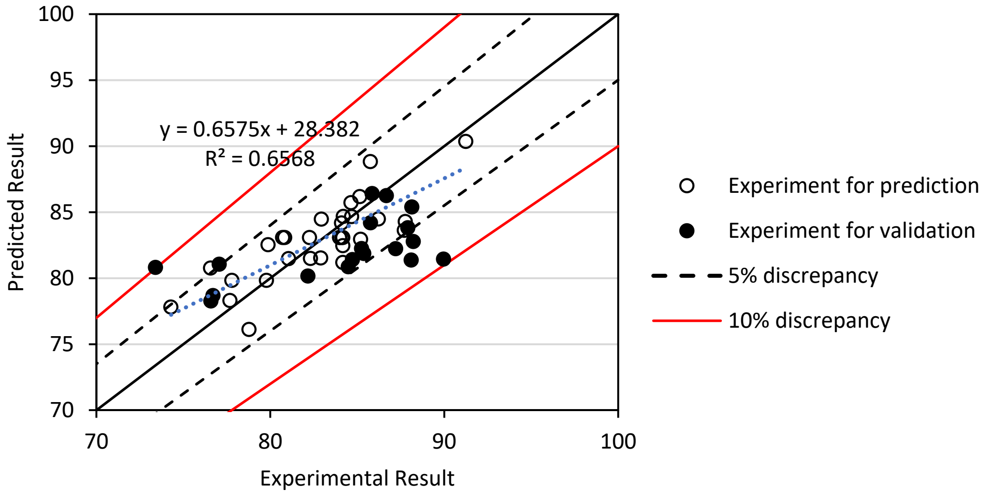

Figure 4.36. Validation of turbidity removal

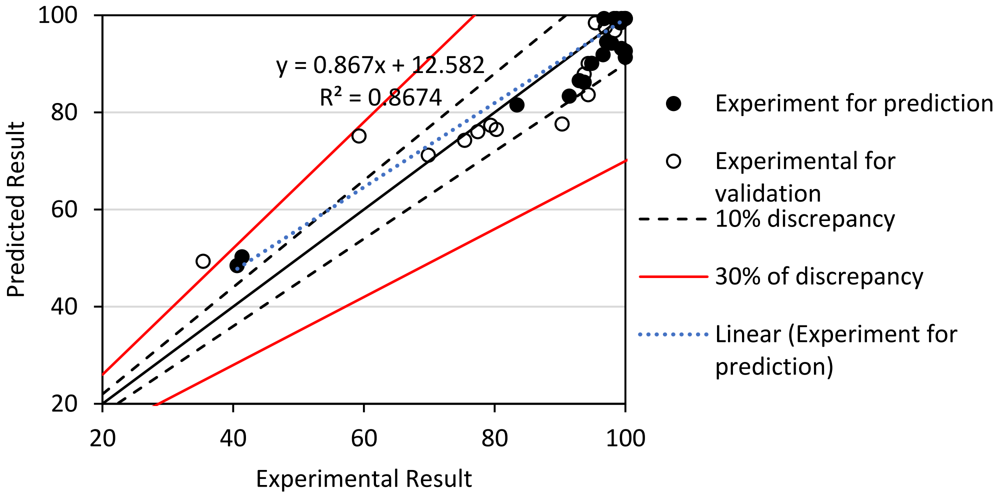

Figure 4.37. Validation of absorbacne removal with overfit data range

- *Humic acid removal*

Figure 4.37 showed the validity of predicted model to new observation of absorbance removal. All validated absorbance removal data which was higher than 70% was fitted to the predicted model and in range 10% error. The results showed that 3 validated values were out of range. If the discrepancy was expand to 30%, most of data values were fitted to the model. Therefore, the validation of HA was in 30% of discrepancy.

4.5.3 Summary results of EC and settling test

The effect of ions and operating condition on turbidity and HA removal was compared with based condition. The improvement was calculated by using eq. 4.24, where ΔR(%) was the improvement, R_i(%) was the efficiency of each conditions, R_o(%) was the efficiency of base condition at current density 1 mA/cm^2 with natural synthetic water pH.

$$\Delta R(\%) = \frac{R_i(\%)\text{-}R_o(\%)}{R_0(\%)} \times 100 \qquad \textit{eq. 4.23}$$

Four conditions were summarized following:

1. Based condition: was operated at 1 mA/cm^2 with natural synthetic pH (pH=7.49).
2. No ion contaminated: current density was varied from 1 to 4 mA/cm^2 with wastewater nature pH

3. The individual terms of ion and operation were:
   - ✓ Current density: pH 7.49 and current density 1, 2, 3, and 4 mA/cm^2
   - ✓ Initial pH: initial pH 5, 7, and 9 and current density 1 mA/cm^3
   - ✓ Calcium: initial pH 7, current density 1 mA/cm^2, and calcium concentration 3.6, 10.8, 18 mg/L. Since the initial pH of effect of calcium was different from base condition; therefore, the improvement of only calcium (ΔR_{Ca}) on base condition (R_o) was the different between the improvement of concentrated calcium (R_{Ca}) to zero calcium ($R_{Ca=0}$) at same pH as expressed in eq.4.34.

     $$\Delta R_{Ca} = \Delta R_{Ca} - \Delta R_{Ca=0} \qquad \textit{eq. 4.24}$$

   - ✓ Ferrous: initial pH 7, current density 1 mA/cm^2, ferrous concentration 1, 13, 25 mg/L. The same equation (eq. 4.35) for calcium was employed to find out the improvement of ferrous.
4. Co-existing ions and operating conditions: initial pH 5-9, current density 1-4 mA/cm^2, calcium 3.6-18 mg/L, and ferrous 1-25 mg/L.

a. <u>Turbidity removal</u>

➢ *Optimal condition*

The result showed the optimal conditions of individual term and co-terms to the based condition as indicated in Table 4.11. At based condition, HA-bentonite was removed around 73.41 mA/cm^2 at nature pH 7.49 with current density 1 mA/cm^2.

At kinetic study, the optimal condition was found at 3 mA/cm^2 for turbidity removal operating with HA-bentonite's natural pH (pH=7.49). Treatment efficiency was improved 16.13% from based condition.

At individual ion and operating condition, current density and ferrous had significant effects on turbidity removal. However, the improvement of adjusting pH was found around 22.56% from the based condition when adjusting initial pH to optimal values (pH 7). Then, finding optimal ion contaminated for turbidity removal was also useful in EC process. The result showed that calcium did not significant effect on the treatment performance when initial pH was 7 and current density 1 mA/cm^2. The existing ferrous contained in solution was decreased in turbidity removal. The optimal condition of co-

Table 4.11. The optimal of the effects of individual and co-terms on turbidity removal

Condition/ parameter		Current density	Initial pH	Calcium	Ferrous
		mA/cm2	-	mg/L	mg/L
Base	Operation	1	7.49±0.15	0	0
	Efficiency (%)	73.41±0.07			
No ions/ Individual study: Current density (1-4 mA/cm^2)	Effect	significant			
	Optimal	3	7.49±0.15	0	0
	Efficiency (%)	85.25±0.10			
	Improve/Reduce efficiency (%)	16.13			
Individual study: Initial pH (5-9)	Effect	insignificant			
	Optimal	1	7	0	0
	Efficiency (%)	89.97±0.21			
	Improve/Reduce efficiency (%)	22.56			
Individual study: Calcium (0-18 mg/L)	Effect	insignificant			
	Optimal	1	7	0	0
	Efficiency (%)	89.97±0.21			
	Improve/Reduce efficiency (%)	22.56			
Individual study: Ferrous (0-25 mg/L)	Effect	significant			
	Optimal	1	7	0	0
	Efficiency (%)	89.97±0.21			
	Improve/Reduce efficiency (%)	22.56			
Co-terms	Effect	insignificant	significant	significant	significant
	Optimal	3.4	8	18	1
	Efficiency	89.45±0.19			
	Improve/Reduce efficiency (%)	21.85			

ions and operating condition was found at current density 3.4 mA/cm^2, initial pH 8, calcium 18 mg/L, and ferrous 1 mg/L. The turbidity could reach 89.45% or improvement 21.85% from based condition. Comparing EC performance between no ion and containing co-ions, the result was not much different (no ion: 85.25% vs. co-ions: 89.45% removal efficiency). Therefore, some ions containing in water may not an obstacle for EC process.

Table 4.12. Summary the worst condition of individual and existing ions on turbidity removal

Condition/ parameter		Current density	Initial pH	Calcium	Ferrous
		mA/cm2	-	mg/L	mg/L
Base	Operation	1	7.49±0.15	0	0
	Efficiency (%)	73.41±0.07			
No ions/ Individual study: Current density (1-4 mA/cm^2)	Effect	significant	-	-	-
	Optimal	1	7.49±0.15	0	0
	Efficiency (%)	73.41±0.07			
	Improve/Reduce efficiency (%)	0			
Individual study: Initial pH (5-9)	Effect	insignificant			
	Value	1	9	0	0
	Efficiency (%)	71.72±0.10			
	Improve/decrease efficiency (%)	-2.30			
Individual study: Calcium (0-18 mg/L)	Effect	insignificant			
	Value	1	7	3.6	0
	Efficiency (%)	87.22±0.44			
	Improve/decrease efficiency (%)	18.81			
Individual study: Ferrous (0-25 mg/L)	Effect	significant			
	Value	1	7	0	25
	Efficiency (%)	76.62±0.18			
	Improve/decrease efficiency (%)	4.37			
Co-terms	Effect	insignificant	significant	significant	significant
	Value	1	5	3.6	18.1
	Efficiency	78.40±1.55			
	Improve/decrease efficiency (%)	6.80			

- *The worst condition*

However, the worst condition of ions contaminated and operation condition might be happening in some case. The effect values were shown in Table 4.12.

b. <u>Humic acid removal</u>

- *Optimal condition*

The optimal conditions of ion and operations on absorbance removal were shown in Table 4.13. When the synthetic water did not contaminate any ions, absorbance removal was 98.41% with optimal current density 3 mA/cm^2. It was improved 41.13% from based condition of current density 1 mA/cm^2. Therefore, current density was very significant effect on absorbance removal.

For single term of ion and operation, the absorbance removal efficiency values were 98.41%, 97.14%, 77.43%, and 93.71% for optimal current density, initial pH, calcium, and ferrous, respectively. Therefore, optimal conditions of current density and initial pH were meaningful to EC process. At initial pH 7 with current density 1 mA/cm^2, the absorbance removal was 80.29% or improved 15.14% from EC operated at current density 1 mA/cm^2 and initial pH 7.49. Therefore, the improvement of ferrous was only 19.25% while calcium decreased absorbance 4.01% from base condition.

The optimal condition of co-existing ions and operations was current density 4 mA/cm^2, initial pH 5, calcium 8 mg/L, and ferrous 25 mg/L. The absorbance was removed 100% or 43.41% from base condition. Therefore, the different of no ions and co-existing ions with optimal operating condition of absorbance was not much different.

- *The worst condition*

The worst conditions ions and operating condition were summarized in Table 4.14. The effect of calcium (Ca^{2+}=10.8 mg/L) in water was decreased the treatment performance around 30.14% from base condition with same operating conditions of EC process. However, at the worst condition of ferrous, ferrous was very slightly decreased the treatment performance, so adding ferrous in the system was only positive effect in EC process in HA removal. The result of co-existing ions and operating condition showed that the worst condition of ions and operations, the treatment of absorbance was reduced

Table 4.13. Optimal condition of different conditions on absorbance removal

Condition/ parameter		Current density	Initial pH	Calcium	Ferrous
		mA/cm^2	-	mg/L	mg/L
Base	Operation	1	7.49±0.15	0	0
	Efficiency (%)	69.73±4.27			
No ions/ Individual study: Current density (1-4 mA/cm^2)	Effect	significant	7.49±0.15	0	0
	Optimal	3			
	Efficiency (%)	98.41±2.25			
	Improve/Reduce efficiency (%)	41.13			
Individual study: Initial pH (5-9)	Effect	insignificant			
	Value	1	5	0	0
	Efficiency (%)	97.14±0.00			
	Improve/decrease efficiency (%)	39.31			
Individual study: Calcium (0-18 mg/L)	Effect	insignificant			
	Value	1	7	5	0
	Efficiency (%)	97.14±0.00			
	Improve/decrease efficiency (%)	39.31			
Individual study: Ferrous (0-25 mg/L)	Effect	insignificant			
	Value	1	7	0	0
	Efficiency (%)	80.29±1.21			
	Improve/decrease efficiency (%)	15.14			
Co-terms	Effect	significant	significant	insignificant	significant
	Value	4	5	8	25
	Efficiency	100			
	Improve/decrease efficiency (%)	43.41			

41.73% from base condition. It could conclude that optimal operation for HA removal was very crucial. Low current density with high pH, absorbance could not remove effectively from EC process.

Table 4.14. Summary the worst conditions in absorbance removal

Condition/ parameter		Current density	Initial pH	Calcium	Ferrous
		mA/cm^2	-	mg/L	mg/L
Base	Operation	1	7.49±0.15	0	0
	Efficiency (%)	69.73±4.27			
No ions/ Individual study: Current density (1-4 mA/cm^2)	Effect	significant			
	Optimal	1	7	0	0
	Efficiency (%)	69.73±4.27			
	Improve/Reduce efficiency (%)	0			
Individual study: Initial pH (5-9)	Effect	insignificant			
	Value	1	9	0	0
	Efficiency (%)	35.43±0.01			
	Improve/decrease efficiency (%)	-49.20			
Individual study: Calcium (0-18 mg/L)	Effect	insignificant			
	Value	1	7	18	0
	Efficiency (%)	75.43±0.81			
	Improve/decrease efficiency (%)	8.17			
Individual study: Ferrous (0-25 mg/L)	Effect	insignificant			
	Value	1	7	0	1
	Efficiency (%)	79.43±1.61			
	Improve/decrease efficiency (%)	13.91			
Co-terms	Effect	significant	significant	insignificant	significant
	Value	1	9	18	1
	Efficiency	40.63±3.21			
	Improve/decrease efficiency (%)	-41.73			

The objective of EC process in this study is to remove the turbidity in water containing turbidity and NOM. Therefore, the optimal conditions of turbidity removal was applied.

c. Settling test

The objective of settling test was to separate sludge and improve treatment of EC effluent. After 20 min treatment of two conditions for turbidity, their effluents were tested with settling test as shown in Table 4.15. The data processing on settling test analyze was shown in Appendix 5.

➢ *synthetic water*

The objective of doing settling test of synthetic water without EC operation was to prevent the sedimentation in EC reactor after design the continuous reactor. The synthetic water contained 70 mg/L of HA and 100 NTU of bentonite. The relationship of overflow rate and efficiency was shown in Figure 4.38. If the overflow rate of EC was lower than 7.8 m/hr, the sedimentation would reach 50% in continuous reactor. Therefore, to prevent sedimentation in reactor, the overflow rate required higher than 1.5 m/hr (sedimentation less than 24%).

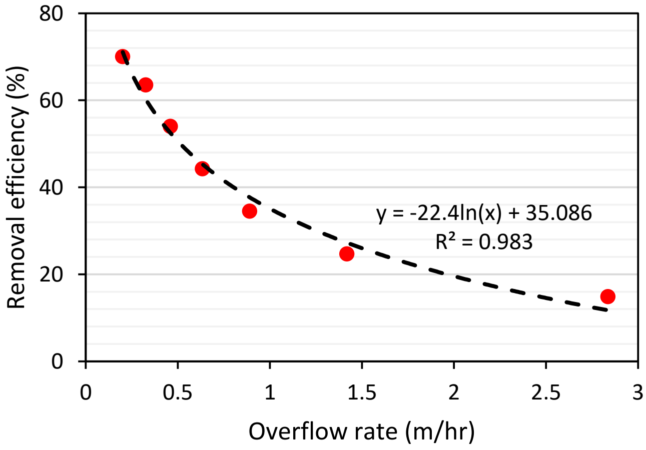

Figure 4.38. Overflow rate and removal efficiency of synthetic water without EC operating

➢ *Optimal co-existing ions and operating conditions*

At optimal co-existing ions an operating conditions, the initial turbidity was 33.9 NTU. The overflowrate and removal efficiency was shown in Figure 4.39. The maximum turbidity removal was 85% or 5 NTU when overflow rate was 0.84 m/hr. Moreover, the overflowrate was 1.4 m/hr for 7 NTU turbidity residual. On the other hand, there was no HA residual after settling test.

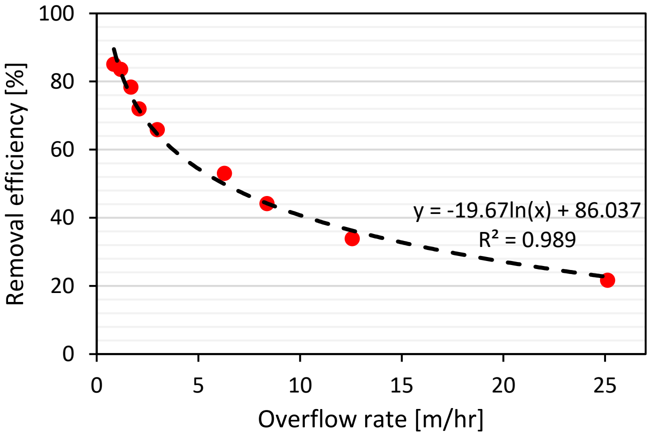

Figure 4.39. Settling graph of optimal co-existing ions and operating for turbidity removal

Table 4.15. Summary results of settling test

Condition/ parameter	Overflowrate for max. turbid removal		
	Time (min)	Turbidity (NTU)	Overflow rate (m/hr)
No operation (EC)	89.7	32.1	0.20
Optimal ions and operation (turbidity)	21.4	5.08	0.59

The summary of turbidity remained after settling test was illustrated in Table 4.15. The result indicated that the optimal ions and operation could improve the treatment of turbidity to 5 NTU.

d. EC effluent

After EC operation of optimal condition of co-ions and operation, HA remained was already lower than WHO standard. Therefore, EO process was not necessary to operate. However, some case of the worst condition of HA was considered. Table 2.2 already showed that the maximum pH of groundwater in Cambodia was 9.95 since it might be polluted by human or natural activity. After 20 minutes HA removal with the worst conditions of co-existing and operating by EC process, the turbidity was around 18 NTU and 37 mg/L of HA remained or 75 mg/L of COD as shown **Error! Reference source not found.**.

Table 4.16. Contaminants remained after EC of the worst condition of HA removal

Real effluent			Synthetic water		
Contaminant	Unit	value	Chemical	Unit	Value
Turbidity	NTU	18.3	HA	mg/L	37
HA	mg/L	37	FeSO4		2.48
Fe^{2+}		0.5	$CaCl_2$		12.88
Ca^{2+}		4.64	NaCl		32.57
Cl^-		28	pH	-	9

4.6 Electrooxidation and design criteria proposition

4.6.1 Electrode condition for EO process

The objective of EO process was to remove HA which remained from EC effluent. The remained ions and HA were synthesized as shown in **Error! Reference source not found.**. Electrode material, arrangement, and effect of chloride were analyzed to improve the treatment performance.

a. <u>Electrode material for cathode side</u>

Electrode type is very important for electrochemical. In this study, aluminum and graphite for cathode side were compared to study the treatment efficiency of HA. Electrode was arranged in mono-polar with gap 1.5 cm and current density 2.5 mA/cm^2. The result in Figure 4.40 showed that aluminum-graphite was better in HA removal than graphite along reaction time. At 50 minutes treatment, graphite-aluminum removed HA around 93.51% while graphite-graphite was 58.33% removal. This might happen since aluminum could produce more hydrogen gas than graphite in EO process. Therefore, graphite-aluminum in monopolar was employed to remove HA from synthetic water since bipolar could not be done by using different material electrodes.

b. <u>Electrode arrangement</u>

Since aluminum electrode was much better than graphite for employing cathode side and the inner electrode of bipolar had two charges, so this part considered the arrangement of EO process. The arrangement of electrode material was shown in Table 4.17. The result showed that bipolar arrangement could improve HA removal slightly at 40 min beginning. After that, the removal efficiency was similar. However, the

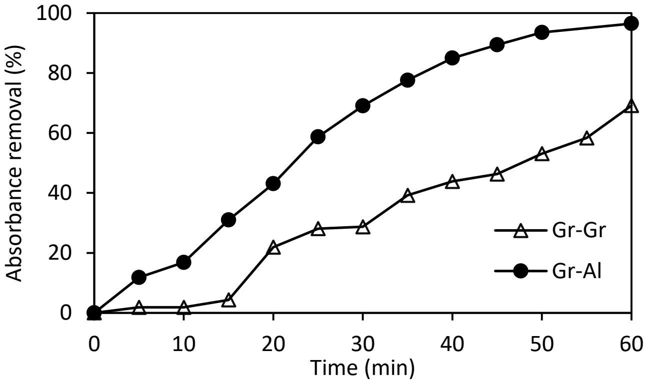

Figure 4.40. Comparison absorbance removal by using Graphite/Graphite and Graphite-Aluminum

voltage consumption in bipolar was much higher than mono one. Therefore, monopolar arrangement was selected in EO process due to energy saving.

c. <u>Conductive carbon coated onto graphite for anode material</u>

To improve the treatment efficiency, many studies were developed electrode material by modifying, coating, or decomposing electrode material. Here, conductive carbon was coated onto graphite electrode to study the removal efficiency with electrode before coated. The benefits of coating this conductive carbon are:

- High conductivity: it reduces the surface resistivity of 42 Ω per square for 1 coat, so it could improve the reaction rate in the system
- Strong adhesion: it can improve adhesion stronger than water-based coatings
- Rub of resistant
- Tough and durable coating
- Corrosion-proof coat slows or prevents substrate oxidation

Figure 4.42 showed that the removal of graphite coated was better than graphite before coated and its appearance was shown in Appendix 8. At 50 min treatment with current

Table 4.17. Comparing electrode arrangement in EO process.

Arrangement	Electrode			
	1	2	3	4
Monopolar	Gr	Al	Gr	Al
Bipolar	Gr	Gr	Gr	Al

Note: electrode 1 and 4 were at anode and cathode side, respectively.

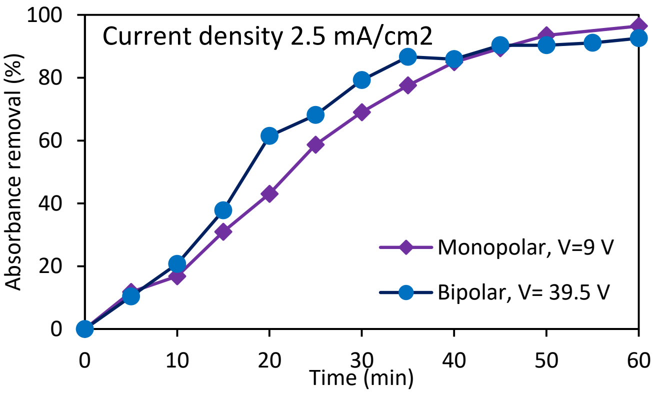

Figure 4.41. Removal efficiency of mono- and bipolar arangement at current density 2.5 mA/cm^2

density 2.5 mA/cm^2, graphite coated could reach 100 % removal while graphite removed only 93.42%. Therefore, graphite coated was consumed in this study. Therefore, electrode material for EO was aluminum for cathode and conductive carbon coated onto graphite for anode in HA removal. Monopolar arrangement was employed.

4.6.2 Kinetic study of EO

Current density was varied from 2.5 to 7 mA/cm^2 for analyze the optimal current density and chemical reaction rate of EO in HA removal. The result showed that the removal of absorbance at 20 minutes were 62.56%, 93.10%, 99.37%, and 99.33% after applying with 2.5, 4, 5.5, and 7 mA/cm^2, respectively. The kinetics of removal efficiency were not much increased when current density was higher than 5.5 mA/cm^2.

By using simple kinetic model of zero-, firs-t, and second order, the constant rate and R-square of observe and model prediction for current density 2.5 mA/cm^2 was summary

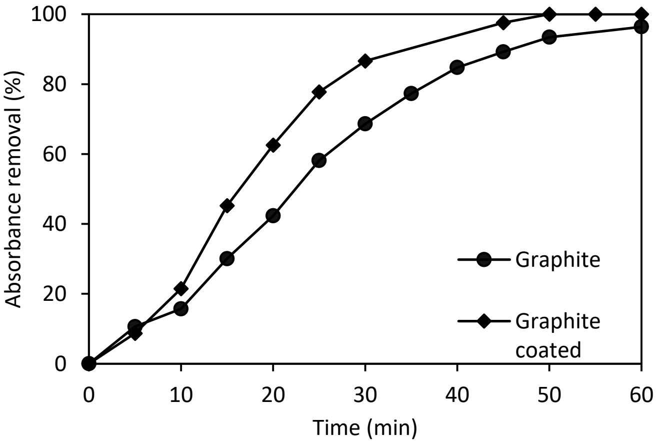

Figure 4.42. Comparison of graphite and graphite coated conductivity carbon on HA removal

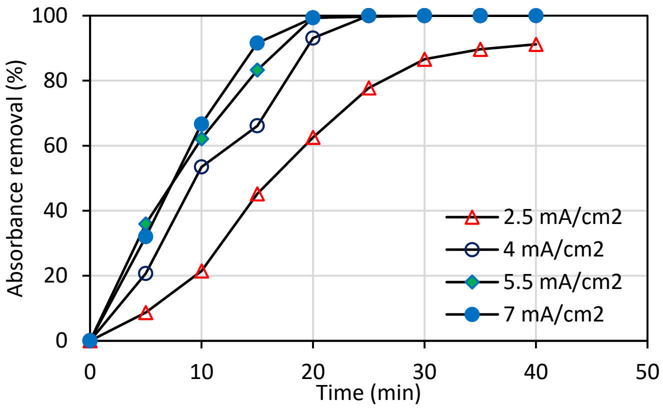

Figure 4.43. Removal efficiency of HA along the time at different current density, EO process

in Figure 4.44. The result showed that HA removal in EO followed first-order kinetic since its R-square was the highest. Tang et al. (2014) also showed that HA was follow first-order chemical reaction. The model prediction of HA in different current density by using solver in Microsoft excel were shown in Appendix 6. The constant rate of model prediction was followed first-order polynomial as shown in Figure 4.45. It could conclude that current density 5.5 mA/cm^2 was an optimal condition since the slope of constant rate was not steep anymore after increasing current density.

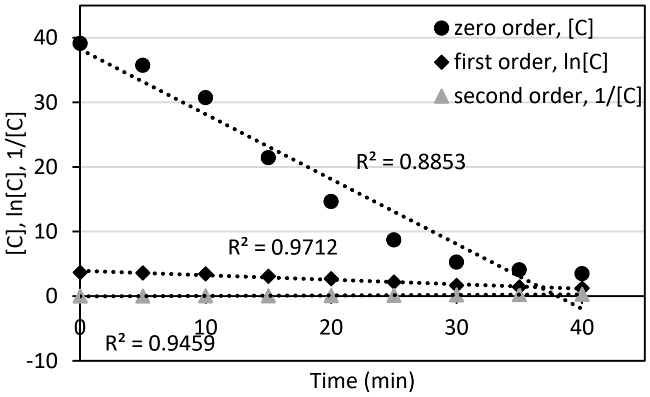

Figure 4.44. Constant rate and R-square of zero, first, and second order kinetic

4.6.3 Effect of chloride on HA removal in EO process

The optimal current density 2.5 mA/cm^2 was taken to study the effect of chloride on HA removal in Electrooxidation process since some studies proved that chloride could improve the treatment efficiency by indirect oxidation of chloride ion, and conductivity in Electrooxidation process (Subramaniam and Halim, 2014). However, the results

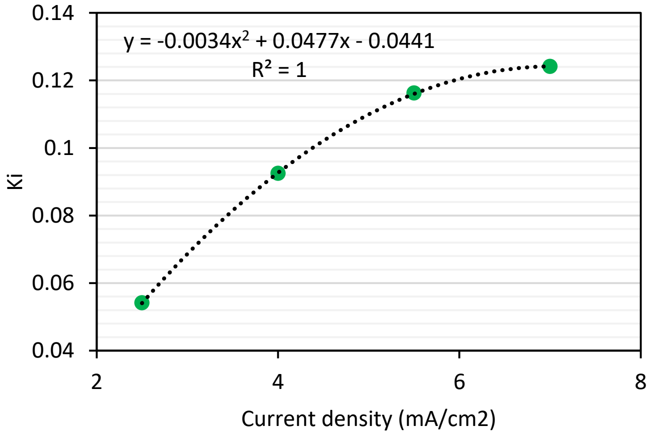

Figure 4.45. Model prediction of k in different current density

showed that adding concentration of chloride 0, 50, 200, and 500 mg/L into the synthetic water, it was not significant effect on HA removal as shown in Figure 4.46 (a). Therefore, another experiment of HA synthetic water without adding sodium chloride or minus 28 mg/L of Cl^- from the previous study was employed. The result still showed that there was no effect on HA removal.

This study was concerned that the current density was too high; therefore, it was not able to see the effect of chloride on HA as the potential of current density on HA removal was much higher than chloride's. Thus, the reduction current densities to 4 mA/cm^2 and 2.5 mA/cm^2 were analyzed the effect of chloride ion again as shown in Figure 4.46 (b) and (c). It was indicated that there was no different after adding chloride from 0 to 280 mg/L when HA concentration was 37 mg/L with current density 2.5 mA/cm^2. At current density 4 mA/cm^2 showed that adding chloride higher than 300 mg/L, the removal was decreased.

Therefore, the result could be concluded that adding chloride in solution did not improve the treatment efficiency. This might be the concentration of HA was low which could not able to see the effect or the structure of HA was not degraded by chlorine. Additionally, adding chloride higher than 300 mg/L would bring negative effect on HA removal. However, adding chloride into solution, it could improve the conductivity which reduced the voltage of DC power supply.

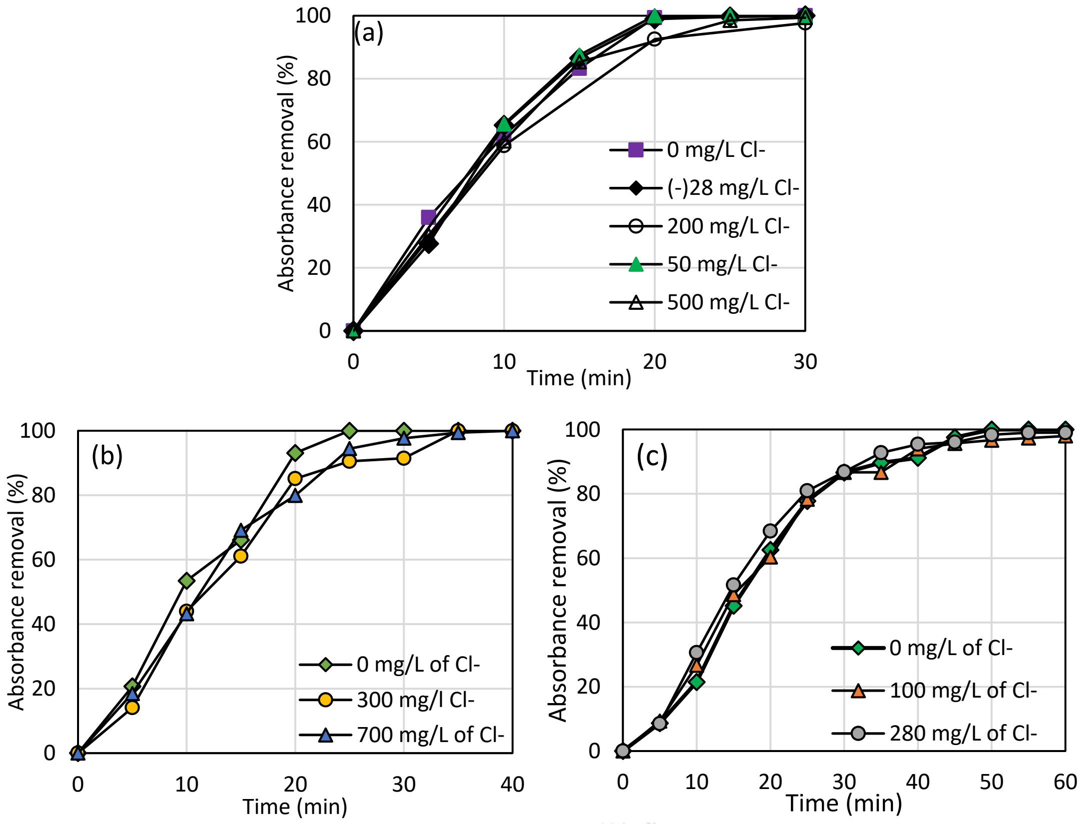

Figure 4.46. Effect of chloride on HA removal at current density (a) 2.5 mA/cm^2,(b) 4 mA/cm^2, and (c) 2.5 mA/cm^2, EO process

4.6.4 Proposition of design scenario and criteria

a. <u>Proposition of design scenario</u>

After EC and EO process in a batch reactor, this section aimed to propose the treatment design for turbidity and HA removal. The continuous reactor was design based on the characteristic of water. As mentioned in settling test, only optimal co-ions and operation condition could reach the standard after settling. However, there was no HA remained after settling test. Then, the worst condition of co-ions and operation for HA was included in this study. Therefore, three scenarios of reactor design with two conditions of wastewater were considered as shown in Figure 4.47 and Table 4.18.

➢ *1st scenario*

1st scenario was shown in Figure 4.47. Wastewater was only treated in electrocoagulation reactor. The effluent had turbidity higher than standard with low HA residual as shown in Table 4.19.

Table 4.18. Three condition for reactor design study

Conditions	Current density applied mA/cm^2	
Scenario 1st and 2nd	**EC**	
Optimal co-ions and operations for turbidity removal	3.4	
Scenario 3rd	**EC**	**EO**
Worst co- ions and operation for HA removal	1	5.5

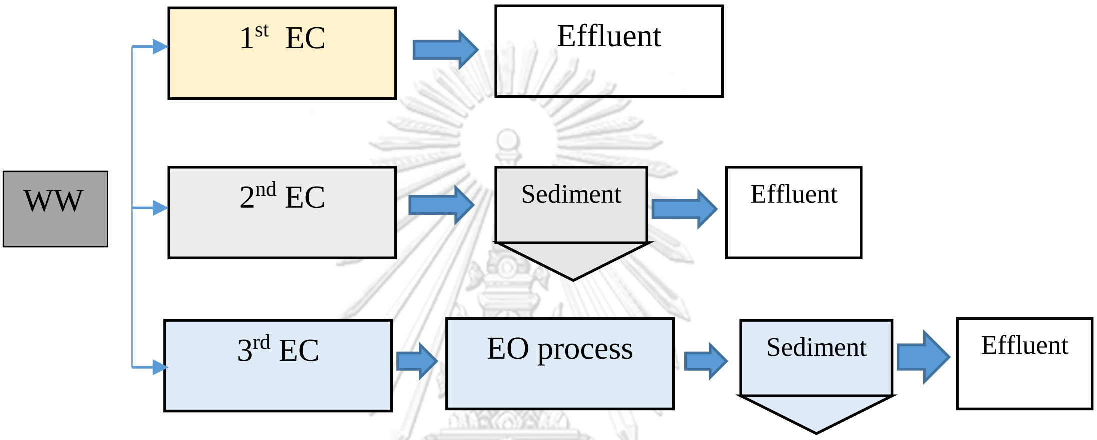

Figure 4.47. Three senarios of reactor design: (1) only EC reactor, (2) EC reactor and sedimetation tank, (3) EC, EO, and sedimentation tank for turbidity and HA removal

- *2nd scenario*

At 2nd scenario, two reactors were designed including EC reactor and sedimentation tank. The result showed that after 20 minutes treatment by EC process and settle down 30 minutes, the effluent of turbidity, COD, Dissolve oxygen (DO), Conductivity, and pH were allowed by WHO drinking water standard as shown in Table 4.15.

- *3rd scenario*

At third scenario, three reactors were designed including EC, EO, and sedimentation tank orderly as shown in Figure 4.47. This condition, EC was operated with current density 1 mA/cm^2 using aluminum electrode in bipolar arrangement. Then, EO was operated with current density 5.5 mA/cm^2 using graphite-coated and aluminum in monopolar arrangement. After EO, 99.34% of HA was removed but the turbidity remained was around 22 NTU. Therefore, sedimentation was required to improve the

Table 4.19. Effluents of 2nd scenario comparing to WHO standard (Omaka et al., 2015)

Parameters	Unite	Values	WHO standard
Turbidity	NTU	5.06	5
DOC	mg/L O_2	2.50	-
DO	mg/L	4.55±0.07	4
Conductivity	µS/cm	330.6±0.42	1250
pH	-	7.88±0.01	6.5-8.5

Note: DOC value was in mean value. The DOC in Thailand tap water was 2.46 mg/L

turbidity removal after EO process. Therefore, only 2nd and 3rd conditions which were able to use in water treatment since they had effluent lower than standard. However, 3rd scenario will cost higher than 2nd scenario as the current density of EO process was already higher than 2nd scenario. Thus, among these three scenarios, the 2nd scenario was employed because the operation cost was low and effluent was under WHO standard.

b. Design criteria

After getting the optimal conditions for 2nd scenario in EC for turbidity and HA removal. Here, the design criteria were proposed. The process of calculation was expressed in Appendix 8. If the raw water flowrate Q=50 m^3/hr , the design criteria for these processes were:

- *Electrocoagulation reactor (ECR)*

The dimension of electrocoagulation continuous reactor was illustrated in Table 4.20. To prevent the sedimentation occurred in EC reactor, the overflow rate (V_o) of EC reactor must be higher than pollutant overflow settling velocity (V_s=1.42 m/hr for 25% removal). Therefore, EC was operated at current density 3.4 mA/cm^2 and 20 min treatment. The tank size was 5 m length, 3.33 m width, and 1.2 m depth. The electrode plates were 4168 sets.

- *Sedimentation tank*

The detention time was 22 min with 1.25 m/hr of overflowrate, so the detention time for studying was 30 min. The design criteria was shown in Table 4.21.

✓ Checking criteria for sedimentation tank

The design criteria was based on Kawamura (2000). The result showed that all parameters were in criteria design as shown in Table 4.22.

$$V = \frac{2(L+W)}{t} = \frac{2\times(5+3.33)}{20} = 0.83m/\min = 49.98m/hr > 1.42m/hr(ok)$$

Therefore, the dimensions of sedimentation tank are 7.68 m length with 5 baffles, 3.33 m width, and 0.98 m height as shown in Figure 4.49.

Table 4.20. The design criterial for electrocoagulation reactor

EC tank	Equation		Hypothesis
Current density: J=3.4 mA/cm^2	-	-	Optimal current density
Volume of wastewater: V=16.67 m^3	$Q = \frac{V}{t}$	V: volume of wastewater (m^3) t: operating time (hr) Q: wastewater discharge (m^3/hr)	Q: 50 m^3/hr t: 20 min
Number of electrode set: N=4168	$N=\frac{V}{4L}$	V: volume of wastewater (L) 4L: volume of wastewater in batch column	V:16.67 m^3=16670 L
Length of reactor: L=5 m	$v = \frac{L}{t}$	v: mean flow (m/min)	v: 0.25 m/min t: 20 min
Cross section: A=3.33 m^2	$A = \frac{V}{L}$	V: volume (m^3) L: length of reactor (m)	V: 16.67 m^3 L: 5 m
Depth and Width: D=1 m +0.2m=1.2m W=3.33 m	$V = L\times W\times D$	L: length of reactor W: width D: depth F: freeboard 0.2m	L: 5m D: 1m

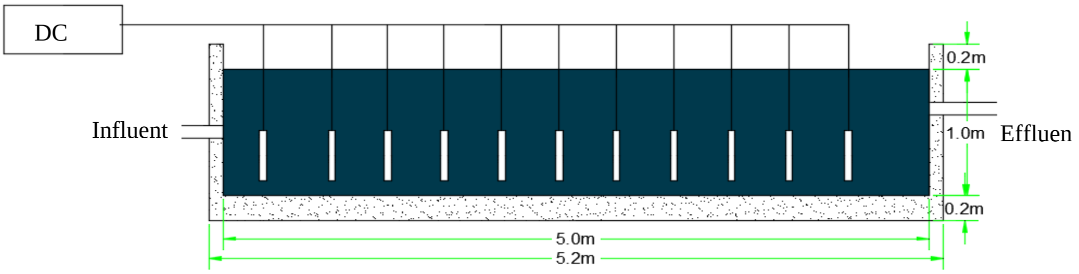

Figure 4.48. Electrocoagulation Reactor (ECR)

Table 4.21. Design criteria of sedimentation tank

Sedimentation tank	Equation		Hypothesis
Volume of the tank: *V=25 m^3*	$Q = \frac{V}{t}$	Q: wastewater flowrate (m^3/hr) V: volume of the tank (m^3) t: detention time (hr)	Q: 50 m^3/hr t: 30 min
Surface tank: As= 40 m^2	$v = \frac{As}{t}$	v: overflowrate (m/hr) t: detention time (hr)	v: 1.25 m/hr t: 30 min
Length and width of tank: L_T=16.67 m W=3.33 m	$As = 2(L_T + W)$	As: surface loading (m^2) L_T: total length (m) W: width (m)	As: 40 m^2 L:W=5:1
Adjust length of tank: L=7.68m	$L_{BF} = \frac{W}{2}$	W: width L_{BF}: length of baffle (m) L_{BF}=W/2	Number of baffle: 5 W=3.33 m
Depth of tank: D=0.98 m D_{Total}=1.2 m	$V = D \times W \times L$ D_{Total}=D+$H_{Freeboard}$	D: depth (m) W: width (m) L: length (m) V: volum (m^3)	W: 3.33 m L: 7.68 m V: 25 m^3 $H_{freeboard}$: 0.22 m

c. <u>Estimated cost of treatment</u>

The operating cost includes material cost (mainly based on electrodes), utility cost (mainly based on electrical energy), as well as labor, maintenance and other fixed costs.

Table 4.22. Checking design criterial for sedimentation tank

Parameters	Criteria	Sedimentation tank
Water depth	Max 4.5 m	0.98 m
Mean flow	0.3 to 1.1 m/min	0.53 m/min
Detention time	max 4 hr	30 min
Surface loading rate	1.25 to 2.5 m/hr	1.25 m/hr
Length: width	Min of 4:1	5:1
Depth: Length	Min of 1:15	1:17.01

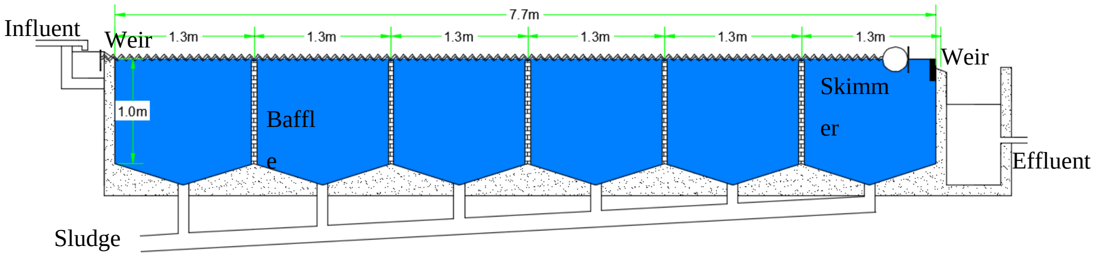

Figure 4.49. Sedimentation tank

In this preliminary economic study, energy and electrode material costs are taken into account as major cost items in the calculation of the operating cost as kWh per kg of turbidity and organic removed. These calculations was carried out after optimizing the operational parameters in EC process as shown in Table 4.23. The process of calculation, electrode and energy consumption cost were followed by Palahouane et al. (2015), Algeria.

Thus, the operation cost in 1 m^3 was US$ 0.2782 or US$ 13.91 in 50 m^3 of wastewater.

4.6.5 Summary

The optimal time was found at 20 minutes treatment with current density 5.5 mA/cm^2 for HA 37 mg/L removal by using electrooxidation. Electrooxidation was not required to operate when the optimal co-ions and operating condition for electrocoagulation (2nd scenario) was chosen. The coagulation tank dimension was 5m length, 1.2 m depth, and 3.33 m width. The sedimentation tank was 7.68 m length with 5 baffles, 3.33 m width, and 1.1 m height height when wastewater discharge was 50 m^3/hr. The cost of EC treatment was US$ 0.28/m^3.

Table 4.23. Cost estimation of EC operation

Procedure of calculation	Equation		Hypothesis
Electrical consumption E=0.011 kwh	E=UiT/1000	E: electrical consumption (kwh) U: voltage (V) i: current (A) T: operation time (h)	U: 46.75 V i: 0.68 A T: 20 min
Amount of aluminum released m_T=0.1522g	m_T =itM/ZF	i: current (A) t: time (s) M: molecular weight of metals (g/mol) Z: number of electrons F: Faraday's constant (Coulombs/mol)	M_{Al}: 27 g/mol Z: 3 F: 96500 C/mol I: 0.68A
current efficiency C_E=181.73%	$C_E = \frac{m_e}{m_T} \times 100$	C_E: current efficiency (%) m_T: theoretical mass of aluminium (g) m_e: actual electrode loss (g)	$m_{electrode}$: 0.2766g m_T:0.076g
specific electrical energy consumption Seec=0.0015kwh	$\text{Seec}=\frac{nF}{3.6\times10^3 MC_E}$	n: number of electrons F: Faraday's constant (Coulombs/mol) M: molecular weight of metals (g/mol) C_E: current efficiency (%)	n: 3 F: 96500 C/mol M: 27 g/mol C_E: 363.45%
energy consumption C_{energy}=0.009kwh	C_{enery} =(E-Seec)	E: electrical consumption (kwh) Seec: specific electrical energy consumption	E=0.011 kwh Seec=0.0015kwh
the total cost 0.2782 US$/$m^3$	$\text{Operating}_{cost} = aC_{energy} + bC_{electrode}$	C_{energy} and $C_{electrode}$, are consumption quantities per kg of turbidity and organic removed a: electrical energy price b: aluminum electrodes cost	a: 0.06 $/kWh b: 2052$/t (Daghrir et al., 2013)

CHAPTER 5
CONCLUSION AND RECOMMENDATION

5.1 Conclusion

This study aimed to study the effects of ion contaminated and operating conditions on Electrocoagulation and Electrooxidation for improving water quality. Therefore, this work could be concluded to the three objectives as following (Figure 5.1):

- To optimize the treatment conditions of Electrocoagulation process in terms of turbidity and natural organic matter removal

The optimal condition of electrode configuration and arrangement was found at current density 1.5 mA/cm^2, gap 2 cm, and bipolar arrangement. Electrocoagulation comparing to chemical coagulation process, it could be concluded that EC was better performed with wastewater containing humic acid while CC was highly treated turbidity in wastewater.

The kinetic of Bentonite removal has three stages: lag, reactive, and stable stage following destabilization mechanism while HA can be removed faster by sweeping flocs mechanism. HA could improve turbidity removal in HA-Bentonite since its colloid that could attach the pollutants. The optimal current density and time were found at 3 mA/cm^2 and 20 minutes treatment, respectively. The turbidity removal in EC was followed S-curve while HA was fitted with first-order chemical rate. Meanwhile, the second-polynomial equation was the most fitted model in these two pollutants in terms of current density and operating time.

- To evaluate the effect of ions (ferrous and calcium) and operating conditions (initial pH and current density) on Electrocoagulation performance in terms of turbidity and natural organic matter removal, and predict mathematical model by using statistical design of experiment (DOE) methodology

In terms of turbidity removal, ferrous, calcium, and initial pH were significant effects in EC process. It was noticed that ferrous brought negative effects while calcium had benefit in turbidity removal. The optimal condition of turbidity removal was identified at current density 3.4 mA/cm^2, initial pH 8, ferrous 1 mg/L, and calcium 18 mg/L. The worst condition was found at current density 1 mA/cm^2, pH 5, calcium 3.6 mg/L, and ferrous 18.1 mg/L.

In terms of humic acid removal, current density, initial pH, and ferrous were significant effects while calcium was not. The optimal condition was found at current density 4 mA/cm^2, initial pH 5, calcium 8 mg/L, and ferrous 25 mg/L. The worst condition was found at current density 1 mA/cm^2, initial pH 9, calcium 18 mg/L, and ferrous 1 mg/L.

The mathematical models for turbidity, HA, and final pH were constructed in terms of current density, initial pH, calcium, and ferrous by using Design of Experiment (DOE). The turbidity and final pH model were validated with overfit data in 10% of discrepancy while absorbance was validated in 30% of discrepancy.

- To analyze electrode material and operating condition on natural organic matter removal in Electrooxidation process

HA was residual 37 mg/L after EC operation at the worst condition of co-ions and operations. The best electrode material for EO was aluminum and conductive carbon coated onto graphite for cathode and anode, respectively. Humic acid was removed following first-order chemical reaction. The optimal current density and operating time were 5.5 mA/cm^2 and 20 min, respectively. Chloride was not effects to HA removal in EO process.

The optimal condition of co-existing ions and operations were chosen to design the continuous flow since it was the most economic condition. The wastewater containing HA 70 mg/L, bentonite 100 NTU, calcium 18 mg/L, and ferrous 1 mg/L was operated at current density 3.4 mA/cm^2 and initial pH 8. After 20 minutes EC treatment, the effluent of HA was already lower than standard, so EO was not necessary to operate. However, sedimentation tank was needed to separate sludge and reduce turbidity in system. If wastewater discharge was 50 m^3/hr, the EC was 5 m length, 3.33 m width, and 1.2 m depth with cost US$ 13.91 and the sedimentation tank was 7.68 m length with 5 baffles, 3.33 m width, and 1.1 m height.

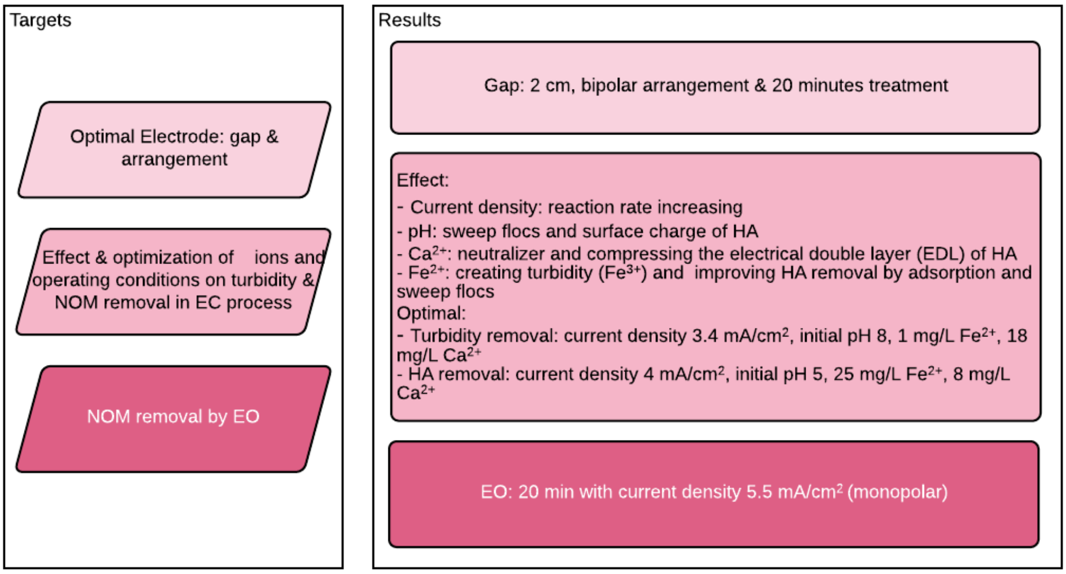

Figure 5.1. Summary results

5.2 Recommendation

The future study of the effects of ion contaminations and operating conditions on EC and EO in water quality improvement still requires elucidation of several key components. A list of future activities for those who are willing in furthering the scientific advancement of EC and EO may look into the following:

- Total aluminum ions in solution should be considered rather than measuring electrode loss for analyzing the optimal condition of EC process.
- The variation of initial concentration of bentonite and HA should be analyzed
- Different concentration of HA would be observed to analyze the effects of chloride on HA removal.
- The proposed design criteria should be constructed and validated.

REFERENCES

Abuzaid, N. S., Bukhari, A. A., and Al-Hamouz, Z. M. Removal of bentonite causing turbidity by electro-coagulation. Journal of Environmental Science & Health Part A 33(7) (1998): 1341-1358.

Adjeroud, N., Dahmoune, F., Merzouk, B., Leclerc, J.-P., and Madani, K. Improvement of electrocoagulation–electroflotation treatment of effluent by addition of Opuntia ficus indica pad juice. Separation and Purification Technology 144 (2015): 168-176.

Ahn, H. Estimation of Response Surface Based on Central Composite Design Using Spatial Prediction. Paper presented at the International Conference on Industrial Engineering, Management Science and Application (ICIMSA), 2016 2016.

Akbal, F., and Camcı, S. Copper, chromium and nickel removal from metal plating wastewater by electrocoagulation. Desalination 269(1-3) (2011): 214-222.

Al-Sameraiy, M. A novel water pretreatment approach for turbidity removal using date seeds and pollen sheath. Journal of Water Resource and Protection 4(02) (2012): 79.

Al-Shannag, M., Al-Qodah, Z., Bani-Melhem, K., Qtaishat, M. R., and Alkasrawi, M. Heavy metal ions removal from metal plating wastewater using electrocoagulation: Kinetic study and process performance. Chemical Engineering Journal 260 (2015): 749-756.

Al Aji, B., Yavuz, Y., and Koparal, A. S. Electrocoagulation of heavy metals containing model wastewater using monopolar iron electrodes. Separation and Purification Technology 86 (2012): 248-254.

Alimohammadi, M., et al. Elimination of natural organic matter by electrocoagulation using bipolar and monopolar arrangements of iron and aluminum electrodes. International Journal of Environmental Science and Technology 14(10) (2017): 2125-2134.

Alimohammadi, M., Askari, M., Dehghani, m. h., Emamjomeh, M., and Nazmara, S. Natural organic matter removal from aqueous solutions by electrocoagulation process using iron and aluminum electrodes. Journal of Advances in Environmental Health Research 2(2) (2014): ??-??

American Public Health Association, American Water Works Association, Water Pollution Control Federation, and Water Environment Federation. Standard methods for the examination of water and wastewater. Vol. 2: American Public Health Association., 1915.

An, C., Huang, G., Yao, Y., and Zhao, S. Emerging usage of electrocoagulation technology for oil removal from wastewater: A review. Sci Total Environ 579 (2017): 537-556. doi: 10.1016/j.scitotenv.2016.11.062.

Anglada, A., Urtiaga, A., and Ortiz, I. Contributions of electrochemical oxidation to waste-water treatment: fundamentals and review of applications. Journal of Chemical Technology and Biotechnology 84(12) (2009): 1747-1755.

Arroyo, M., Pérez-Herranz, V., Montanes, M., Garcia-Anton, J., and Guinon, J. Effect of pH and chloride concentration on the removal of hexavalent chromium in a batch electrocoagulation reactor. Journal of Hazardous Materials 169(1) (2009): 1127-1133.

Asgharian, F., Khosravi-Nikou, M., Anvaripour, B., and Danaee, I. Electrocoagulation and ultrasonic removal of humic acid from wastewater. Environmental Progress & Sustainable Energy 36(3) (2017): 822-829.

Ashery, A. F., Radwan, K., and Rashed, M. The effect of ph control on turbidity and NOM removal in conventional water treatment. Paper presented at the Proceedings of the Fifteen International Water Technology Conference, Alexandria, Egypt. 2011.

Asselin, M., Drogui, P., Benmoussa, H., and Blais, J.-F. Effectiveness of electrocoagulation process in removing organic compounds from slaughterhouse wastewater using monopolar and bipolar electrolytic cells. Chemosphere 72(11) (2008): 1727-1733.

Athreya, S., and Venkatesh, Y. Application of Taguchi method for optimization of process parameters in improving the surface roughness of lathe facing operation. International Refereed Journal of Engineering and Science 1(3) (2012): 13-19.

Bazrafshan, E., Biglari, H., and Mahvi, A. H. Humic acid removal from aqueous environments by electrocoagulation process using iron electrodes. Journal of Chemistry 9(4) (2012): 2453-2461.

Bazrafshan, E., Mahvi, A. H., Naseri, S., and Mesdaghinia, A. R. Performance evaluation of electrocoagulation process for removal of chromium (VI) from synthetic chromium solutions using iron and aluminum electrodes. Turkish Journal of Engineering and Environmental Sciences 32(2) (2008): 59-66.

Bejjany, B., et al. Treatment of the surface water by Electrocoagulation-Electroflotation process in internal loop airlift reactor: Conductivity effect on turbidity removal and energy consumption. (2017a).

Bejjany, B., et al. Treatment of the surface water by Electrocoagulation-Electroflotation process in internal loop airlift reactor: Conductivity effect on turbidity removal and energy consumption. Journal of Materials and Environmental Sciences 8(8) (2017b): 2757-2768.

Black, A., Buswell, A. M., Eidsness, F. A., and Black, A. Review of the jar test. Journal (American Water Works Association) 49(11) (1957): 1414-1424.

Bob, M., and Walker, H. W. Enhanced adsorption of natural organic matter on calcium carbonate particles through surface charge modification. Colloids and Surfaces A: Physicochemical and Engineering Aspects 191(1-2) (2001): 17-25.

Brahmi, K., et al. Use of electrocoagulation with aluminum electrodes to reduce hardness in tunisian phosphate mining process water. Mine Water and the Environment 35(3) (2016): 310-317.

Butler, E., Hung, Y.-T., Yeh, R. Y.-L., and Suleiman Al Ahmad, M. Electrocoagulation in wastewater treatment. Water 3(2) (2011): 495-525.

Butler, E., Hung, Y., Yeh, R. Y., and Ahmad, M. S. A. Electrocoagulation in Wastewater Treatment. Water 3(4) (2011): 495-525. doi: 10.3390/w3020495.

Caccavale, F., Iamarino, M., Pierri, F., and Tufano, V. The Chemical Batch Reactor Control and Monitoring of Chemical Batch Reactors (pp. 9-38): Springer. 2011.

Cañizares, P., et al. Electrochemical oxidation of azoic dyes with conductive-diamond anodes. Industrial & Engineering Chemistry Research 45(10) (2006): 3468-3473.

Chawaloesphosiya, N., Mongkolnauwarat, J., Prommajun, C., Wongwailikhit, K., and Painmanakul, P. Treatment of cutting-oily wastewater by electrocoagulation-flotation (ECF) process: modeling approach. Environmental Engineering Research 20(4) (2015): 392-396.

Chen, X., Chen, G., and Yue, P. L. Separation of pollutants from restaurant wastewater by electrocoagulation. Separation and Purification Technology 19(1) (2000): 65-76.

Chou, W.-J., Sun, C.-H., Yu, G.-P., and Huang, J.-H. Optimization of the deposition process of ZrN and TiN thin films on Si (1 0 0) using design of experiment method. Materials Chemistry and Physics 82(1) (2003): 228-236.

Chou, W.-L., Wang, C.-T., and Chang, S.-Y. Study of COD and turbidity removal from real oxide-CMP wastewater by iron electrocoagulation and the evaluation of specific energy consumption. Journal of Hazardous Materials 168(2) (2009): 1200-1207.

Comninellis, C., et al. Advanced oxidation processes for water treatment: advances and trends for R&D. Journal of Chemical Technology and Biotechnology 83(6) (2008): 769-776.

Crittenden, J. C., Trussell, R. R., Hand, D. W., Howe, K. J., and Tchobanoglous, G. MWH's water treatment: principles and design. John Wiley & Sons, 2012.

Daghrir, R., Drogui, P., and Zaviska, F. Effectiveness of a hybrid process combining electro-coagulation and electro-oxidation for the treatment of domestic wastewaters using response surface methodology. Journal of Environmental Science and Health, Part A 48(3) (2013): 308-318.

Daneshvar, N., Oladegaragoze, A., and Djafarzadeh, N. Decolorization of basic dye solutions by electrocoagulation: an investigation of the effect of operational parameters. Journal of Hazardous Materials 129(1-3) (2006): 116-122.

Dean, J. G., Bosqui, F. L., and Lanouette, K. H. Removing heavy metals from waste water. Environmental science & technology 6(6) (1972): 518-522.

Derayat, J., Motlagh, Z., Pirsaheb, M., sharafi, K., and Motlagh, R. Survey of electrocoagulation process Performance (with iron-rod electrode) in treatment of drinking water- case study: Kermanshah Soleymanshah dam. International Research Journal of Applied and Basic Sciences 9(8) (2015): 1453-1459.

Duan, J., and Gregory, J. Coagulation by hydrolysing metal salts. Advances in colloid and interface science 100 (2003): 475-502.

Duan, J., Wilson, F., Graham, N., and Tay, J. H. Adsorption of humic acid by powdered activated carbon in saline water conditions. Desalination 151(1) (2003): 53-66.

Durst, R. A. Ion-selective electrodes: proceedings. US National Bureau of Standards; for sale by the Supt. of Docs., US Govt. Print. Off., Washington, 1969.

El Azher, N., Gourich, B., Vial, C., Soulami, M. B., and Ziyad, M. Study of ferrous iron oxidation in Morocco drinking water in an airlift reactor. Chemical Engineering and Processing: Process Intensification 47(9-10) (2008): 1877-1886.

Emamjomeh, M. M., and Sivakumar, M. Review of pollutants removed by electrocoagulation and electrocoagulation/flotation processes. Journal of environmental management 90(5) (2009): 1663-1679.

Emamjomeh, M. M., and Sivakumar, M. Review of pollutants removed by electrocoagulation and electrocoagulation/flotation processes. J Environ Manage 90(5) (2009): 1663-1679. doi: 10.1016/j.jenvman.2008.12.011.

Essadki, A. H., Gourich, B., Vial, C., Delmas, H., and Bennajah, M. Defluoridation of drinking water by electrocoagulation/electroflotation in a stirred tank reactor with a comparative performance to an external-loop airlift reactor. Journal of Hazardous Materials 168(2) (2009): 1325-1333.

FENG, Q.-y., LI, X.-d., CHENG, Y.-j., Lei, M., and MENG, Q.-j. Removal of humic acid from groundwater by electrocoagulation. Journal of China University of Mining and Technology 17(4) (2007): 513-520.

Freiser, H. Ion-selective electrodes in analytical chemistry. Springer Science & Business Media, 2012.

Gao, S., et al. Effects of chloride ions on electro-coagulation-flotation process with aluminum electrodes for algae removal. Journal of Hazardous Materials 182(1) (2010): 827-834.

Ghernaout, D., Ghernaout, B., and Boucherit, A. Effect of pH on electrocoagulation of bentonite suspensions in batch using iron electrodes. Journal of dispersion science and technology 29(9) (2008): 1272-1275.

Ghosh, D., Solanki, H., and Purkait, M. Removal of Fe (II) from tap water by electrocoagulation technique. Journal of Hazardous Materials 155(1) (2008): 135-143.

Ghosh, D., Solanki, H., and Purkait, M. K. Removal of Fe(II) from tap water by electrocoagulation technique. J Hazard Mater 155(1-2) (2008): 135-143. doi: 10.1016/j.jhazmat.2007.11.042.

Ghosh, K., and Schnitzer, M. Macromolecular structures of humic substances. Soil Science 129(5) (1980): 266-276.

Gomez, F., and Sartaj, M. Optimization of field scale biopiles for bioremediation of petroleum hydrocarbon contaminated soil at low temperature conditions by response surface methodology (RSM). International Biodeterioration & Biodegradation 89 (2014): 103-109.

Greeson, P. E. Organic Substances in Water. US Geological Survey, 1981.

Han, M., Song, J., and Kwon, A. Preliminary investigation of electrocoagulation as a substitute for chemical coagulation. Water Science and Technology: Water Supply 2(5-6) (2002): 73-76.

Hayden, P., and Rubin, A. J. Systematic investigation of the hydrolysis and precipitation of aluminum (III). Aqueous-Environmental Chemistry of Metals (1974): 317-381.

Holt, P., Barton, G., and Mitchell, C. Electrocoagulation as a wastewater treatment. The third annual australian environmental engineering research event 1000 (1999): 41-46.

Hossain, M., Mahmud, I., Parvez, S., and Cho, H. M. Impact of current density, operating time and pH of textile wastewater treatment by electrocoagulation process. Environmental Engineering Research 18(3) (2013): 157-161.

Ibarra-Taquez, H. N., GilPavas, E., Blatchley III, E. R., Gómez-García, M.-Á., and Dobrosz-Gómez, I. Integrated electrocoagulation-electrooxidation process for the treatment of soluble coffee effluent: Optimization of COD degradation and operation time analysis. Journal of environmental management 200 (2017): 530-538.

Irvine, K., Richey, J., Holtgrieve, G., Sarkkula, J., and Sampson, M. Spatial and temporal variability of turbidity, dissolved oxygen, conductivity, temperature, and fluorescence in the lower Mekong River–Tonle Sap system identified using continuous monitoring. International Journal of River Basin Management 9(2) (2011): 151-168.

Jaramillo, M. Riverbank filtration: an efficient and economical drinking-water treatment technology. Dyna 79(171) (2012): 148-157.

Jeong, J., Kim, J. Y., Cho, M., Choi, W., and Yoon, J. Inactivation of Escherichia coli in the electrochemical disinfection process using a Pt anode. Chemosphere 67(4) (2007): 652-659.

Jiang, J.-Q., Graham, N., André, C., Kelsall, G. H., and Brandon, N. Laboratory study of electro-coagulation–flotation for water treatment. Water Research 36(16) (2002): 4064-4078.

Joseph, L., et al. Removal of natural organic matter from potential drinking water sources by combined coagulation and adsorption using carbon nanomaterials. Separation and Purification Technology 95 (2012): 64-72.

Kabdaşlı, I., Arslan-Alaton, I., Ölmez-Hancı, T., and Tünay, O. Electrocoagulation applications for industrial wastewaters: a critical review. Environmental Technology Reviews 1(1) (2012): 2-45. doi: 10.1080/21622515.2012.715390.

Kac, F. U., Kobya, M., and Gengec, E. Removal of humic acid by fixed-bed electrocoagulation reactor: Studies on modelling, adsorption kinetics and HPSEC analyses. Journal of Electroanalytical Chemistry (2017).

Karichappan, T., Venkatachalam, S., and Jeganathan, P. M. Optimization of electrocoagulation process to treat grey wastewater in batch mode using response surface methodology. Journal of Environmental Health Science and Engineering 12(1) (2014): 29.

Kawamura, S. Integrated design and operation of water treatment facilities. john Wiley & sons, 2000.

Khairi, K., Ghazi, N., and Mohammed, A. Hardness Removal from Drinking Water Using Electrochemical Cell. Egg. & Tech. Journal 33(1) (2011): 78-88.

Kobya, M., Can, O. T., and Bayramoglu, M. Treatment of textile wastewaters by electrocoagulation using iron and aluminum electrodes. Journal of Hazardous Materials 100(1) (2003): 163-178.

Kobya, M., Gebologlu, U., Ulu, F., Oncel, S., and Demirbas, E. Removal of arsenic from drinking water by the electrocoagulation using Fe and Al electrodes. Electrochimica Acta 56(14) (2011): 5060-5070.

Kuehn, W., and Mueller, U. Riverbank filtration: an overview. American Water Works Association. Journal 92(12) (2000): 60.

Kuokkanen, V., Kuokkanen, T., Rämö, J., and Lassi, U. Recent applications of electrocoagulation in treatment of water and wastewater—a review. Green and Sustainable Chemistry 3(02) (2013): 89.

Lamsal, R., Walsh, M. E., and Gagnon, G. A. Comparison of advanced oxidation processes for the removal of natural organic matter. Water Research 45(10) (2011): 3263-3269.

Lawson, M., Polya, D. A., Boyce, A. J., Bryant, C., and Ballentine, C. J. Tracing organic matter composition and distribution and its role on arsenic release in shallow Cambodian groundwaters. Geochimica et Cosmochimica Acta 178 (2016): 160-177.

Lekhlif, B., Oudrhiri, L., Zidane, F., Drogui, P., and Blais, J.-F. Study of the electrocoagulation of electroplating industry wastewaters charged by nickel (II) and chromium (VI). J. Mater. Environ. Sci 5(1) (2014): 111-120.

Logsdon, G. S., Kohne, R., Abel, S., and LaBonde, S. Slow sand filtration for small water systems. Journal of Environmental Engineering and Science 1(5) (2002): 339-348.

Mac Berthouex, P., and Brown, L. C. Chemical Processes for Pollution Prevention and Control. CRC Press, 2017.

Mahvi, A. H., Ebrahimi, S. J. A.-d., Mesdaghinia, A., Gharibi, H., and Sowlat, M. H. Performance evaluation of a continuous bipolar electrocoagulation/electrooxidation–electroflotation (ECEO–EF) reactor designed for simultaneous removal of ammonia and phosphate from wastewater effluent. Journal of Hazardous Materials 192(3) (2011): 1267-1274.

Malakootian, M., Mansoorian, H., and Moosazadeh, M. Performance evaluation of electrocoagulation process using iron-rod electrodes for removing hardness from drinking water. Desalination 255(1-3) (2010): 67-71.

Malakootian, M., and Yousefi, N. The efficiency of electrocoagulation process using aluminum electrodes in removal of hardness from water. Iranian Journal of Environmental Health Science & Engineering (IJEHSE) 6(2) (2009a).

Malakootian, M., and Yousefi, N. The efficiency of electrocoagulation process using aluminum electrodes in removal of hardness from water. Journal of Environmental Health Science & Engineering 6(2) (2009b): 131-136.

Manea, F., Jakab, A., Ardelean, M., Pop, A., and Vlaicu, I. Boron-doped diamond electrode-based advanced treatment methods for drinking water. Environmental Engineering and Management Journal 13(9) (2014): 2167-2172.

Matilainen, A., and Sillanpää, M. Removal of natural organic matter from drinking water by advanced oxidation processes. Chemosphere 80(4) (2010): 351-365.

Merzouk, B., Gourich, B., Sekki, A., Madani, K., and Chibane, M. Removal turbidity and separation of heavy metals using electrocoagulation–electroflotation technique: A case study. Journal of Hazardous Materials 164(1) (2009): 215-222.

Mills, D. A new process for electrocoagulation. Journal-American Water Works Association 92(6) (2000): 34-43.

Ministry of Rural Development, D. o. R. W. S. (2002). *Drinking Water Quality in Cambodia* Hanoi, Vietnam: Country Report.

Mohammad, M. E., and Mahdi, F. Flouride Removal by Electrocoagulation (EC) Process: Aluminum Chemistry and Speciation. International Journal of Advances in Science Engineering and Technology 4(2016) (2016): 82-85.

Mollah, M. Y., et al. Fundamentals, present and future perspectives of electrocoagulation. Journal of Hazardous Materials 114(1) (2004): 199-210.

Montgomery, D. C. Design and Analysis of Experiments, John Wiley & Sons. New York (2001): 64-65.

Montgomery, D. C. Design and analysis of experiments, minitab manual. John Wiley & Sons, 2010.

Motheo, A. J., and Pinhedo, L. Electrochemical degradation of humic acid. Science of the Total Environment 256(1) (2000): 67-76.

Motlagh, J. Survey of electrocoagulation process Performance (with iron-rod electrode) in treatment of drinking water-case study: Kermanshah Soleymanshah dam. (2015).

Nasrullah, M., Siddique, M. N. I., and Zularisam, A. Effect of High Current Density in Electrocoagulation Process for Sewage Treatment. Asian Journal of Chemistry 26(14) (2014): 4281-4285.

National Institute of Statistics, N. C. (2008). Summary of Groundwater Data. Retrieved 18 September, 2017, from http://rdic.org/groundwater-summary-data/

O'melia, C., Becker, W., and Au, K.-K. Removal of humic substances by coagulation. Water Science and Technology 40(9) (1999): 47-54.

Omaka, O. N., Offor, I. F., and Onwe, I. M. Hydrogeochemical attributes and ground water quality of Ngbo Community in Ohaukwu Area Council, Ebonyi State, Nigeria. Revista Ambiente & Água 10(1) (2015): 35-47.

Palahouane, B., Drouiche, N., Aoudj, S., and Bensadok, K. Cost-effective electrocoagulation process for the remediation of fluoride from pretreated photovoltaic wastewater. Journal of Industrial and Engineering Chemistry 22 (2015): 127-131.

Park, S.-j., and Yoon, T.-i. Effects of iron species and inert minerals on coagulation and direct filtration for humic acid removal. Desalination 239(1-3) (2009): 146-158.

Parmar, K. A., Prajapati, S., Patel, R., and Dabhi, Y. Effective use of ferrous sulfate and alum as a coagulant in treatment of dairy industry wastewater. J. Eng. Appl. Sci. 6(9) (2011): 42-45.

Pettit, R. E. Organic matter, humus, humate, humic acid, fulvic acid and humin: Their importance in soil fertility and plant health. CTI Research (2004).

Ray, C., Melin, G., and Linsky, R. B. Riverbank filtration: improving source-water quality. Vol. 43: Springer Science & Business Media, 2003.

Rezaei, H., et al. Humic acid removal by electrocoagulation process from natural aqueous environments. International Journal of Electrochemical Science 13(3) (2018): 2379-2389.

Rodrigues, A., Brito, A., Janknecht, P., Proença, M. F., and Nogueira, R. Quantification of humic acids in surface water: effects of divalent cations, pH, and filtration. Journal of Environmental Monitoring 11(2) (2009): 377-382.

Sahu, O., Mazumdar, B., and Chaudhari, P. Treatment of wastewater by electrocoagulation: a review. Environmental science and pollution research international 21(4) (2014a): 2397-2413.

Sahu, O., Mazumdar, B., and Chaudhari, P. Treatment of wastewater by electrocoagulation: a review. Environmental science and pollution research 21(4) (2014b): 2397-2413.

Sarkar, M. S. K. A., Donne, S. W., and Evans, G. M. Utilization of hydrogen in electroflotation of silica. Advanced Powder Technology 22(4) (2011): 482-492. doi: 10.1016/j.apt.2011.05.007.

Särkkä, H., Bhatnagar, A., and Sillanpää, M. Recent developments of electro-oxidation in water treatment—a review. Journal of Electroanalytical Chemistry 754 (2015): 46-56.

Särkkä, H., Vepsäläinen, M., and Sillanpää, M. Natural organic matter (NOM) removal by electrochemical methods—A review. Journal of Electroanalytical Chemistry 755 (2015): 100-108.

Seid-Mohammadi, A., Sharifi, Z., Shabanlo, A., and Asgari, G. Simultaneous Removal of Turbidity and Humic Acid Using Electrocoagulation/Flotation Process in Aqua Solution. Avicenna Journal of Environmental Health Engineering 2(1) (2015).

SEID, M. A., Sharifi, Z., Shabanlo, A., and Asgari, G. Simultaneous Removal of Turbidity and Humic Acid Using Electrocoagulation/Flotation Process in Aqua Solution. (2015).

Shestakova, M., and Sillanpää, M. Electrode materials used for electrochemical oxidation of organic compounds in wastewater. Reviews in Environmental Science and Bio/Technology 16(2) (2017): 223-238.

Silberberg, M. Chemistry: The molecular Nature of Matter and Change. McGraw Hill. New York, NY (2006).

Singer, P. C., and Bilyk, K. Enhanced coagulation using a magnetic ion exchange resin. Water Research 36(16) (2002): 4009-4022.

Subramaniam, D., and Halim, A. A. Effect of electrochemical oxidation on biodegradability and toxicity of batik industry wastewater. Paper presented at the AIP Conference Proceedings. 2014.

Sudoh, R., et al. Removal of dissolved humic acid from water by coagulation method using polyaluminum chloride (PAC) with calcium carbonate as neutralizer and coagulant aid. Journal of Environmental Chemical Engineering 3(2) (2015): 770-774.

Sundararajan, K. (2016). Design of experiments–a primer: iSixSigma.

Tang, C., Yan, W., and Zheng, C. Electrochemical oxidation of humic acid at the antimony-and nickel-doped tin oxide electrode. Frontiers of Environmental Science & Engineering 8(3) (2014): 337-344.

Tchamango, S., Kamdoum, O., Donfack, D., Babale, D., and Ngameni, E. COMPARISON OF ELECTROCOAGULATION AND CHEMICAL COAGULATION IN THE TREATMENT OF ARTISANAL TANNERY EFFLUENTS. Nigerian Journal of Technology 35(1) (2016): 219-225.

Tran, N., and Drogui, P. Electrochemical removal of microcystin-LR from aqueous solution in the presence of natural organic pollutants. Journal of environmental management 114 (2013): 253-260.

Vepsäläinen, M., Pulliainen, M., and Sillanpää, M. Effect of electrochemical cell structure on natural organic matter (NOM) removal from surface water through electrocoagulation (EC). Separation and Purification Technology 99 (2012): 20-27.

Vik, E. A., Carlson, D. A., Eikum, A. S., and Gjessing, E. T. Electrocoagulation of potable water. Water Research 18(11) (1984): 1355-1360.

Volk, C., et al. Monitoring dissolved organic carbon in surface and drinking waters. Journal of Environmental Monitoring 4(1) (2002): 43-47.

Waller, R. M., Ground Water and the Rural Homeowner, Pamphlet, U.S. (2016, 02-Dec-2016 12:51:57 EST). Contaminants Found in Groundwater. Retrieved 12 December, 2017, from http://water.usgs.gov/edu/groundwater-contaminants.html

Wang, Q., et al. Effect of pH on humic acid removal performance in coagulation–ultrafiltration process and the subsequent effects on chlorine decay. Separation and Purification Technology 80(3) (2011): 549-555.

Water, U. S. O. o. D., and Smith, J. E. Technologies for upgrading existing or designing new drinking water treatment facilities. Office, US EPA, 1990.

Worch, E., Grischek, T., Börnick, H., and Eppinger, P. Laboratory tests for simulating attenuation processes of aromatic amines in riverbank filtration. Journal of Hydrology 266(3) (2002): 259-268.

Xie, J., et al. pH modeling for maximum dissolved organic matter removal by enhanced coagulation. Journal of Environmental Sciences 24(2) (2012): 276-283.

You, H. J., and Han, I. S. Effects of dissolved ions and natural organic matter on electrocoagulation of As (III) in groundwater. Journal of Environmental Chemical Engineering 4(1) (2016): 1008-1016.

Zhang, M., Trompette, J.-L., and Guiraud, P. Role of Humic Acid in Enhancing Dissolved Air Flotation for the Removal of TiO2 Nanoparticles. Industrial & Engineering Chemistry Research 56(8) (2017): 2212-2220. doi: 10.1021/acs.iecr.6b04572.

Zhao, S., Huang, G., Cheng, G., Wang, Y., and Fu, H. Hardness, COD and turbidity removals from produced water by electrocoagulation pretreatment prior to reverse osmosis membranes. Desalination 344 (2014): 454-462.

Zularisam, A., Ismail, A., and Salim, R. Behaviours of natural organic matter in membrane filtration for surface water treatment—a review. Desalination 194(1-3) (2006): 211-231.

APPENDIX

Appendix 1: Kinetic model

- S-curve model of bentonite

Turbidity model prediction of Bentonite synthetic water followed Sigmoid function.

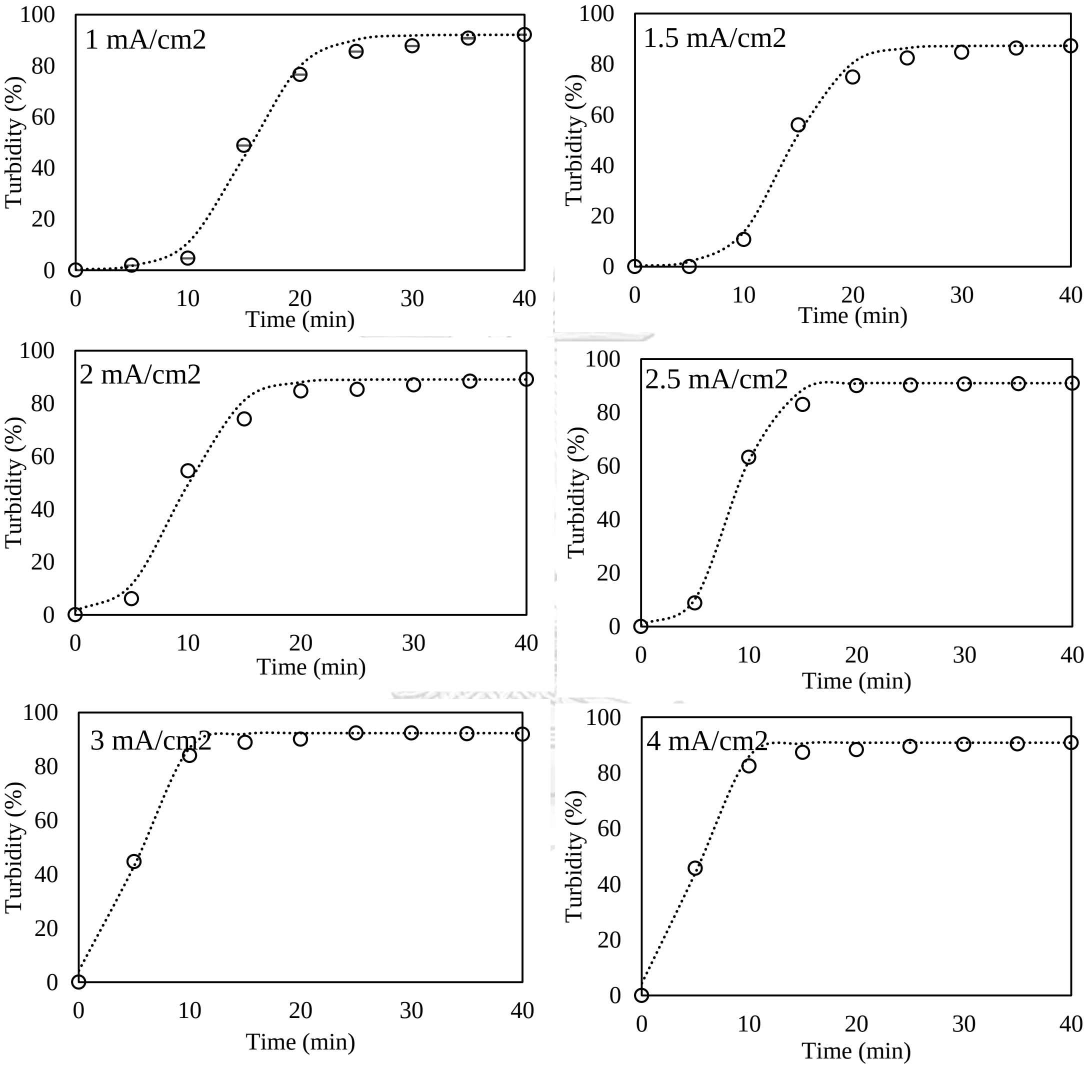

- S-curve model of HA-bentonite

Turbidity prediction of HA-Bentonite synthetic water followed Logistic function

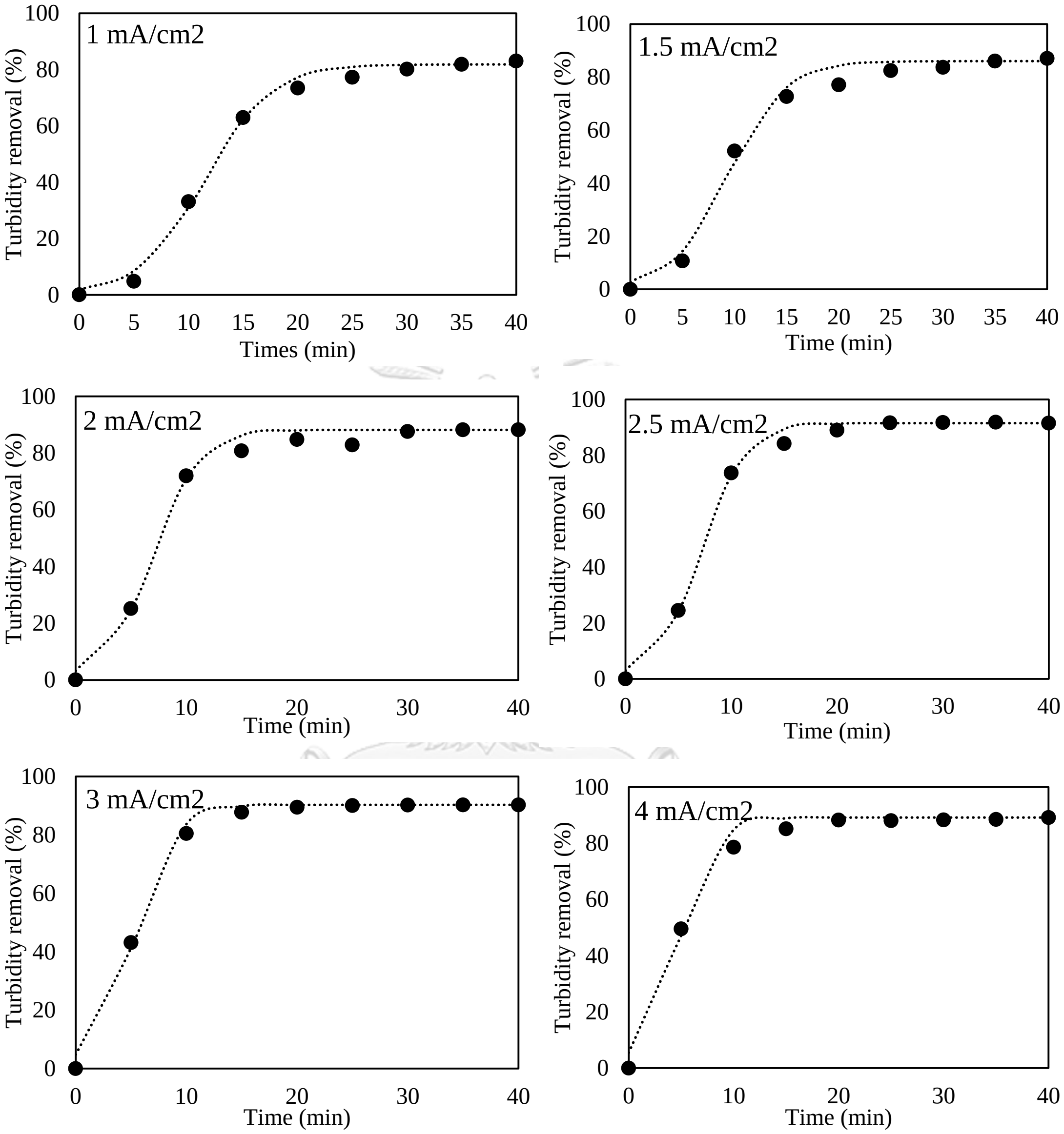

- First order kinetic of HA

Absorbance removal of HA synthetic water followed first-order kinetic

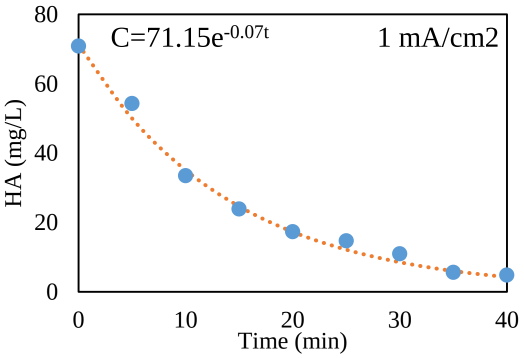

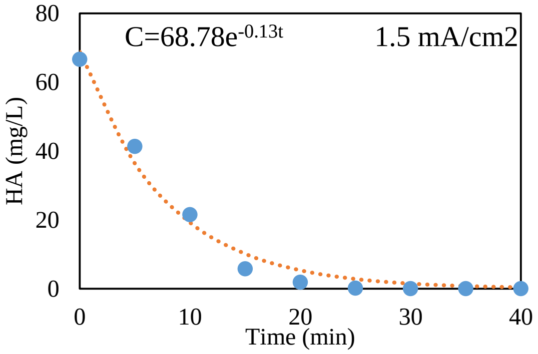

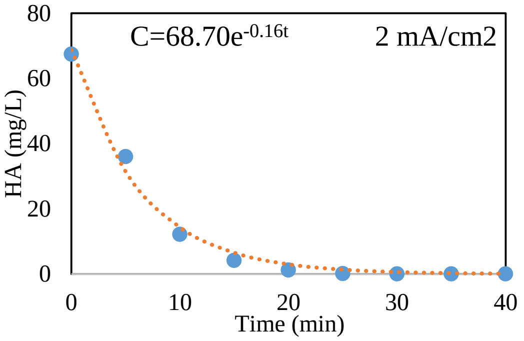

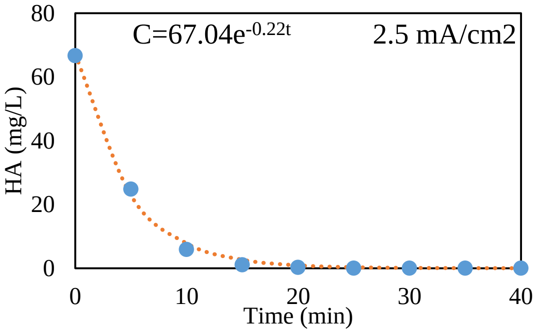

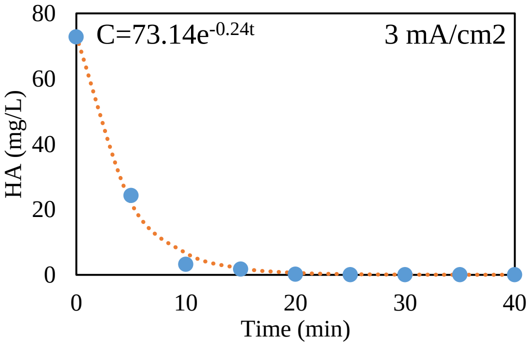

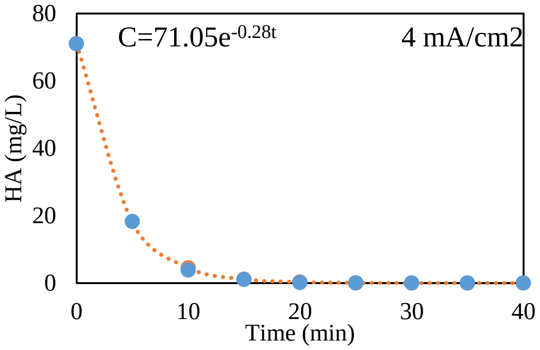

➢ First-order kinetic of ha-bentonite

Absorbance removal of HA-Bentonite synthetic water followed first-order kinetic

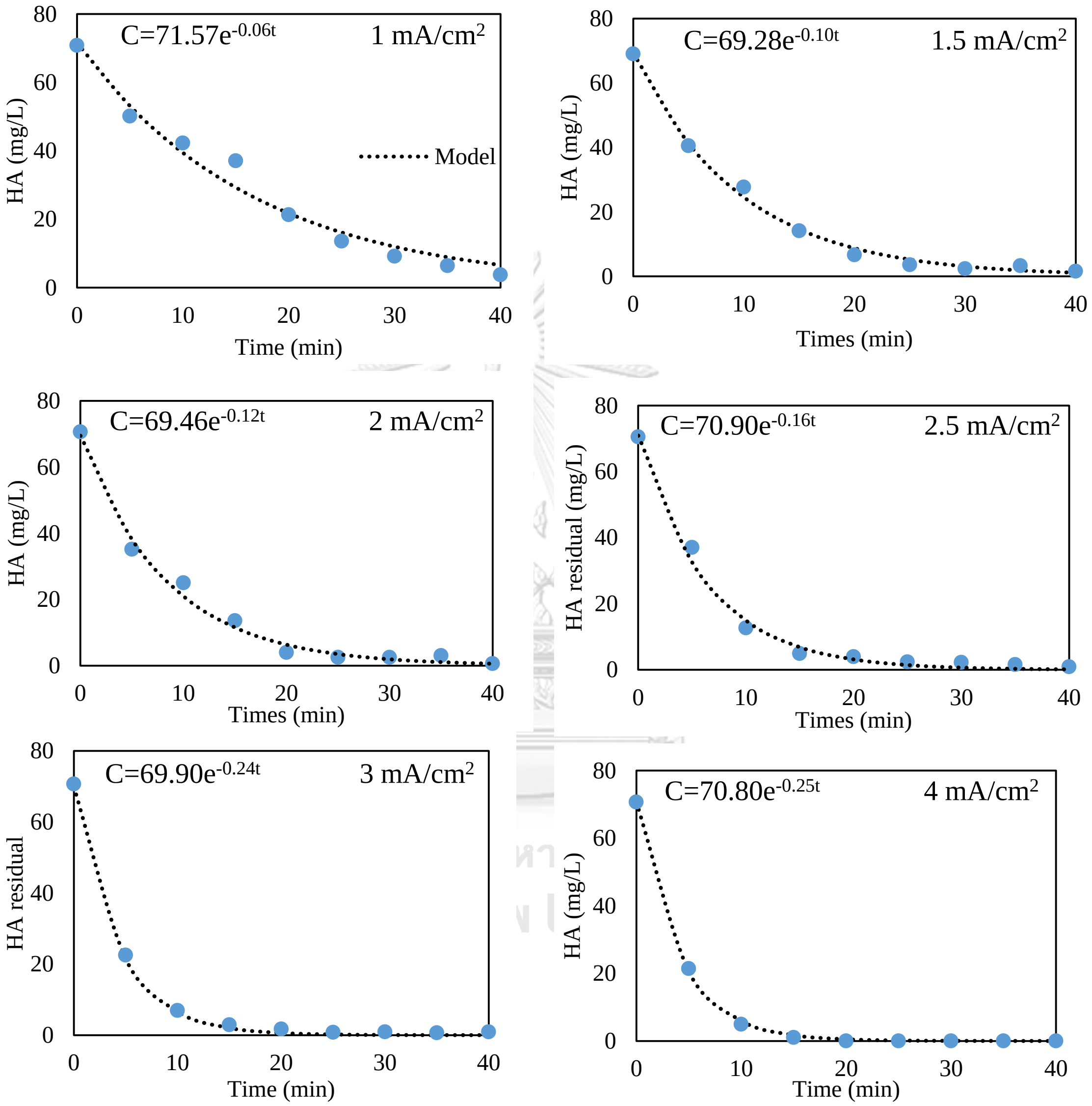

Appendix 2: Observed data

Result of turbidity and absorbance of HA in various conditions of four factors including ferrous, calcium, current density, and pH.

No	StdOrder	Parameters				Response		
		Fe^{2+}	Ca^{2+}	J	pH	Turbidity	Absorbance	Final pH
		mg/L	mg/L	mA/cm2	(-)	(%)	(%)	(-)
1	19	13	3.6	2.5	7	82	98	8.14
2	8	25	18	4	5	74	100	6.3
3	11	1	18	1	9	83	41	8.85
4	20	13	18	2.5	7	85	99	7.6
5	7	1	18	4	5	84	99	6.21
6	29	13	10.8	2.5	7	82	97	8.23
7	28	13	10.8	2.5	7	81	99	8.33
8	24	13	10.8	2.5	9	84	94	8.48
9	9	1	3.6	1	9	80	41	8.85
10	25	13	10.8	2.5	7	81	98	7.46
11	2	25	3.6	1	5	78	99	5.5
12	13	1	3.6	4	9	85	97	8.76
13	21	13	10.8	1	7	80	93	7.19
14	10	25	3.6	1	9	78	91	8.54
15	27	13	10.8	2.5	7	84	99	7.96
16	14	25	3.6	4	9	84	99	8.69
17	3	1	18	1	5	85	100	6
18	5	1	3.6	4	5	77	99	6.6
19	22	13	10.8	4	7	88	100	8.39
20	31	13	10.8	2.5	7	84	100	7.6
21	26	13	10.8	2.5	7	84	100	8.11
22	23	13	10.8	2.5	5	81	100	6.15
23	6	25	3.6	4	5	79	99	6.33
24	15	1	18	4	9	91	95	8.56
25	16	25	18	4	9	86	94	8.93

No	StdOrder	Parameters				Response		
		Fe^{2+}	Ca^{2+}	J	pH	Turbidity	Absorbance	Final pH
		mg/L	mg/L	mA/cm2	(-)	(%)	(%)	(-)
26	12	25	18	1	9	85	83	8.65
27	1	1	3.6	1	5	86	97	6.07
28	4	25	18	1	5	83	94	5.75
29	30	13	10.8	2.5	7	84	100	7.95
30	18	25	10.8	2.5	7	84	98	8.32
31	17	1	10.8	2.5	7	88	98	7.64

Appendix 3: Design of Experimental results

- **Turbidity**
  - Analysis of variance using Response surface methodology for turbidity removal

Source	DF	Adj SS	Adj MS	F-Value	P-Value
Model	14	272.33	19.45	2.87	0.023
Linear	4	138.66	34.66	5.12	0.008
J	1	5.25	5.25	0.78	0.392
pH	1	45.47	45.47	6.72	0.020
Ca^{2+}	1	44.99	44.99	6.65	0.020
Fe^{2+}	1	42.95	42.95	6.35	0.023
Square	4	19.23	4.81	0.71	0.597
J*J	1	0.53	0.53	0.08	0.784
pH*pH	1	6.78	6.78	1	0.332
$[Ca^{2+}]*[Ca^{2+}]$	1	1.44	1.44	0.21	0.651
$[Fe^{2+}]*[Fe^{2+}]$	1	7.73	7.73	1.14	0.301
2-Way Interaction	6	114.44	19.07	2.82	0.046
J*pH	1	92.05	92.05	13.6	0.002
$J*[Ca^{2+}]$	1	0.70	0.70	0.1	0.753
$J*[Fe^{2+}]$	1	0.64	0.64	0.09	0.763
$pH*[Ca^{2+}]$	1	8.67	8.67	1.28	0.274
$pH*[Fe^{2+}]$	1	9.73	9.73	1.44	0.248
$[Ca^{2+}]*[Fe^{2+}]$	1	2.66	2.66	0.39	0.540
Error	16	108.26	6.77		
Lack-of-Fit	10	93.299	9.33	3.74	0.060
Pure Error	6	14.964	2.49	-	-
Total	30	380.591	-	-	-

Note: DF: Degree of freedom, Adj SS: adjust sum of squares, Adj MS: adjust mean of squares

- Code coefficients of four factors on turbidity removal

Term	Effect	Coef	SE Coef	T-Value	P-Value	VIF
Constant	-	83.51	0.77	108.22	0.000	-

Term	Effect	Coef	SE Coef	T-Value	P-Value	VIF
J	1.08	0.54	0.61	0.88	0.392	1.00
pH	3.18	1.59	0.61	2.59	0.020	1.00
$[Ca^{2+}]$	3.16	1.58	0.61	2.58	0.020	1.00
$[Fe^{2+}]$	-3.09	-1.55	0.61	-2.52	0.023	1.00
J*J	-0.90	-0.45	1.61	-0.28	0.784	2.91
pH*pH	-3.23	-1.62	1.61	-1.00	0.332	2.91
$[Ca^{2+}]*[Ca^{2+}]$	-1.49	-0.74	1.61	-0.46	0.651	2.91
$[Fe^{2+}]*[Fe^{2+}]$	3.45	1.73	1.61	1.07	0.301	2.91
J*pH	4.80	2.40	0.65	3.69	0.002	1.00
$J*[Ca^{2+}]$	-0.42	-0.21	0.65	-0.32	0.753	1.00
$J*[Fe^{2+}]$	-0.40	-0.20	0.65	-0.31	0.763	1.00
$pH*[Ca^{2+}]$	1.47	0.74	0.65	1.13	0.274	1.00
$pH*[Fe^{2+}]$	1.56	0.78	0.65	1.20	0.248	1.00
$[Ca^{2+}]*[Fe^{2+}]$	-0.82	-0.41	0.65	-0.63	0.540	1.00

Note: SE Coef: standard error coefficient, VIF: variance inflation factor

- Contour plots for turbidity removal

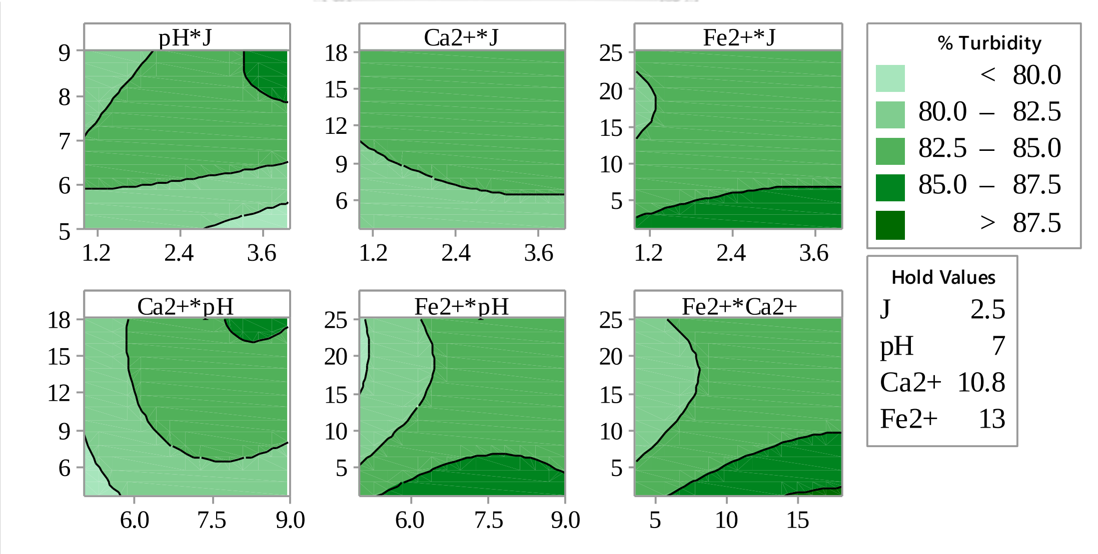

- Surface plots for turbidity removal (%)

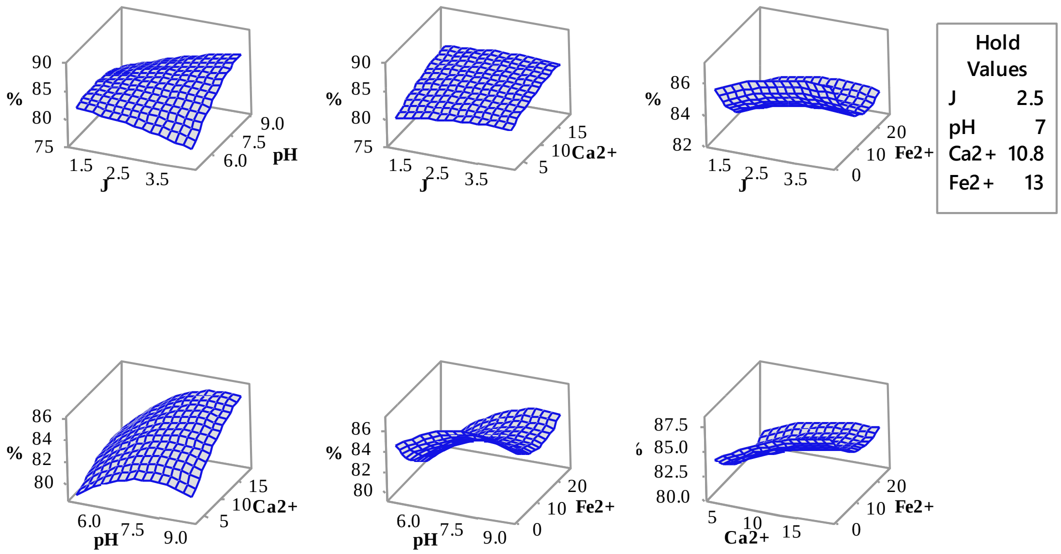

➢ Humic acid

- Analysis of variance for absorbance removal

Source	DF	Adj SS	Adj MS	F-Value	P-Value
Model	14	5514.5	393.89	8.12	0.000
Linear	4	2900.86	725.22	14.96	**0.000**
[Fe^{2+}]	1	462.74	462.74	9.54	**0.007**
[Ca^{2+}]	1	14.64	14.64	0.3	0.590
J	1	1096.86	1096.86	22.62	**0.000**
pH	1	1326.62	1326.62	27.36	**0.000**
Square	4	616.30	154.07	3.18	**0.042**
[Fe^{2+}]*[Fe^{2+}]	1	12.56	12.56	0.26	0.618
[Ca^{2+}]*[Ca^{2+}]	1	3.45	3.45	0.07	0.793
J*J	1	32.40	32.40	0.67	0.426
pH*pH	1	25.79	25.79	0.53	0.476
2-Way Interaction	6	1997.34	332.89	6.87	**0.001**
[Fe^{2+}]*[Ca^{2+}]	1	21.23	21.23	0.44	0.518
[Fe^{2+}]*JA	1	477.08	477.08	9.84	**0.006**
[Fe^{2+}]*pH	1	576.63	576.63	11.89	**0.003**
[Ca^{2+}]*J	1	1.62	1.62	0.03	0.857
[Ca^{2+}]*pH	1	13.48	13.48	0.28	0.605
J*pH	1	907.30	907.30	18.71	**0.001**
Error	16	775.76	48.48		-
Lack of fit	10	767.29	76.73	54.36	**0.000**

Source	DF	Adj SS	Adj MS	F-Value	P-Value
Pure error	6	8.47	1.41		-
Total	30	6290.25	-		-

- Code coefficient

Term	Effect	Coef	SE Coef	T-Value	P-Value	VIF
Constant	-	99.46	2.07	48.15	0.000	
Fe2+	10.14	5.07	1.64	3.09	0.007	1
Ca2+	-1.80	-0.9	1.64	-0.55	0.59	1
J	15.61	7.81	1.64	4.76	0.000	1
pH	-17.17	-8.58	1.64	-5.23	0.000	1
Fe2+*Fe2+	-4.40	-2.2	4.32	-0.51	0.618	2.91
Ca2+*Ca2+	-2.30	-1.15	4.32	-0.27	0.793	2.91
J*J	-7.07	-3.53	4.32	-0.82	0.426	2.91
pH*pH	-6.30	-3.15	4.32	-0.73	0.476	2.91
Fe2+*Ca2+	-2.30	-1.15	1.74	-0.66	0.518	1
Fe2+*J	-10.92	-5.46	1.74	-3.14	0.006	1
Fe2+*pH	12.01	6.00	1.74	3.45	0.003	1
Ca2+*J	0.64	0.32	1.74	0.18	0.857	1
Ca2+*pH	-1.84	-0.92	1.74	-0.53	0.605	1
J*pH	15.06	7.53	1.74	4.33	0.001	1

- Contour plots for interception factor effects of co-existing ions and operating condition on HA removal

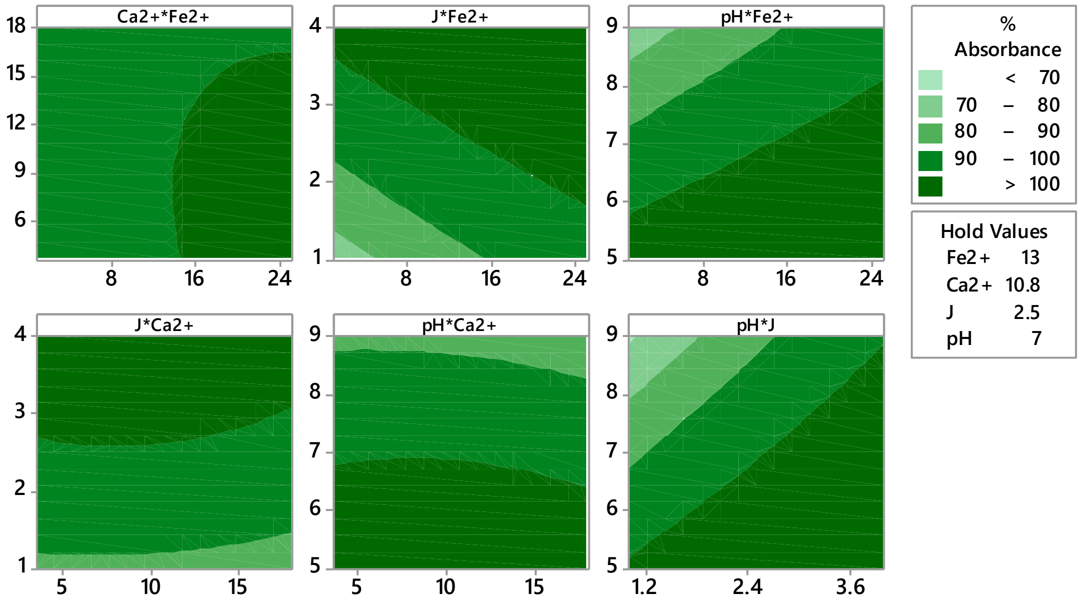

- Surface plots of efects of interception factos

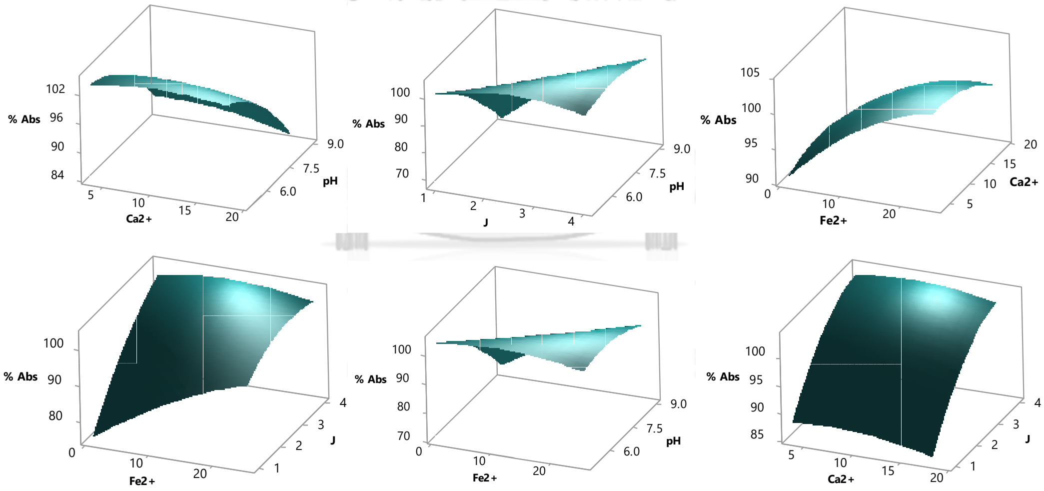

Appendix 4: Model validation

New experimental data values for model validation of turbidity, absorbance, and final pH

No	Factors				Observe data values			Predicted responses		
	Fe^{2+} mg/L	Ca^{2+} mg/L	J $mA.cm^{-2}$	Init pH (-)	Turb (%)	Abs (%)	Final pH	Turb (%)	Abs (%)	Final pH
1	0	0.0	1	7.45	73.41	69.87	8.18	80.84	91.71	8.02
2	0	0.0	1.5	7.58	77.08	90.35	8.32	82.97	94.24	8.15
3	0	0.0	2	7.67	84.73	94.34	8.5	84.41	96.20	8.24
4	0	0.0	2.5	7.62	85.39	94.33	8.34	85.09	97.65	8.27
5	0	0.0	3	7.36	85.25	98.40	8.49	84.73	98.52	8.19
6	0	0.0	4	7.25	88.24	100.00	8.31	81.50	97.70	8.24
7	0	0.0	1	5	85.77	97.14	6.09	83.86	96.13	5.78
9	0	0.0	1	9	76.72	35.43	8.69	78.94	88.92	8.64
10	1	0.0	1	7	88.11	79.43	7.44	80.77	92.65	7.73
11	13	0.0	1	7	82.17	93.71	7.35	76.19	94.16	7.73
12	25	0.0	1	7	76.59	95.43	6.98	77.19	95.68	7.73
13	0	3.6	1	7	87.21	77.43	7.97	82.49	92.64	7.73
14	0	10.8	1	7	87.91	59.27	8.17	84.67	92.88	7.73
15	0	18.0	1	7	88.15	75.43	7.81	86.85	93.11	7.73
16	13	25.2	2.5	7	86.69	96.95	8.47	87.34	96.56	7.91
17	13	0.7	2.5	7	84.49	99.14	7.52	79.91	99.79	7.91
18	1	18.0	4	7	85.86	97.90	8.21	85.86	98.22	8.10
20	14	40.0	1	9	88.83	60.57	9.11	87.42	79.65	8.64
21	1	18.0	3.4	8	82.23	99.70	8.46	89.58	97.50	8.51
22	18	3.6	3.4	8	78.75	100.00	8.5	81.41	99.55	8.51

Note: Init : initial , Turb: Turbidity, Abs: absorbance

Appendix 5: Settling test

- Settling test for synthetic water contained 70 mg/L of HA and 100 NTU

1. Removal efficiency *of different density along the time (15 to 105 min)*

Port Nº	**Depth [cm]**	**Turbidity [%]**						
		Sampling Time [min]						
		15	**30**	**45**	**60**	**75**	**90**	**105**
I	-15	25	46	57	64	66	70	73
II	-20	23	45	56	63	65	70	73
III	-25	22	46	54	62	63	70	73
IV	-30	24	42	55	62	66	70	73

2. Retention time of different removal efficiency at depth 0 to 30 cm

Depth [cm]	**Time (min)**						
	10%	**20%**	**30%**	**40%**	**50%**	**60%**	**70%**
0	0	0	0	0	0	0	0
-15	6.1	12.2	18.8	25.9	35.5	51.5	88.9
-20	6.4	12.9	19.6	26.4	36.7	53.9	88.7
-25	6.8	13.7	20.0	26.1	37.3	56.9	89.0
-30	6.3	12.7	20.2	28.4	39.1	55.2	89.7

3. Graph of removal efficiency at different depth along the time

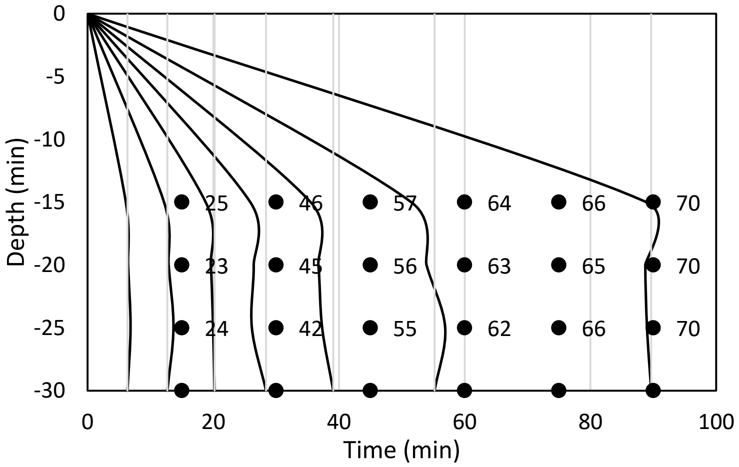

4. The overflow rate and removal efficiency

Time (min)	Overflow rate (cm/min)	Removal efficiency [%]		Vol (m/hr)
6	4.73	RT (10%) =	14.83	2.84
13	2.36	RT (20%) =	24.67	1.42
20	1.48	RT (30%) =	34.47	0.89
28	1.06	RT (40%) =	44.22	0.63
39	0.77	RT (50%) =	53.95	0.46
55	0.54	RT (60%) =	63.50	0.33
90	0.33	RT (70%) =	70.00	0.20

- Settling test after 20 min EC treatment of optimal condition of co-existing and operation

1. Removal efficiency of different density along the time (3 to 21 min)

Port N^o	**Depth [cm]**	**Turbidity [%]**						
		Sampling Time [min]						
		3	**6**	**9**	**12**	**15**	**18**	**21**
I	-15	37	65	68	75	81	85	87
II	-20	48	59	69	78	82	86	87
III	-25	46	61	75	78	82	85	85
IV	-30	42	50	61	77	80	83	83

2. Retention time of different removal efficiency at depth 0 to 30 cm

Depth [cm]	Time (min)								
	10%	20%	30%	40%	50%	60%	70%	80%	85%
0	0	0	0	0	0	0	0	0	0
-15	0.8	1.6	2.5	3.4	4.4	5.4	10.0	14.6	18.2
-20	0.6	1.2	1.9	2.5	3.4	6.2	9.2	13.6	17.2
-25	0.6	1.3	1.9	2.6	3.8	5.8	7.9	13.5	19.8
-30	0.7	1.4	2.1	2.9	6.0	8.6	10.7	15.2	21.4

3. Graph of removal efficiency at different depth along the time

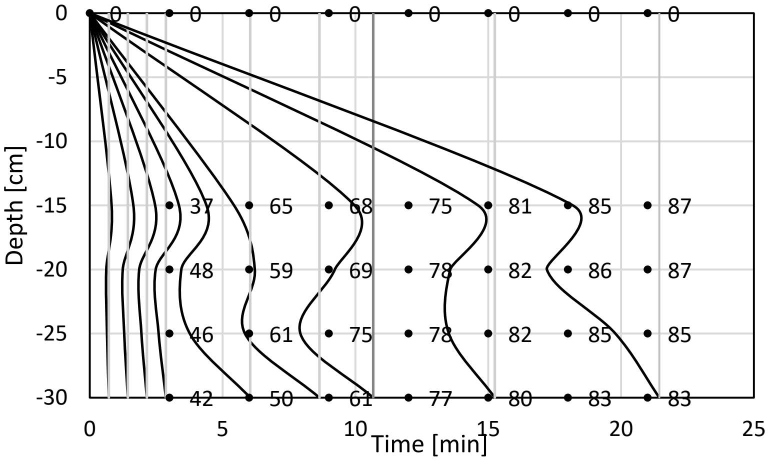

4. The overflow rate and removal efficiency

Time (min)	Vol (cm/min)	RT [%]		Vol (m/hr)
0.7	41.89	RT (10%) =	21.62	25.13
1.4	20.94	RT (20%) =	33.84	12.57
2.1	13.96	RT (30%) =	44.10	8.38
2.9	10.47	RT (40%) =	53.01	6.28
6.0	4.97	RT (50%) =	65.83	2.98
8.6	3.47	RT (60%) =	71.93	2.08
10.7	2.81	RT (70%) =	78.33	1.69
15.2	1.97	RT (80%) =	83.51	1.18
21.44	1.40	RT (85%) =	85	0.84

Appendix 6: Chemical reaction rate of EO in ha removal

First-order kinetic of HA removal at current density 2.5, 4, 5.5, and 7 mA/cm^2 in Electrooxidation.

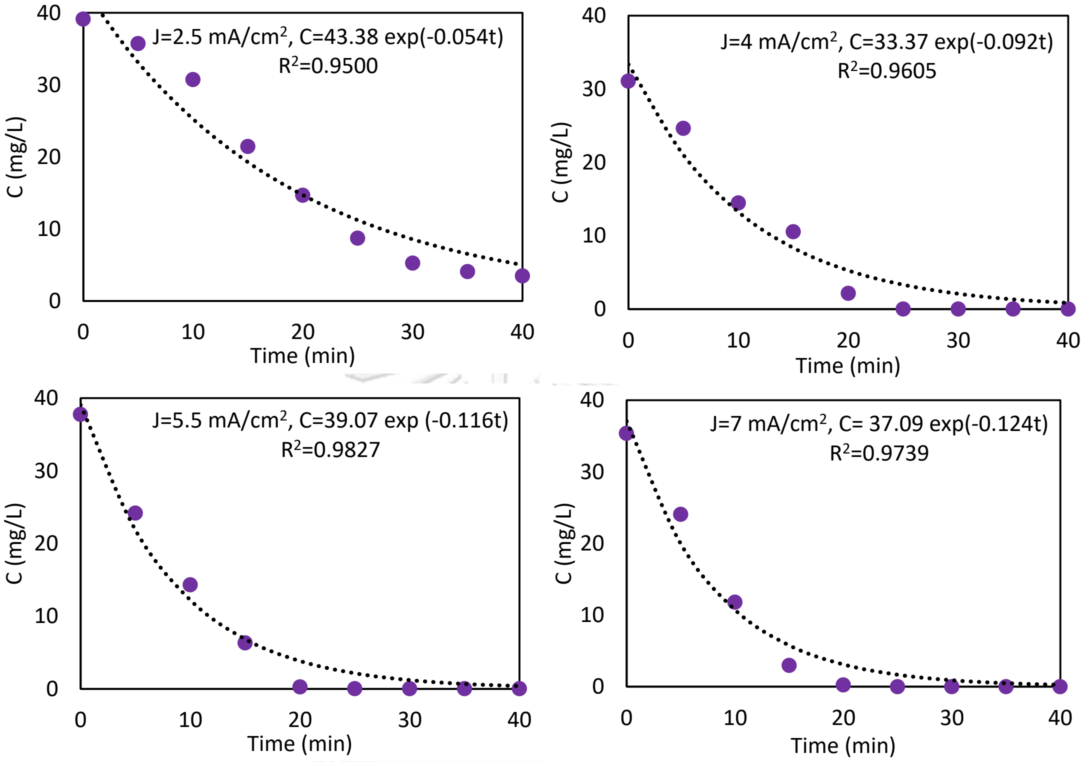

Appendix 7: Appearances of synthetic water, material, and reactor

- Settling column

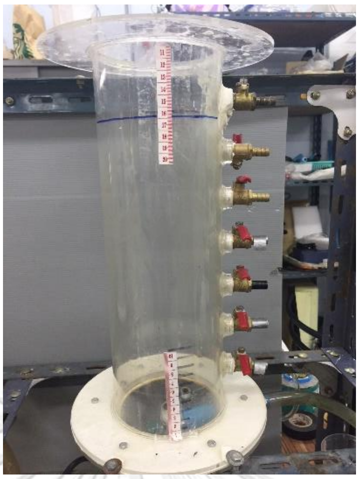

- Graphite

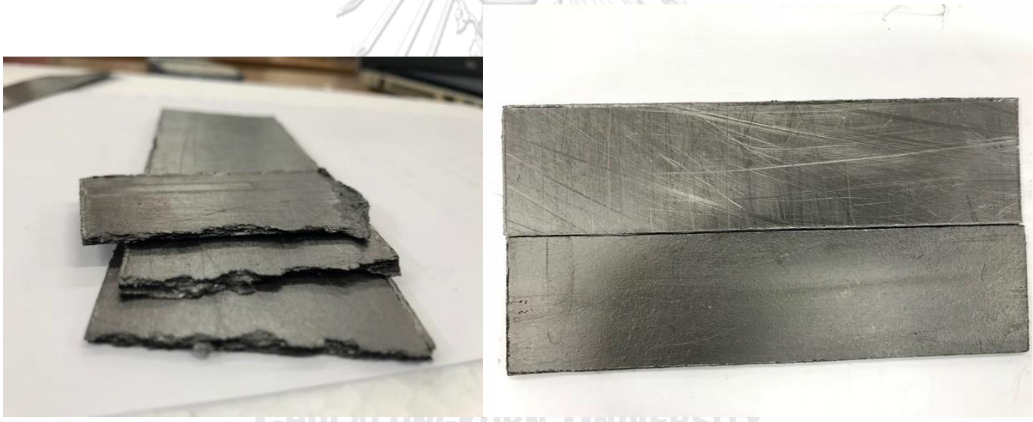

- Conductive carbon coated onto graphite

- Before and after EC process at optimal condition (HA-Bentonite synthetic water)

- Before and after EO process (Effluent synthetic from EC)

VITA

Ms. Vouchlay Theng was born in 1992 in Kompong Cham province, Cambodia. She graduated Bachelor's degree of Engineering in Department of Water Resources Engineering and Rural Infrastructure, Institute of Technology of Cambodia (ITC), Phnom Penh, Cambodia in July 2016. She awarded a scholarship from Asian Development Bank (ADB) and Ministry of Water Resources and Meteorology (MOWRAM), Cambodia.

She pursued Master's degree of Engineering in Department of Environmental Engineering, Faculty of Engineering, Chulalongkorn University, Thailand in August 2016 supported by ASEAN University Network Southeast Asia Engineering Education Development Network Program (AUN/SEED-Net) of Japan International Cooperation Agency (JICA).